AD-A124 671 DEVELOPMNT OF AN IMPROVED EXPLOSIVELY DRIVEN RUPTURED CONDUCTOR OPENING SWITCH(U) AIR FORCE INST OF TECH WRIGHT-PATTERSON AFB OH SCHOOL OF ENGI.. 1/2

UNCLASSIFIED J D WATSON ET AL. DEC 82 AFIT/GE/EE/82D-39 F/G 9/1 NL

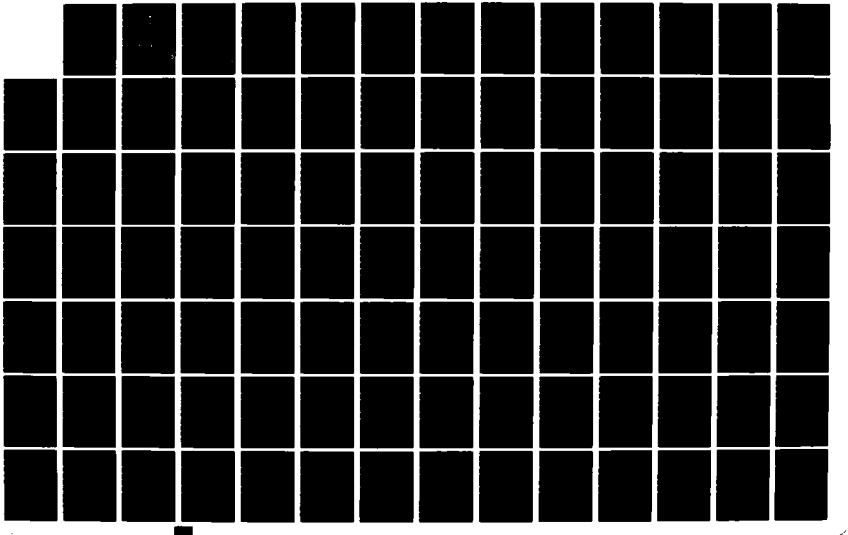

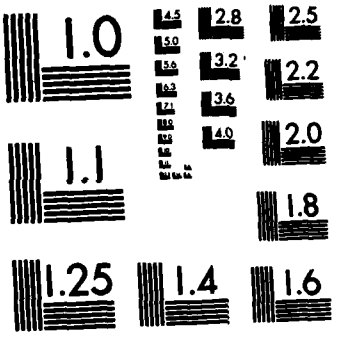

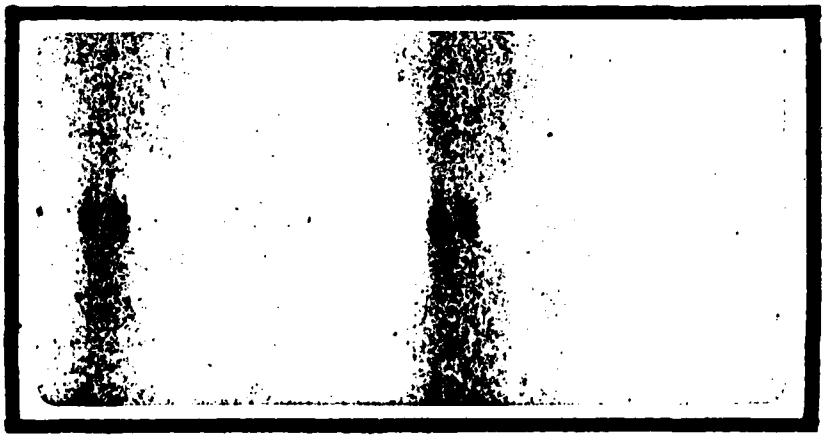

DEPARTMENT OF THE AIR FORCE
AIR UNIVERSITY (ATC)

AIR FORCE INSTITUTE OF TECHNOLOGY

Wright-Patterson Air Force Base, Ohio

AFIT/GE/EE/82D-39

DEVELOPMENT OF AN IMPROVED EXPLOSIVELY DRIVEN RUPTURED CONDUCTOR OPENING SWITCH

THESIS

John D. Watson, Capt, USAF
Michael L. Hines, 2Lt, USAF

AFIT/GE/EE/82D-39

Approved for public release; distribution unlimited

AFIT/GE/EE/82D-39

DEVELOPMENT OF AN IMPROVED EXPLOSIVELY DRIVEN RUPTURED CONDUCTOR OPENING SWITCH

THESIS

Presented to the Faculty of the School of Engineering
of the Air Force Institute of Technology
Air University
In Partial Fulfillment of the
Requirements for the Degree of
Master of Science

by

John D. Watson
Captain USAF

Michael L. Hines
2d Lt USAF

Graduate Electrical Engineering

December 1982

Preface

The purpose of this study was to determine the performance characteristics and limitations of two types of explosively driven ruptured conductor opening switches. Previous investigation by Ihor M. Vitkovitsky and R. D. Ford at the Naval Research Laboratories in Washington, D.C., have shown that these switches can be used effectively for energy compression in pulse power systems.

The major finding of this study is that these switches can be used to combine the commandability of a ruptured conductor opening switch with the fast switching characteristics of a fuse opening switch. We believe that the results in this report have direct applications to pulse power systems where commandable switching of high power pulses at low repetition rates is required.

We would like to thank our advisor, Major Timothy J. Skvarenina of the Air Force Institute of Technology at Wright-Patterson AFB, Ohio, for his patient assistance during this project. We are especially grateful to Dr. Robert E. Reinovsky of the Air Force Weapon Lab (AFWL) at Kirtland AFB, NM. His guidance and assistance were extremely helpful. We are also very grateful to 1Lt Paul Levi of AFWL for his tireless technical assistance during the experiments.

This effort was jointly funded by the Air Force Weapons Laboratory and the Defense Nuclear Agency.

Contents

Contents

List of Figures

List of Tables

Abstract

Two types of explosively driven ruptured conductor opening switches were tested. Each used a length of detonator cord to rupture an aluminum conductor. The first type used a cylindrical conductor with pusher media of either paraffin or water to break the conductor and absorb the arc energy. The second type used detonator cord in direct contact with a flat conductor. This design used the high pressure from the explosive to break the conductor and extinguish the arc.

The cylindrical switches interrupted 115 KA in approximately 35 μsec with switching delays of 68 μsec to 87 μsec. Peak load powers of up to 334 MW were achieved using a 61 KJ supply circuit. Increasing the explosive weight was found to have a detrimental effect on the switch opening time.

The flat conductor switches interrupted 185 KA with initial resistance rise rates of up to 117 mΩ/μsec. Peak load powers of up to 3.5 GW were achieved using a 137 KJ supply circuit.

The planar switch showed characteristics of both a ruptured conductor opening switch and a fuse opening switch. As the switch current was increased, the opening time decreased, eventually to a time smaller than the detonator cord burn time. This indicated that after the detonator cord was ignited, the unsevered portion of the conductor was burned open like a fuse due to the increased current density.

DEVELOPMENT OF AN IMPROVED EXPLOSIVELY DRIVEN RUPTURED CONDUCTOR OPENING SWITCH

I Introduction

Background

An inductive energy store seems a likely system for energy storage since inductive storage has a potential for energy densities several orders of magnitude greater than does capacitive storage (Ref 1). The energy stored in an inductor is proportional to the square of the current through it. Therefore, large inductive energy storage implies large currents. Transferring the stored inductive energy to a load requires an opening switch. To be useful, the opening switch must be able to interrupt large currents reliably and quickly.

Several types of opening switches are in use today. Mechanical breakers can interrupt relatively large currents but characteristic opening times are in the millisecond range and then only at a "current zero" (Ref 2). Fuses possess desirable opening times in the sub-microsecond range, but consume a large amount of electrical energy during the vaporization of the fuse element (Ref 8). In addition the delay time for opening a fuse is determined by the size of the fuse, and they generally cannot conduct current very long before opening. Explosive opening switch possess opening times in the

microsecond range and if the circuit permits, may dissipate little electrical energy. They are thus able to transfer a large amount of the stored energy to the load in a short period of time resulting in increased power input to the load. These switches can be designed to conduct for an indefinite period of time as discussed in Chapter III and then open on command with a short predetermined delay.

Previous investigations of explosive opening switches have been done primarily in the USSR and at the Naval Research Laboratory (Ref 2). The Air Force Weapons Laboratory (AFWL) is interested in explosive opening switches for application in x-ray simulators involving energy storage of as much as 100 MJ.

Problem

The purpose of this thesis was to test explosive opening switches developed by the Air Force Weapons Laboratory. These switches were modified designs of previous devices tested by the Naval Research Laboratory (Ref 2). The experiments were designed to determine the current interrupting and voltage holdoff capability of the switches in order to predict scaling potential for practical applications.

Scope

The study done in this thesis was limited to the testing of two specific explosive switch designs, using planar and cylindrical geometries. These designs are explained in Chapter III. Minor changes in the mechanical design of

each switch were made during this study to improve switch life and performance.

The criteria used to evaluate the switches are the change in switch resistance with respect to time, consistency of the current interrupting capability and the voltage hold off capability.

Assumptions

The electrical circuit used in the experiment consisted of a capacitor bank, a closing switch, a parallel plate transmission line, a storage inductor, an opening switch and a load as shown in Figure 1.

It was assumed that the circuit could be modelled by lumped-parameter elements of capacitance, inductance and resistance. Lumped-parameter elements can be assumed provided:

a. circuit dimensions are small compared to the wavelength

b. inductors and capacitors dissipate negligible energy

c. the magnetic field associated with resistances and capacitors is negligible

d. the displacement current associated with all circuit elements, except that between capacitor plates, is negligible (Ref 3).

Assuming a lumped-parameter network permitted an RLC circuit analysis approach on all tests performed.

General Approach

In this experiment two different opening switch geometries, planar and cylindrical, were tested. In order to

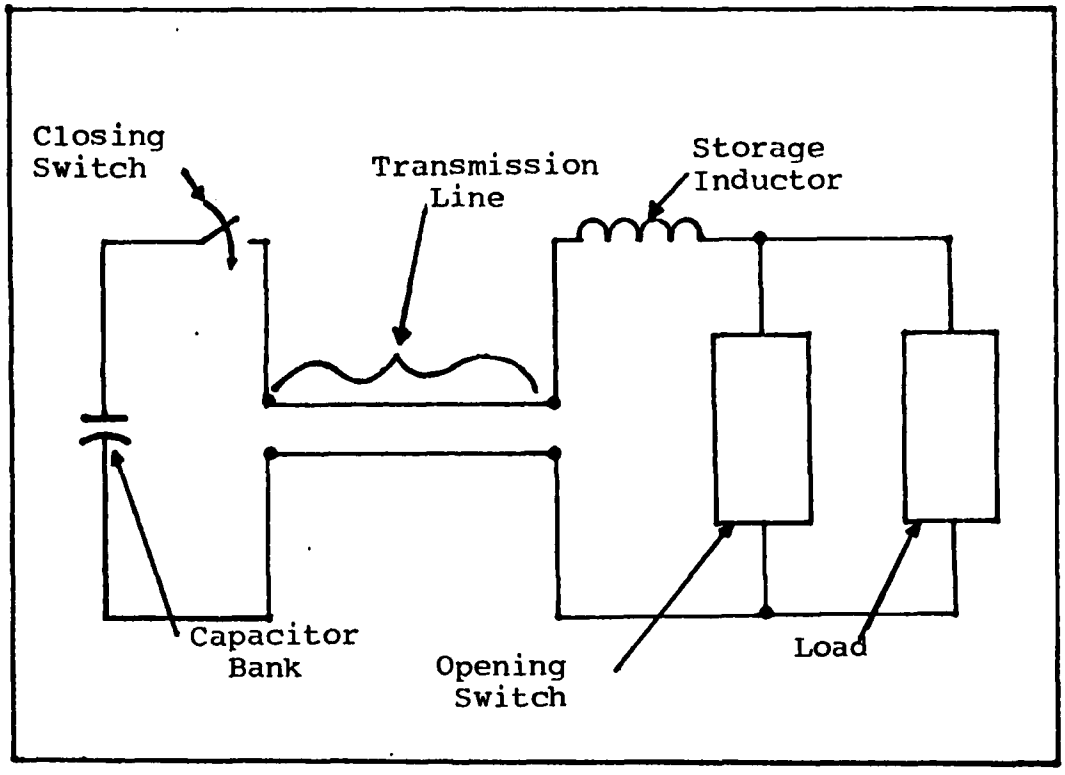

Fig. 1 Schematic Diagram of Circuit Component Layout.

analyze the circuit the constant circuit parameters were determined. These were determined by discharging the capacitor bank into a series of load circuits, one at a time. Current measurements were then used to determine these values.

The cylindrical switch was tested using two different pusher media, paraffin and water. In addition, the weight of the explosive charge and switch current were varied to determine switch characteristics.

The planar switch was tested using three different explosive weights and a sequence of increasing switch currents. The switch inductance was also lowered by modifying the conductor geometry.

For all the tests performed voltage across the switch was measured with a resistive divider. The derivatives of the currents through the switch and load were measured using Rogowski coils. Currents were obtained with passive intergrators. All values were displayed on oscilloscopes and recorded on photographs.

Switch resistances and circuit energy distributions were calculated and plotted with the aid of a computer.

II Theory of Opening Switches

This chapter describes how the energy in the circuit is distributed among the circuit components before, during and after the switching period. Also two equations for the switch resistance are derived for comparison in experimental results. Minimum conductor sizes are estimated for use as a scaling criterion.

Energy Distribution

The capacitor of Figure 1 is charged to some initial voltage, V_o. At time t_o the closing switch is closed and the capacitor discharges into the transmission line. The circuit model is shown in Figure 2. The resistors and inductors numbered 1, 2, and 3 represent the transmission line (and storage inductor), the opening switch and the load, respectively. The values of the circuit elements result in an underdamped response, i.e., the voltage and currents are damped sinusoids.

The energy stored in the capacitor at time t_o is

$$W_C = CV_o^2/2 \qquad (1)$$

At the time of the first current peak, t_1, the energy stored in the capacitor at t_o has been transferred to the circuit inductances or dissipated in the resistances. The amounts of energy transferred and dissipated are

$$W_L = LI^2/2 \qquad (2)$$

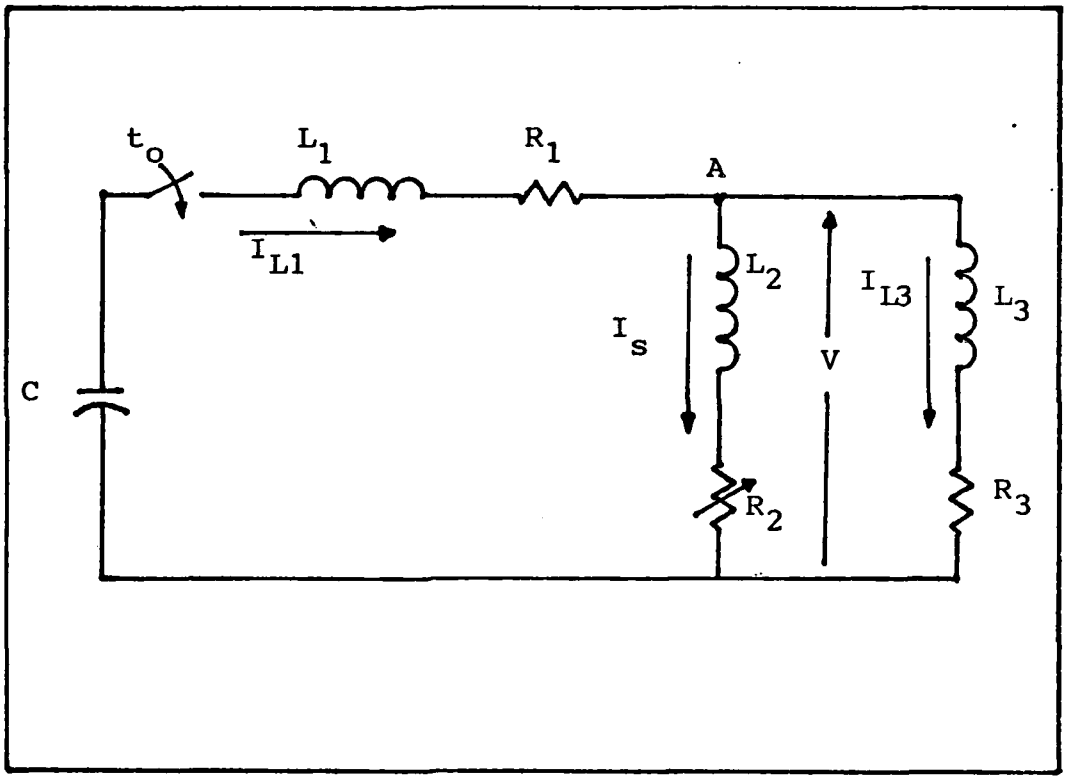

Fig. 2 Schematic Diagram of Circuit Model

and

$$W_R = \int_{t_o}^{t_i} RI^2 \, dt \tag{3}$$

For times when the load resistance R_3 of Figure 3 is much greater than the switch resistance R_2, the load current I_{L3} is much smaller than the switch current I_s. Thus I_{L3} can be neglected for the period t_o to t_1 and

$$I_s \approx I_{L1} \tag{4}$$

Therefore, at time t_1, the original energy, minus a small amount dissipated in R_1 and R_2, is stored L_1 and L_2.

At time t_1 the switch begins to open. This process is modeled by increasing the switch resistance R_2. If the switch opens over a short period of time Δt, then the energy lost in the source and load resistances during switching is insignificant.

Assuming that $R_3 \gg R_2$ prior to the switch opening and that the switch opens quickly, the energy distribution can be modeled as shown in Figure 3. Switches S_1 and S_2 shown in Figure 3 were not physically in the circuit but are used here for purposes of describing the switching interval. Switches S_1 and S_2 operate simultaneously over the switching interval Δt.

The energy and the flux linkage in the storage inductor at time t_1 are

$$W_{L1}(t_1) = L_1 I_s^2(t_1)/2 \tag{5}$$

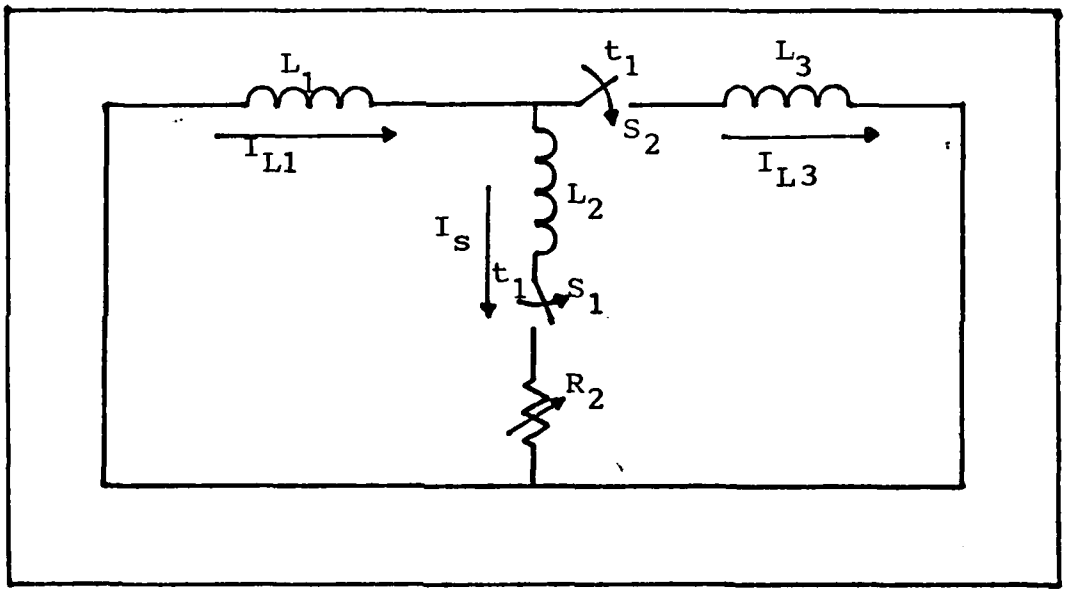

Fig. 3 Schematic Diagram of Energy Distribution Model

$$\lambda(t_1) = L_1 I_s(t_1) \tag{6}$$

The energy in the switch at t_1 is

$$W_{sw}(t_1) = L_2 I_s^2(t_1)/2 \tag{7}$$

and is dissipated in the switch during the switching interval. At the end of the switching interval, t_2, the source current I_{L1} flows through the load because now $R_2 >> R_3$ and

$$I_{L1} = I_{L3} \tag{8}$$

Neglecting the energy dissipated in R_1 and R_3 the flux linkage is conserved, and

$$\lambda(t_1) = \lambda(t_2) \tag{9}$$

and

$$L_1 I_s(t_1) = (L_1+L_3) I_{L3}(t_2) \tag{10}$$

solving for $I_{L3}(t_2)$ yields

$$I_{L3}(t_2) = I_s(t_1) L_1/(L_1+L_3) \tag{11}$$

The energy in the source and load inductors at t_2 is

$$\begin{aligned} W_{L1}(t_2) &= L_1 I_{L3}^2(t_2) \\ &= L_1 [L_1/(L_1+L_3)]^2 I_s^2(t_1)/2 \\ &= [L_1/(L_1+L_3)]^2 W_{L1}(t_1) \end{aligned} \tag{12}$$

$$W_{L3}(t_2) = L_3 I_{L3}^2(t_2)$$

$$= L_3[L_1/(L_1+L_3)]^2 I_s^2(t_1)/2$$

$$= L_1 L_3/(L_1+L_3)^2 W_{L1}(t_1)/2 \qquad (13)$$

Some of the energy originally in L_1 at t_1 has been dissipated in the switch during the switching interval Δt. That energy is

$$W_{LOSS} = W_{L1}(t_1)-W_{L1}(t_2)-W_{L3}(t_2) \qquad (14)$$

Substituting equations (12) and (13) into (14) yields

$$W_{LOSS} = W_{L1}(t_1)L_3/(L_1+L_3) \qquad (15)$$

The total energy dissipated by the switch is W_{LOSS} plus the energy stored in the switch inductance L_2 at the t_1. Therefore,

$$W_{DISS}(t_2) = W_{LOSS}+W_{sw}(t_1) \qquad (16)$$

Substituting equations (7) and (15) into (16) gives

$$W_{DISS}(t_2) = W_{L1}(t_1)[L_1L_3+L_2(L_1+L_3)]/L_1(L_1+L_3) \qquad (17)$$

Assume now that some energy is dissipated in the source resistance R_1 and the load resistance R_3 of Figure 2 during the switching interval Δt. This results in a peak load current, I_{Lp}, which is less than $I_{L3}(t_1)$ given by equation (11). Using the linear approximations for load and switch current shown in Figure 4, the equation of the line for I'_{L1} during

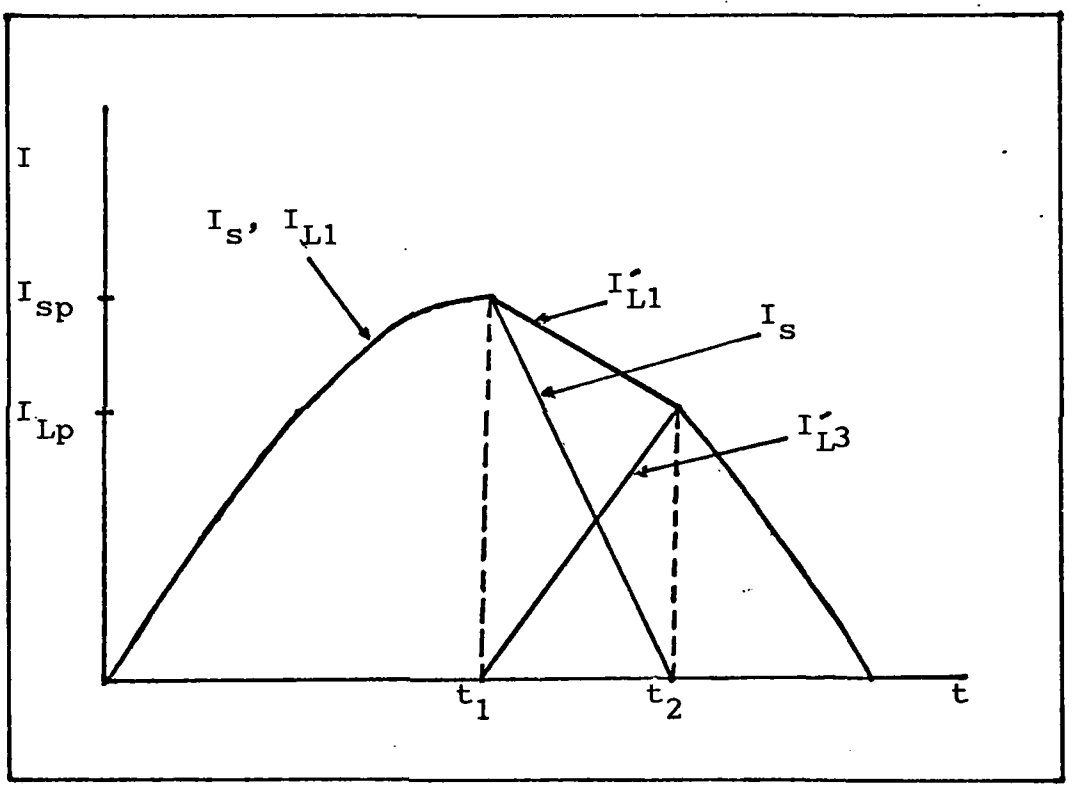

Fig. 4 Model of Circuit Currents

the switching interval is

$$I'_{L1}(t) = [(I_{Lp}-I_{sp})(t-t_1)/\Delta t]+I_{sp} \quad (18)$$

and the equation of the line of I'_{L3} during the switching interval is

$$I'_{L3}(t) = I_{Lp}(t-t_1)/\Delta t \quad (19)$$

Substituting equation (18) into (3) and integrating gives

$$W_{R1} = R_1\Delta t(I_{Lp}^2+I_{sp}I_{Lp}+I_{sp}^2)/3 \quad (20)$$

Substituting (19) into (3) gives

$$W_{R3} = R_3I_{Lp}^2\Delta t/3 \quad (21)$$

Since W_{R1} represents a loss from the energy in $W_{L1}(t_1)$ which cannot be transferred to the load and W_{R3} represents a loss from the energy that was transferred to the load, the energy in the load inductor at t_2 is

$$W'_{L3}(t_2) = L_3I_{Lp}^2/2$$

$$= W_{L3}(t_2)-W_{R1}-W_{R3} \quad (22)$$

Substituting equations (13), (20) and (21) into (22) and solving for I_{Lp} gives

$$I_{Lp} = [I_{sp}/(3_{L3}+2\Delta t(R_1+R_3))][-R_1\Delta t+$$

$$(-\Delta t^2(3R_1^2+4R_1R_3)+6\Delta tL_3((R_1+R_3)L_1^2/(L_1+L_3)^2$$

$$+R_1)+(3L_3L_1/(L_1+L_3))^2)^{1/2}] \quad (23)$$

If $\Delta t = 0$ or $R_1 = 0$ and $R_3 = 0$, equation (23) reduces to the same form as equation (11). For the case where the source resistance, R_1, is very small,

$$I_{Lp} \approx [L_1 I_{sp}/(L_1+L_3)][1+(4\Delta t^2 R_3^2)/(6L_3R_3\Delta t+9L_3^2)]^{-\frac{1}{2}} \quad (24)$$

Therefore, the estimated energy in L_1 and L_3 at t_2 is

$$W'_{L1}(t_2) = L_1 I_{Lp}^2/2 \quad (25)$$

and

$$W'_{L3}(t_2) = L_3 I_{Lp}^2/2 \quad (26)$$

It can be seen from equation (23) that the peak load current, I_{Lp}, is a function of the switch current peak I_{sp}, the source and load resistances (R_1 and R_3), the load and source inductances and the switching interval Δt.

In this section equations for energy and current have been derived for the source, switch and load currents at different points in time. These equations will be used later in Chapter V as a comparison with the actual measured values.

Circuit Analysis

From Figure 2 two equations can be written and solved for the switch resistance R_2. At node A, the voltage, V_2 across the switch can be written as

$$V = L_2\dot{I}_s + R_2 I_s \tag{27}$$

Solving for R_2 gives

$$R_2 = (V - L_2\dot{I}_s)/I_s \tag{28}$$

Now writing a loop equation around the switch and load mesh gives

$$L_2\dot{I}_s + R_2 I_s - R_3 I_{L3} - L_3\dot{I}_{L3} = 0 \tag{29}$$

Solving for R_2 gives

$$R_2 = (L_3\dot{I}_{L3} - L_2\dot{I}_s + R_3 I_{L3})/I_s \tag{30}$$

Equations (28) and (30) provide two different ways to calculate the switch resistance since equation (28) depends on V while equation (30) depends on $\dot{I}_{L3}$. Both V and $\dot{I}_{L3}$ were measured, providing a check on the results.

III Switch Design and Operation

This chapter describes the construction and operation of the two types of switches, cylindrical and planar, which were tested.

Cylindrical Switch

Construction. The cylindrical switch is constructed around an aluminum tube with .035 inch wall thickness as shown in Figure 5. Mounted around the tube and held in place by polyethylene rings, are steel cutting and bending rings. The cutting rings have sharp square inner edges which cut the tube when it is forced against them. The bending rings have rounded inner edges which allow the cut tube sections to form around it. A bending ring is placed at both ends of the switch while alternating cutting and bending rings, separated by the polyethylene rings, lie along the length of the tube.

Enclosing the steel and polyethylene ring assembly is an aluminum cylinder of 0.25 inch wall thickness which contains the explosion. On each end of the switch, attached to the outer cylinder, is a steel end plate. Attached to the end plates and extending the length of the switch are 3/8 inch bolts which provide axial containment of the switch.

Steel plugs are inserted into each end of the inner aluminum tube to provide a place to attach the switch to the

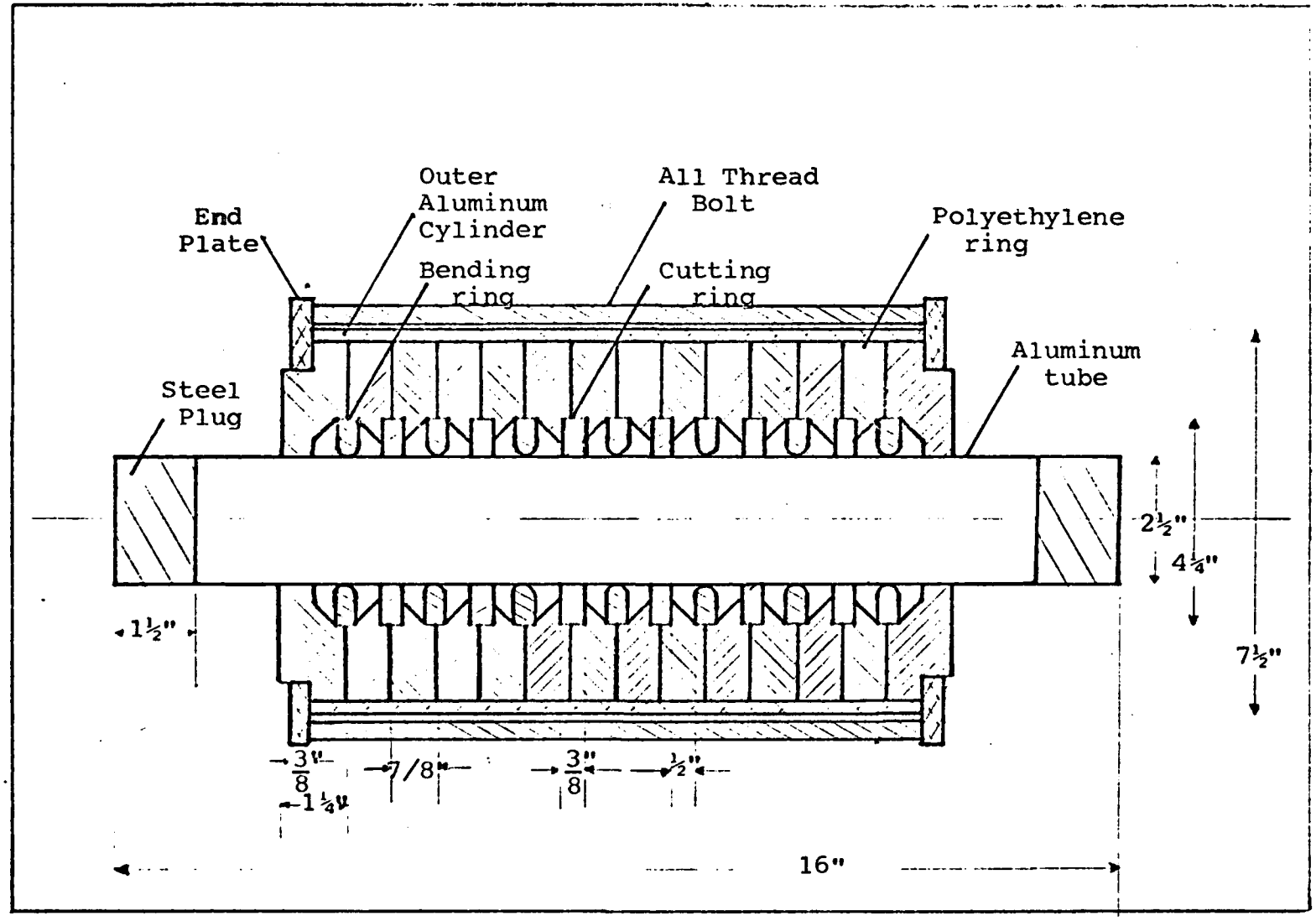

Fig.5 Cross Section of Cylindrical Switch

electrical circuit and prevent venting of the explosive gasses out the ends of the tube.

Operation. As shown in Figure 5, the inner aluminum tube is filled with a non-conducting pusher medium. Paraffin and water as were used in this study. The high explosive PETN cord extends the length of the pusher medium in the center of the tube.

The pusher medium serves a dual purpose in the operation of the switch. First, the pusher medium transmits the radial pressure wave created by the burning PETN cord. Second, the pusher medium cools and extinguishes the arc formed as the aluminum tube, now conducting high currents, is cut at the cutting rings.

Figure 6b shows a section of the switch in the open position. The inner aluminum tube is shown cut at both edges of the cutting ring leaving a circular piece of the conductor, the width of the ring, on the inside surface of the ring. As the tube is cut at the cutting ring the pusher medium forces the cut end of the tube further outward resulting in the length of the tube lying between two cutting rings to fold around the inner surface of the enclosed bending ring. This action provides maximum conductor separation (Ref 2) and the dielectric pusher material is now separating the steel rings.

The delay inherent in the opening of the switch can be attributed to three factors: (1) the PETN cord detonation velocity, (2) the time required to compress the pusher medium

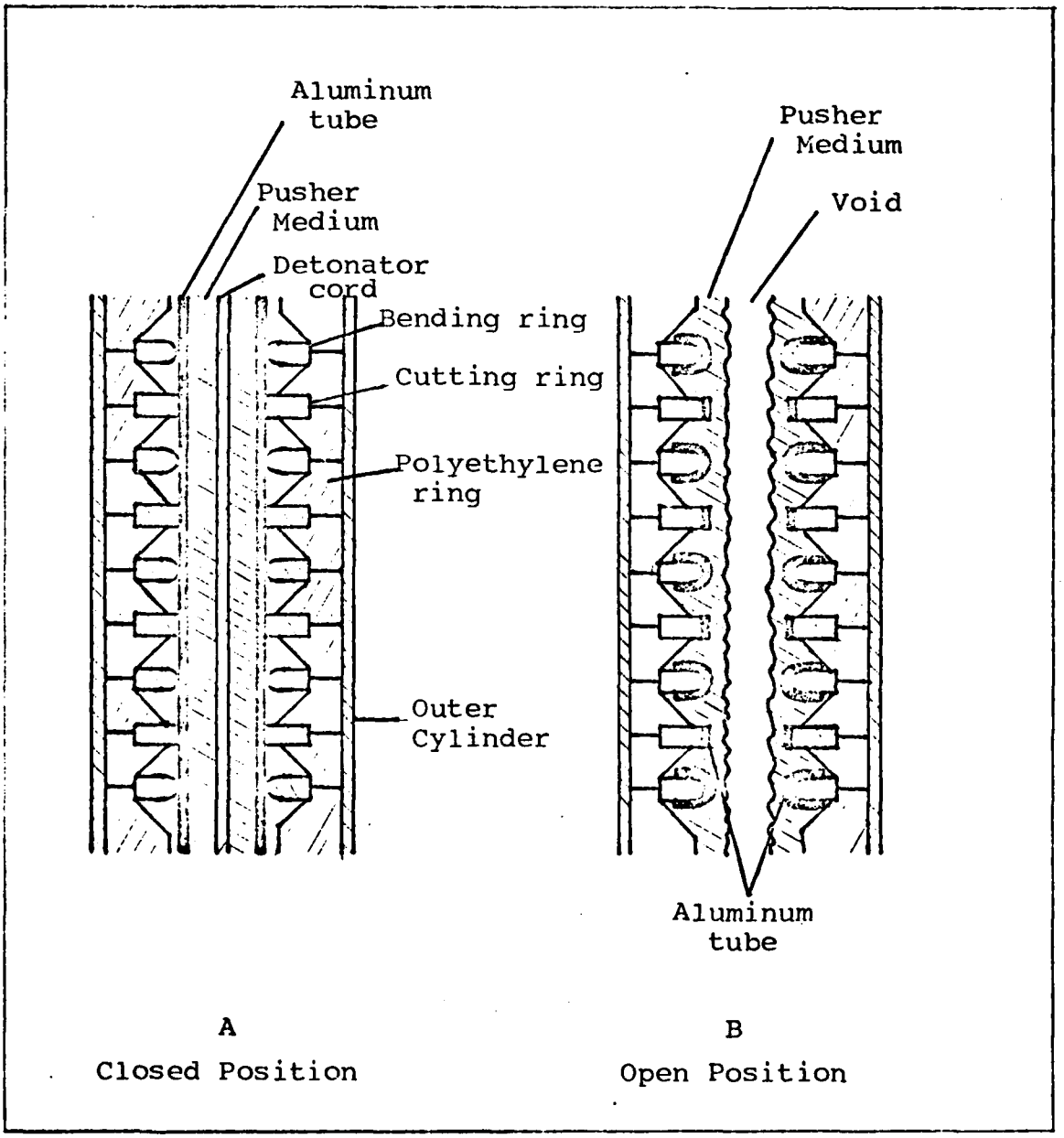

Fig. 6 Cross Section of Cylindrical Switch in the Open and Closed States.

and (3) the radial velocity of the pusher medium (Ref 2).

The PETN cord detonation velocity is 7 mm/μsec (Ref 4). The velocity of the pusher medium can be calculated approximately as (Ref 2)

$$V_p = [2WC_nN_gN_{IE}/M]^{\frac{1}{2}} \qquad (31)$$

where

M = pusher medium mass (Kg)

W = explosive energy of PETN (J/gm)

C_n = explosive charge (gm)

$N_g = \left(\frac{\text{initial explosive volume}}{\text{final explosive volume}}\right)^{\gamma-1} \approx 50\%$,

$\gamma = 1.2$

N_{IE} = efficiency of transferring the internal energy of the gas to kinetic motion of a pusher ≈ 50%

therefore

$$V_p = [WC_n/2M]^{\frac{1}{2}} \qquad (32)$$

The PETN cord was detonated at each end simultaneously. Therefore, knowing the cord detonation velocity (V_c), the distance from the end of the cord to the center of the switch (ℓ), the tube wall thickness (t_T), and using equation (31), a time from detonation (T_{delay}) to complete switch opening, as in Figure 6b, can be calculated by

$$T_{delay} = (\ell/V_c)+(t_T/V_p) \qquad (33)$$

Planar Switch

The planar switch is constructed so the force of the explosive charge acts directly on the conductor. The design is based on a concept described by Ford and Vitkovitsky (Ref 5). Nothing is between the explosive and the conductor but a thin layer of air, so the arc must be extinguished by the blast effects of the explosive. The arc is compressed and extended by the shock wave at the expanding explosion front until extinguished. The torn ends of the switch conductor are insulated by the explosive products and the high pressure behind the shock wave until the current is interrupted. The description of these effects is beyond the scope of this thesis. They have been the subject of experiments by Zubkov, et. al., in the Soviet Union (Ref 6).

Construction. The planar switches used for these experiments were assembled as shown in Figure 8. Each switch tested used four sections like that in Figure 8, connected in series. The earliest switches tested used connections to the circuit at each end of the switch. This configuration facilitated the connection to the circuit but caused a high inductance. Beginning with planar switch number 8, the conductor was folded back under the switch as shown in Figure 7. This reduced the switch inductance.

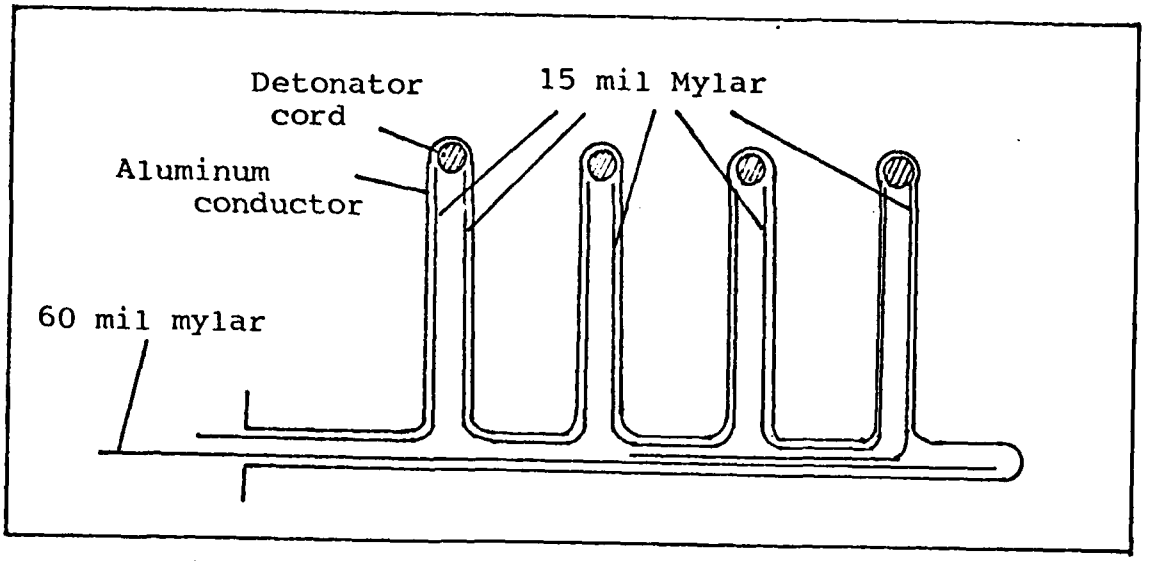

Fig. 7 Configuration of Planar Switch Conductor and Mylar Insulation

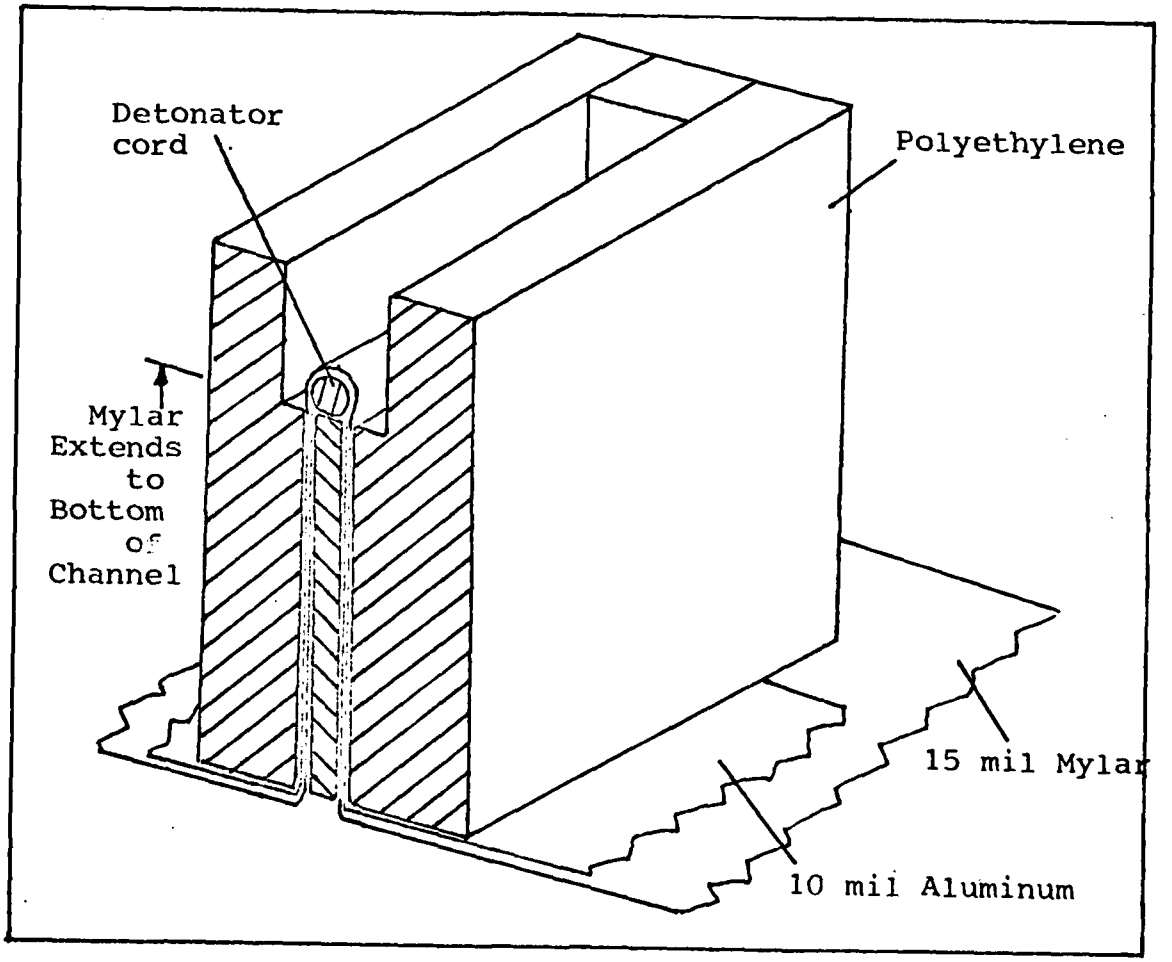

Fig. 8 Planar Switch Cross Section

The conductor was formed before assembly. The large polyethylene insulator blocks were loosely assembled upside down, then the conductor was inserted. A rod the size of the detonator cord was placed in each loop of the conductor to form spaces for the detonator cords. Then the thin polyethylene separator was inserted and the assembly was loosely clamped.

Clamping was accomplished by two steel end braces connected by two threaded rods. The clamp was made wide enough to preclude arcing to the clamp. The end braces were separated from the switch by 20 mils of mylar.

Mylar insulation was inserted as diagrammed in Figures 7 and 8. The mylar extended beyond the polyethylene blocks to give a long tracking path between the conductor edges everywhere except in the channel. The most probable conducting path through the open switch was across the channels.

The assembled switch was tightly clamped and placed upright on a wooden platform. The corners of the clamp were attached to this platform with nylon straps. A hole the size of the detonator was cut in the conductor at the center of each channel for later placement of the detonators.

The conductor ends were formed around wooden cross pieces attached to the wooden platform at the end of the switch. The circuit cabling was attached to the conductor ends at these cross pieces.

Operation. The switches were assembled in the shop and transported to the test site. The switches were

attached to the circuit by lag screws through cable terminal lugs and the conductor into the cross pieces. The cable terminals used throughout the circuit to connect the cables were attached to the cables by set screws. These connections were the source of much of the resistance measured in the circuits.

The metal rods used to form the space for the detonator cord were removed and the cord was inserted. Polyethylene blocks were glued in at the ends of each channel to prevent venting of explosive gasses and pressure out the sides during switching. The detonators were glued in place in the channel, contacting the detonator cord through the hole in the center of the conductor.

The placement of the detonators caused the conductor to tear from the center outward to the edges. The conductors used for these experiments were all 6 in. wide. Each switch section was detonated at the same time. These switches used the same type of detonator cord (PETN) as the cylindrical switches. The cord burns across the 3 in. to the edge of the conductor at 7 mm/μsec. If the increased current density at the edges of the rupturing conductor does not vaporize the ends of the conductor the explosive will mechanically open the switch in 10.9 usec. All of the current flows toward the edges of the conductor as the rupture spreads outward. The arc will ignite at the corners of each conductor section after it mechanically opens. This arc is then extinguished by the explosive pressure and gasses.

Conductor Sizing

The conductor of the switch will heat and can eventually melt from the Joule heating caused by the current flow. The conductor can be cooled externally to prevent melting, either actively or with radiators. The designs used for this study had no cooling equipment and were well insulated. Therefore, the conductors had to be large enough to absorb the heat without melting.

The energy absorbed by the switch during conduction is assumed to remain in the conductor due to the insulation. This energy is

$$W_s = \int_o^{t_{delay}} RI_{peak}^2 SIN^2(2\pi t/Period)dt \quad J$$

$$\approx RI_{peak}^2(Period/8) \qquad (34)$$

where t_{delay} is the time where the switch is detonated. The switch resistance is a function of temperature, and therefore of time, so precise definition of the absorbed energy would have to include this. The resistivity of aluminum increases by approximately a factor of 3.5 when heated from room temperature to melting temperature (659^{o}C). This derivation will approximate this by using an average resistance of three times the room temperature resistance.

For frequencies where skin depth is greater than the thickness of the metal conductor (less than 105MHz for 10 mil aluminum), conductor resistance is

$$R_{AV} \approx 3\ell/\sigma_o A \quad \Omega \tag{35}$$

The room temperature conductivity of aluminum, σ_o, is 3.72×10^5 m ho/cm so

$$W_s \approx \ell I^2_{peak}(\text{Period})/(0.99\text{x}10^6)(A) \tag{36}$$

The energy required to melt aluminum with an initial temperature of 25^oC is

W_m = volume x density x melting specific energy

$$= (\ell)(A)(2.7\text{gm}/\text{Cm}^3)(970\ \text{J/gm}) \tag{37}$$

To prevent conductor melting before detonation of the switch explosive,

$$W_s < W_m \tag{38}$$

$$A > (I_{peak})(\text{Period})^{\frac{1}{2}}/51.0\text{x}10^3 \quad \text{CM}^2 \tag{39}$$

The conductors used for this study were much larger than the minimum required by this approximation. The results of this derivation will be used in Chapter VI to discuss scaling requirements.

IV Experimental Apparatus

In this chapter the components shown in Figure 1 and the measurement and diagnostic equipment are described in detail.

Capacitor Bank

A capacitor bank served as the current source for this study. The capacitor bank consisted of fifty 6.1μF 60KV capacitors connected in parallel to give a total nominal capacitance of 305μF. Charge voltages of 20KV and 30KV were used. The bank was charged with a Maxwell Labs charging system and discharged into the transmission line and storage inductor using a closing switch.

Closing Switch

The closing switch was constructed of two 6 ft. long by 8 in. high by 0.5 in. thick steel plates. The connection of the closing switch to the capacitor bank and the transmission line is as shown in Figure 9.

Plate 1 was almost immovable as it was attached to the solid center conductor of the coax cable from the capacitor bank. Plate 2 was attached to the top of the transmission line and could be lifted up to facilitate switch cleaning and rebuilding.

Mylar is placed between the plates to serve as the main switch insulation during charging. A 1 mil thickness

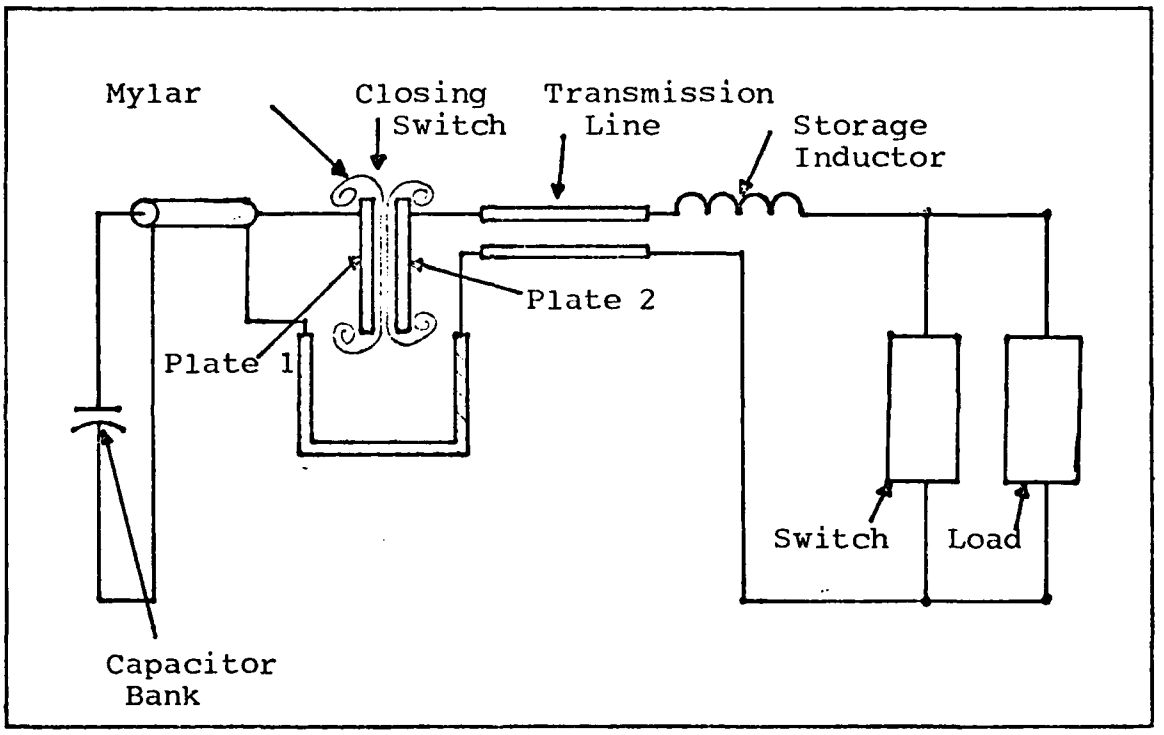

Fig. 9 Closing Switch in the Test Circuit

of mylar was used for each 1KV of potential across the switch plates. The plate separation was therefore determined by the thickness of mylar between the plates, which in turn depended on the charge voltage for the experiment.

Plate 2 had ½ in. holes along the top edge of the plate which accommodated shaped charge detonators. Two detonators per shot were employed to puncture the mylar, thus closing the switch, and allowing the capacitor bank to discharge its energy into the transmission line and connected components.

After each shot the switch was rebuilt by replacing the mylar insulation and installing new detonators in plate 2.

Transmission Line

The transmission line consisted of two 60 mil aluminum sheets each 40 ft. long by 4 ft. wide. The aluminum sheets were separated by 12 sheets of 5 mil mylar each 6 ft. wide for a total insulation thickness of 60 mils. This gave a line capacitance of

$$C = \epsilon A/d = 0.26\mu F \tag{40}$$

Since $C_{line} << C_{bank}$, C_{line} was neglected in all circuit calculations.

The mylar sheets separating the two transmission line sheets extended 1 ft. on each side of the transmission line. A piece of .5 in. Tygon tubing was placed between the sixth

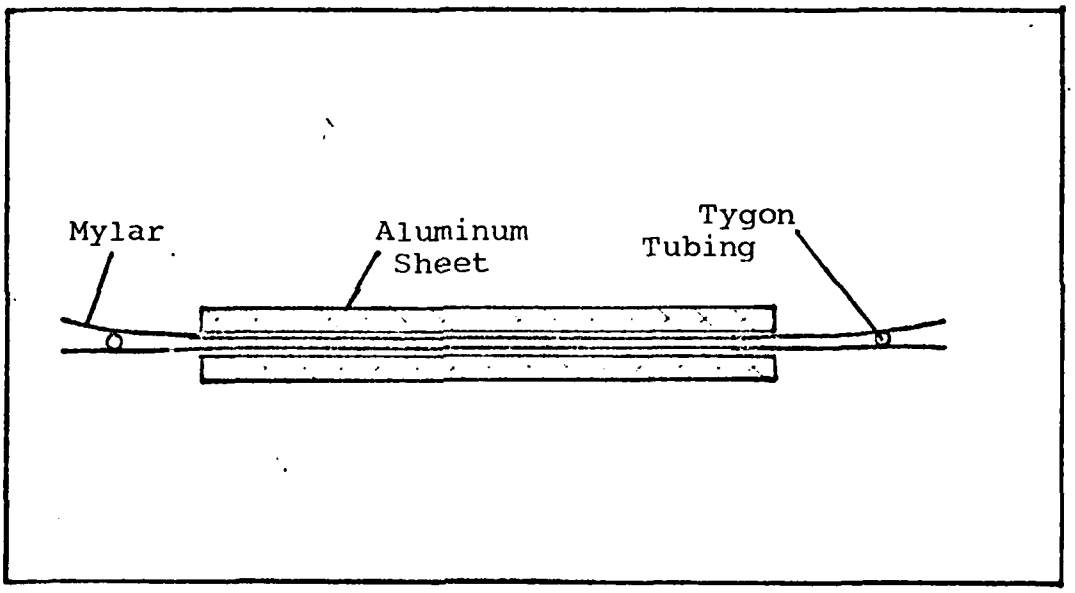

Fig. 10 End View of Transmission Line with Mylar and Tygon Insulation in Place.

and seventh sheets of mylar along the entire length of the transmission line, as shown in Figure 10. This tubing has been demonstrated to improve the insulation capability of mylar sheets by altering the insulation capacitance (Ref 9).

Storage Inductor

The primary storage inductor was constructed of 12 in. PCV pipe with two 1/0 AWG insulated standard copper cables spirally wrapped on the inside surface. The cables were held in place by metal cable clamps at each end of the pipe and were strapped to the pipe with nylon ties on opposite sides of each loop.

The purpose of attaching the inductor to the transmission line was to increase the period of the sinusoidal current produced by the RLC circuit. The period T is

$$\begin{aligned} T &= 2\pi/W_d \\ &\approx 2\pi/W_o \\ &\approx 2\pi(LC)^{\frac{1}{2}} \end{aligned} \tag{41}$$

and is directly proportional to the square root of the circuit inductance. Increasing the period held the current at a peak for a longer period of time allowing the switch to be opened at peak current more reliably. In addition the extra inductance limited the peak current delivered by the capacitor bank. If the capacitor was charged to V_o, then the peak current is given by:

$$I_p = V_o(C/L)^{\frac{1}{2}} \tag{42}$$

Resistor

A resistor served as the load throughout this experiment. The resistor was connected in parallel with the opening switch thus serving as a commutating circuit which dissipated energy transferred to it by the opening switch.

The resistor as shown in Figure 11 was constructed of two parallel aluminum plates separated by polyethylene separators at the top and bottom of the plates. The plates were submerged in a solution of ammonium chloride and water. Resistance could be varied as desired by changing the concentration of ammonium chloride in the water.

Diagnostics

Rogowski Coil. The Rogowski coil provides a means of measuring the derivative of time varying high currents and responds only to the current passing through the coil loop (Ref 7).

Four Rogowski coils were used as shown in Figure 12. Coils A and B were used to measure the load current derivative, $\dot{I}_{L3}$ while coils C and D were used to measure switch current derivative, $\dot{I}_s$. The load current, I_{L3} also passes through coils C and D but it goes through twice in opposite directions cancelling the signal.

To maintain uniformity in this experiment, the Rogowski coils were wrapped around a piece of 4 in. PCV pipe and then placed around the cables which were held fixed in the center of the loop. This procedure provided a constant coil area and orientation around the conductor giving nearly constant coil gain for all the tests.

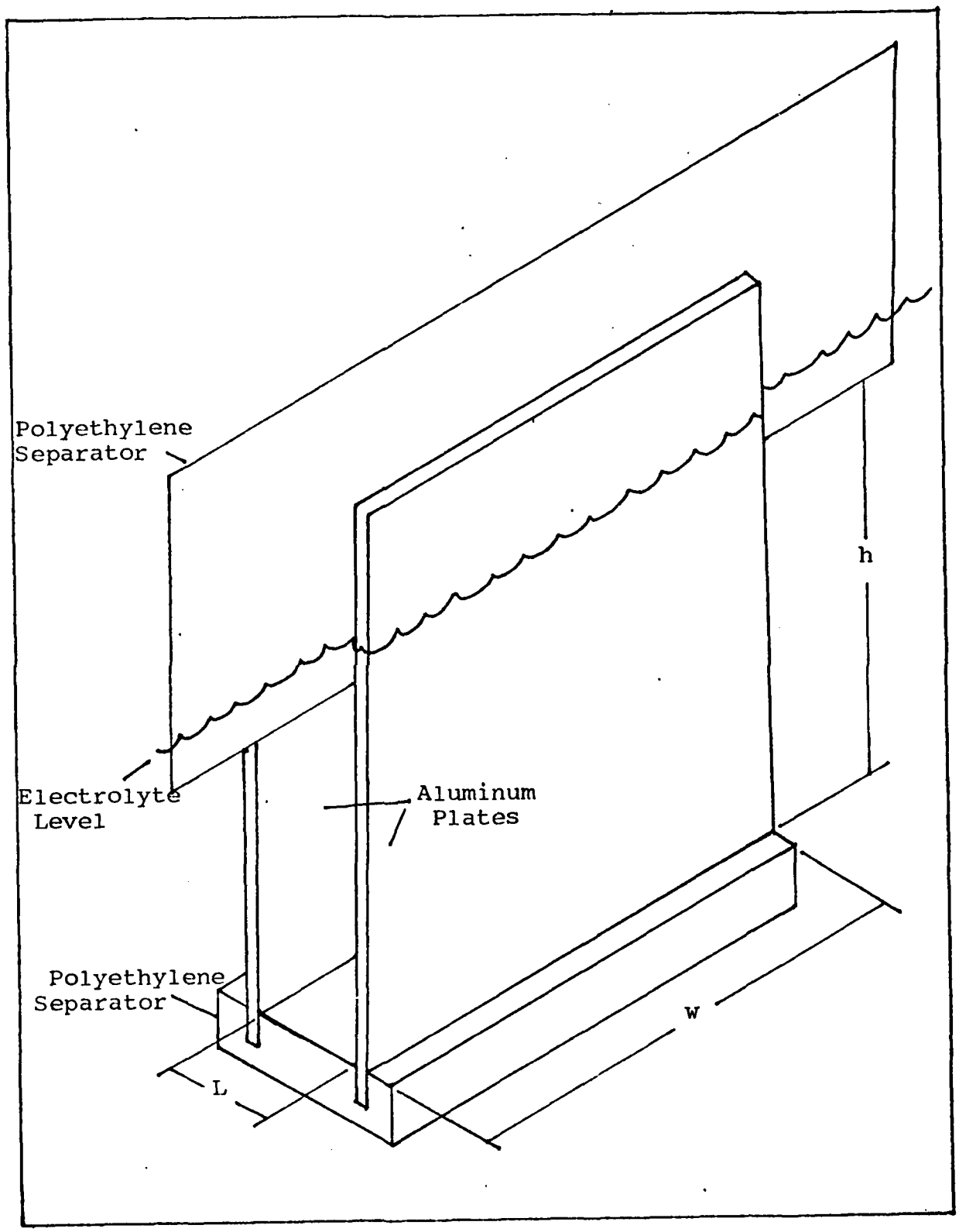

Fig. 11 Resistor Load

Two coils were used for each current derivative measurement. The coil in each pair encircled the conductor in opposite directions. The two signals were connected to a differential amplifier which summed the two signal magnitudes and eliminated any common mode signals.

Voltage Probe. A resistive divider was used to measure the voltage across the switch. It was connected to the circuit as shown in Figure 12. The two resistors, R, in the voltage probe leads were constructed of plastic tubing filled with a copper sulfate solution with copper electrodes sealing each end. The copper sulfate solution was adjusted to give a resistance on the order of 50KΩ. Coaxial cables fed the signal to 50Ω terminators across the oscilloscope inputs. Thus a 1 volt signal was measured at the oscilloscope for every 1 KV across the switch. The cable shields were shorted together at the resistors and at the oscilloscope input to balance any induced shield currents. The two signals were then connected to a differential amplifier which eliminated any common mode signals (Ref 7).

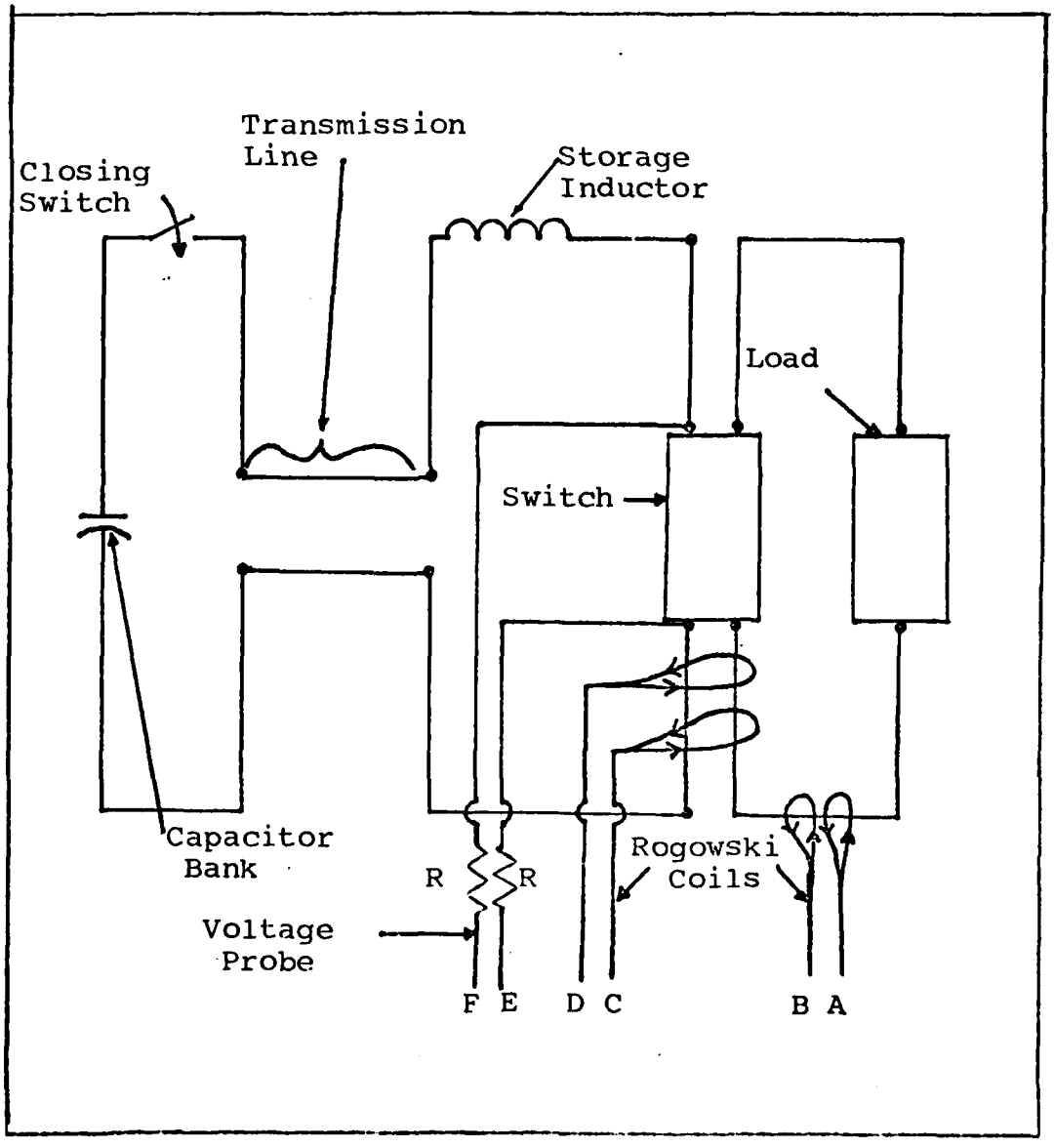

Fig. 12 Schematic Diagram of Diagonistics Placement

V Experimental Procedure

This chapter describes the experiments which were conducted for this study. Preliminary experiments were required to obtain circuit element values for the equivalent circuit model. These were followed by actual testing of the two types of switches under varying conditions.

Determination of Circuit Parameters

This section describes the general procedure used to obtain values for the elements of the equivalent circuit used to represent the experiment.

The only known values in the experimental set-up were the bank capacitance (C_b) and the charge voltage (V_o). All other capacitances were neglected because they were much less than C_b.

The unknown resistances and inductances remaining to be found were in the transmission line, the two switches, the load, the storage inductor and cables and terminals used to connect the circuit components together.

To find the transmission line resistance and inductance, the end of the transmission line was bolted together resulting in a short circuit. The capacitor bank was charged and then discharged. The ringing discharge current was measured. As expected, a damped sinusoidal response was observed.

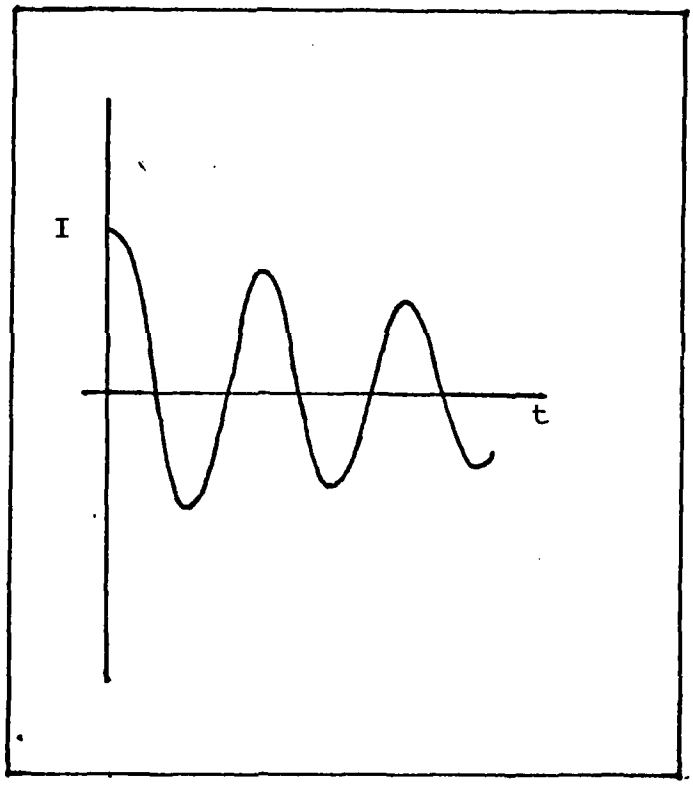

Fig. 13 Plot of Typical Short Circuit Current

A typical response of current through the short is shown in Figure 13. From the oscilloscope traces the period, T can be found.

For a time invariant RLC circuit we may assume that the sinusoidal waveform decayed exponentially. A least squares fit was done on the waveform peaks yielding a damping factor α in the exponential decay. Knowing T, C and α, the circuit inductance was calculated from:

$$T = 2\pi/W_d$$
$$= 2\pi/[(W_o)^2-(\alpha)^2]^{\frac{1}{2}} \qquad (43)$$

where $W_o = \frac{1}{\sqrt{LC}}$

and solving for the inductance yields

$$L = T^2/C(4\pi^2+T\alpha^2) \qquad (44)$$

The circuit resistance was then calculated since:

$$R = 2\alpha L \qquad (45)$$

Once the transmission line resistance and inductance were known, each of the remaining circuit components (the storage induction, each switch and the load) was connected individually to the end of the line and the same procedure was used to find the resistance and inductance added to the circuit by the individual component.

These tests well called "short shots" as all that was desired was the determination of the inductance and resistance of each piece tested.

Cylindrical Switch Tests

Seven cylindrical switches were tested. The tests were performed by connecting each switch into the test circuit as shown in Figure 12. The switches were then armed with detonator cord and electrical detonators. The capacitor bank was charged and then the closing switch was fired to discharge the energy into the circuit. The current would then ring through the source and the switch. The switch acts essentially as a short circuit until shortly after it is detonated.

The switch detonation was timed in an attempt to cause switching at the first peak of the switch current. Due to the long delay experienced with the switch, some switches were detonated simultaneously with the closing switch. An increased storage inductance was used on the last three switch tests to increase the period without significantly reducing the current.

Measurements were made of $\dot{I}$ and switch voltage in the same manner as the short shots described in the previous section.

Shown in Table 1 is a summary of the cylindrical switches tested in this study. The main parameters varied throughout the tests were detonation cord weight, pusher medium and delay. Since the peak current was held essentially

TABLE I

Cylindrical Switch Test Summary

Switch	V(KV)	L (μH)	I (KA)	Detonator Cord (gr/ft)	Pusher Medium	Delay (μsec)	Comments
CYL1	30	7	190	100	Paraffin	30	No load
CYL2	20	7	115	100	Water	30	No Data
CYL3	20	7	115	100	Water	30	Good
CYL4	20	7	115	175	Water	0	Good
CYL5	20	10	115	175	Paraffin	0	Good
CYL6	20	10	115	175	Paraffin	100	Extended delay
CYL7	20	10	115	100	Paraffin	0	Bad Data

constant for all shots except CYL1, the switches were studied on the basis of the effects of detonation cord weight and pusher medium on interruption time.

CYL1 was a first test situation with a new switch design. Switch detonation was delayed for 30 μsec after the closing switch was fired. This delay was based on previous work done by NRL (Ref 2). No load was provided, thus requiring the switch to absorb more energy than it was capable of in a reasonable switching interval. A load was added to provide a commutating element for all subsequent tests.

At this point a plan was decided on for further testing. The next two switches would use water as the pusher medium but the explosive weight would be changed. The following shots would use paraffin as the pusher medium and also vary the explosive weight. These tests would give sufficient results to evaluate the switch performance.

CYL2 was loaded with 100 gr/ft. detonator cord and a water pusher medium. Switch firing was delayed 30 μsec. The closing switch did not fire, therefore, no data was obtained.

CYL3 was constructed the same as CYL2. Test results confirmed a long delay before the switch opening. CYL4 used 175 gr/ft. detonator cord, water pusher medium and zero delay to overcome the long delay experienced in CYL3. CYL5 was altered from CYL4 to test the effects of different pusher medium on switch performance. CYL6 was delayed for such a long period of time to initiate switch opening at a reduced current of the other tests. CYL7 was to compare the two

pusher medium with 100 gr/ft. detonator cord but bad data was obtained.

Planar Switch Tests

The same test procedures were used for the planar switch tests as for the cylindrical switch tests. A test sequence was chosen which would alternately increase explosive weight and peak switch current.

The first three switches tested, called Mod 1, used a tab fixed to each end of the thin polyethylene separator shown in Figure 8 (the tabs are not shown). These tabs extended into the explosive channel and acted as baffles to prevent venting of the explosive gases from the ends of the conductor. This was the design tested by Ford and Vitkowitsky in 1981 (Ref. 5). In all succeeding tests, these tabs were replaced with removable polyethylene blocks which filled the full width of the channel, as shown in Figure 8. This change was made to facilitate switch assembly, though there was some hope that the blocks would improve switching somewhat, since they completely sealed the ends of the explosive channels. When the tabs were used, the switch had to be assembled at the test site. The explosive was inserted during assembly. With the removable end blocks, the switches could be completely assembled in the shop. At the test site, the explosive was inserted and the blocks were glued in after switch installation. The first switch with this change was called Mod 2.

The first two switches tested did not have a load. The switching time was long and the current continued to ring through the switch. A load resistor of 20 mΩ was used to dissipate the circuit energy on the third and fourth switch tests. This resistance was increased for the remaining tests to reduce load current before switching.

The first four switches were connected to the circuit with an input at one end of the switch and an output at the other end. Since the circuit was connected with large cables, this presented the easiest method to connect the cables to the switch. All succeeding switches, called Mod 3, had the conductor folded back under the switch, as shown in Figure 7, to decrease switch inductance.

The first four switches were armed with 50 gr/ft. detonator cord. They were all tested at 120 KA. These included one successful experiment with tabs in the channels and one successful experiment with the polyethylene end blocks. One switch was tested with 100 gr/ft. cord at 120 KA and one at 190 KA. The second of these experienced triggering problems and only three channels fired. The first showed that switching at 120 KA improved when accomplished with 100 gr/ft. cord. All succeeding tests were done with 175 gr/ft. cord.

The current was increased by changing the capacitor changing voltage from 20 KV to 30 KV and by decreasing the storage inductance from 6.3 μH to 3.25 μH. Higher voltages were avoided due to the age of the transmission line. At least one good experiment was performed at 120 KA and at 190 KA.

The triggering system became less reliable as the tests progressed, resulting in no completely successful experiments at 290 KA.

VI Results and Conclusions

This chapter describes the methods used to analyze the test data. Calculated and measured load currents and system energies are compared.

Analysis Procedure

The oscilloscope trace photographs from each experiment were manually digitized and used as input files for a set of digital computer programs. The programs interpolated the input points to 1 μsec intervals and shifted each curve if necessary to improve alignment. The realignment was necessary to correct for magnification and distortion in the cameras and oscilloscopes and to compensate for the small inaccuracies inherent in reading small photographs. The alignment was especially sensitive where several related curves each had very steep slopes, and a reading error of a fraction of a milimeter could produce a significant error in magnitude.

The switch resistance was calculated at each microsecond from equations (28) and (30). The two methods generally showed good agreement. No reconciliation of differences was possible except by adjustments to curve alignments. Equation (30) was used only as an indicator of confidence in the result from equation (28). The switch resistance from equation (28), the other measured values, and the predetermined constant circuit parameter values were used to

calculate instantaneous energy in each inductor, accumulated energy dissipated in each resistor and the load power at each microsecond.

Cylindrical Switch Results

Table 1 summarizes the seven cylindrical switch tests done in this study. Three tests had results which permitted a complete analysis of the switch performance. CYL3, CYL4 and CYL5 showed the effects of the two different pusher media with the same explosive weight and the effects of the same pusher medium with different explosive weights.

Table 2 summarizes switch and load currents for times t_1 and t_2 shown in Figures 14 and 15.

Points t_1 and t_2 in Figures 14 and 15 were obtained by noticing significant changes in the plotted curves. Points 1 and 2 in Figure 14 shows sharp drop in $\dot{I}_s$ and an increase in $\dot{I}_{L3}$. This indicates that the conductor is being cut at the first cutting ring and a small resistance results. Points 3 and 4 show another decrease in $\dot{I}_s$ and a sharp increase in $\dot{I}_{L3}$. This indicates that a larger resistance is occurring in the switch. This time, t_1, is assumed to be the end of the switch delay where the conductor is ruptured at all the cutting rings. Points 5 and 6 in Figure 14 show the peaks of $\dot{I}_s$ and $\dot{I}_L$. This indicates that I_s is dropping sharply and that I_{L3} is rising at its greatest rate. The arc is being cooled rapidly at this point. At point 7 as shown in Figure 15 I_{L3} is at a peak and I_s is zero indicating that the switch is completely open. This point is labeled

TABLE II

Cylindrical Switch Current Switching Characteristics

Switch	t_{delay} (μsec)	Δt (μsec)	t_1				t_2			
			I_s (KA)		I_{L3} (KA)		I_s (KA)		I_{L3} (KA)	
			Meas.	Calc.	Meas.	Calc.	Meas.	Calc.	Meas.	Calc.
CYL3	68	36	75.35	--	17.07	--	.29	--	32.63	43.07
CYL4	87	36	102	--	10.74	--	.50	--	47.07	53.20
CYL5	82	34	101	--	15.08	--	1.37	--	58.76	62.63

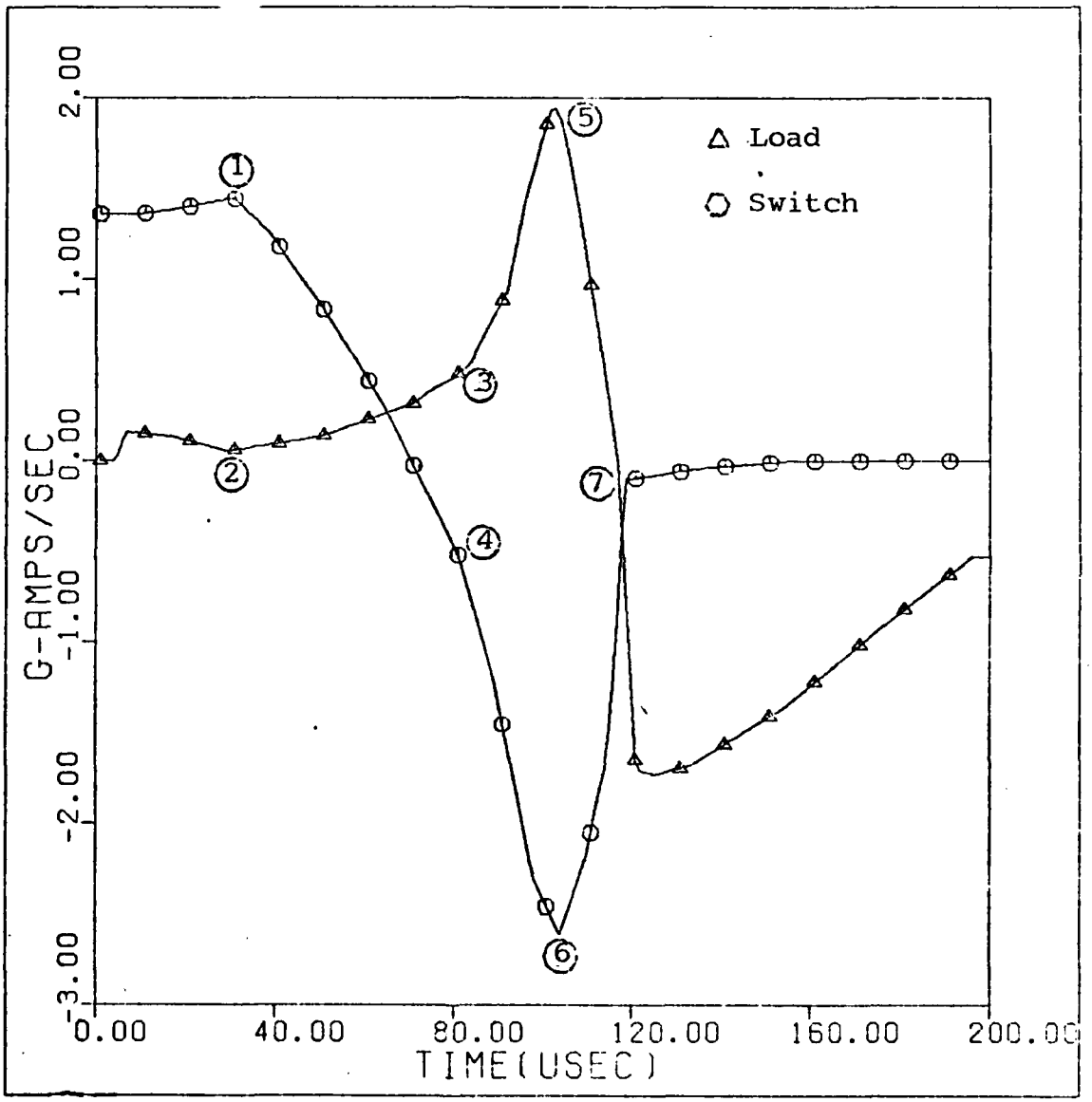

Fig. 14 Plot of Switch C5 Current Derivatives

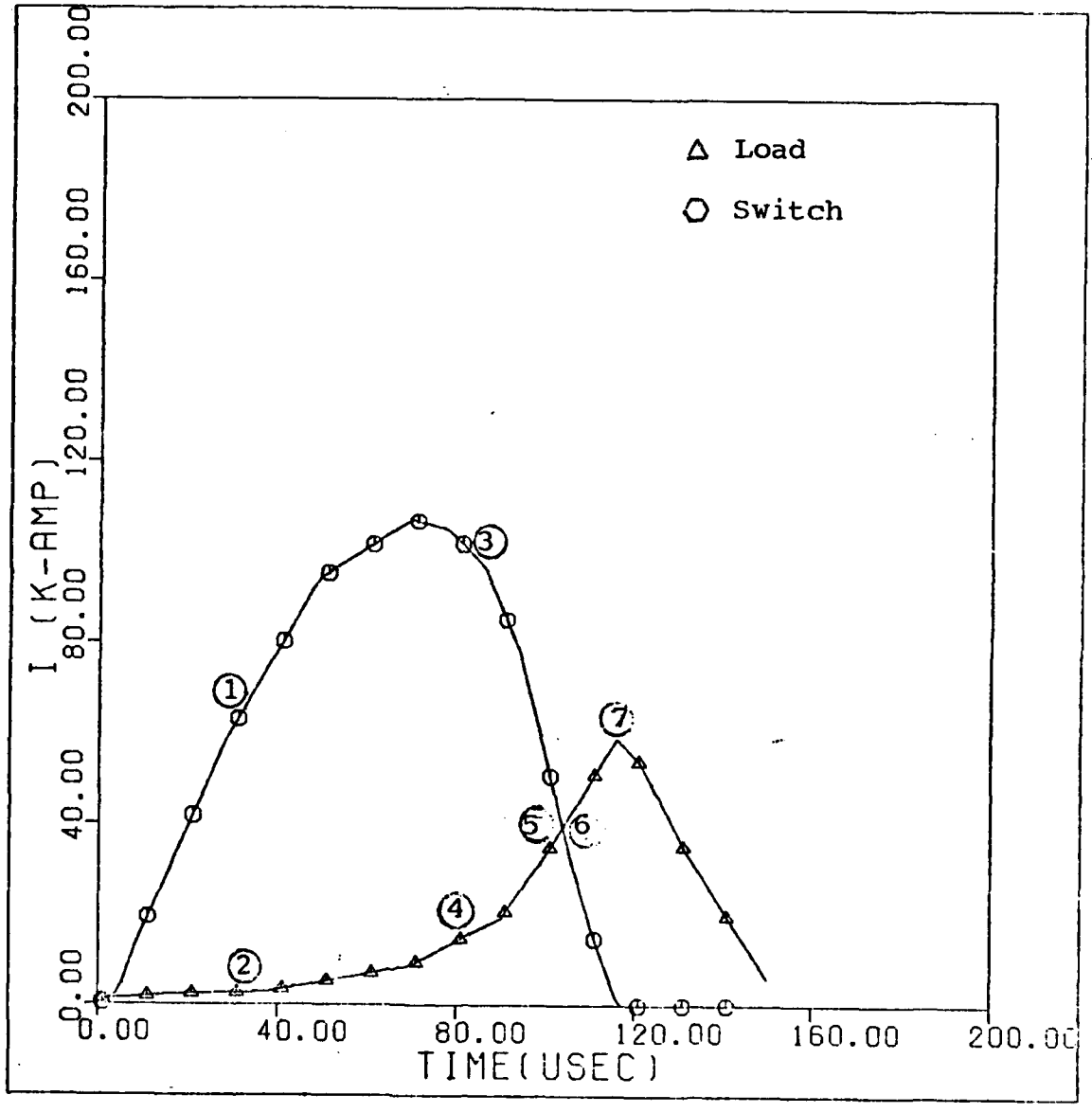

Fig. 15 Plot of Switch C5 Currents

TABLE III

Cylindrical Switch Energy Distribution

SWITCH	$W_{L1}(t_1)$ (KJ)		$W'_{L1}(t_2)$ (KJ)		$W'_{L3}(t_2)$ (KJ)		$W_{DISS}(t_2)$ (KJ)		Peak Load Power (MW)
	Meas.	Calc.	Meas.	Calc.	Meas.	Calc.	Meas.	Calc.	
CYL3	16.67	19.59	3.74	6.70	.857	1.49	13.54	5.41	48.08
CYL4	44.37	26.37	7.81	9.76	1.78	2.28	12.21	10.04	334.37
CYL5	66.97	50.62	18.04	19.57	2.78	3.15	9.19	10.07	322.50

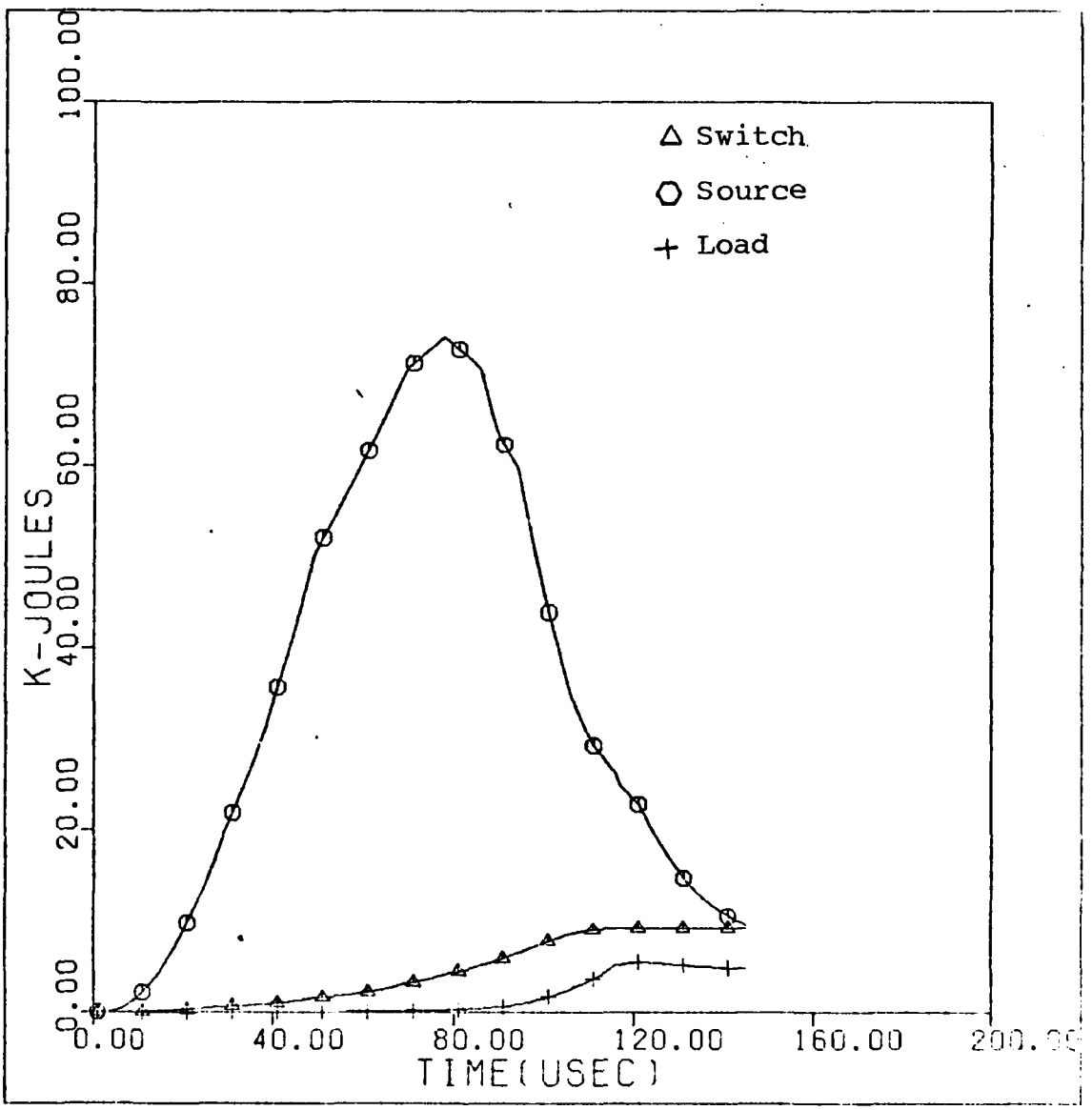

Fig. 16 Plot of Switch C5 Energy Distribution

t_2 and the opening time of the switch, Δt, is taken to be the difference between t_2 and t_1.

Switch delay times, t_{delay}, and opening times, Δt, are shown in Table 2 for each switch.

Table 3 shows the energy distribution at the end of switching, t_2. The peak load power, calculated from load current and switch voltage, shows the energy transfer.

The measured values of energy for the storage inductor, the switch and the load were obtained from Figure 16. Calculated values for these energies were obtained by using equations (25), (26) and (17).

Plots of I, $\dot{I}$, V, R, W and P were produced for each switch tested and are contained in the Appendix.

Planar Switch Results

Twelve planar switches were tested. Each of these tests and the significant test conditions are summarized in Table 4. Six of these tests were chosen for analysis. The Mod 2 switch (P6) and the single good Mod 1 (P5) switch were analyzed to compare any differences caused by the different channel end baffles. Mod 3, number 1, (P8) was selected as a representative test with 100 gr/ft. detonator cord. Mod 3, number 3, (P10) was chosen as the single good test at 175 gr/ft. or 210 KA. P13 and P14 were chosen to represent the 290 KA tests. Since these switches each had a misfire in one section, they were undersized for the voltage that would be generated during opening. Two similar tests were analyzed to provide a comparison with these conditions.

TABLE IV

Planar Switch Test Summary

SWITCH TEST NO.	MOD NO.	COMMENT	DET CORD gr/ft.	STORAGE INDUCTANCE μH	CHARGE VOLTAGE KV	I_{pK} KA	LOAD RESISTANCE mΩ	TRIGGER DELAY μs
P1	1	Short	-	6.3	20	140	-	
P2	1	Short	-	6.3	20	140	-	
P3	1	Prefire	50	6.3	20	140	None	
P4	1	Poor	50	6.3	20	140	None	
P5	1	Good	50	6.3	20	140	18	30
P6	2	Good	50	6.3	20	140	21	30
P7	3	Short	-	6.3	20	140	-	
P8	3	Good	100	6.3	20	140	120	55
P9	3	3 Channel	100	6.3	30	210	120	
P10	3	Good	175	6.3	30	210	120	59
P11	3	3 Channel	175	3.25	30	290	120	
P12	3	Prefire	175	3.25	30	290	120	
P13	3	3 Channel	175	3.25	30	290	50	38
P14	3	3 Channel	175	3.25	30	290	50	38
P15	3	2 Channel	175	3.25	30	290	50	

Tables 5, 6 and 7 summarize the results of the analysis of these six tests. The last three columns of Table 5 are determined from a plot of switch resistance and voltage. An example is in Figure 17. The initial resistance rise is taken from the point where the resistance first starts sharply upward and the point where the resistance first changes to a reduced rate. In Figure 17 this is the slope between point 1 and point 2. Each of the switches showed a restrike of the arc, as evidenced by the reduction in resistance and voltage after point 2. The time between the point where the resistance first starts to rise (point 3 in Figure 17) and where the rate of resistance rise decreases is given as time to breakdown in Table 5. The voltage at this time is divided by the number of sections fired to determine section breakdown voltage.

The current relationships during switching are shown in Table 6. The delay time is the period between the triggering delay of the switch and the time when the switch current begins to decrease. The switching interval, Δt, is taken from the peaks of the switch and load currents. In Figure 18, point 1, at 59 μsec, represents the time when the switch was detonated. Point 2, at 69 μsec, is the time (t_1) where the switch current begins shifting to the load. The difference in these times is the switching delay. The time to the load current peak (t_2) at point 3 is used as the switching interval. Switch currents are taken from the curves at t_1 and t_2. Load current is read from the curve at t_2 and calculated from equation (23).

TABLE V

Planar Switch Resistance and Voltage Characteristics

SWITCH NUMBER	PEAK CURRENT KA	EXPLOSIVE WEIGHT gr/ft	NO. OF SECTIONS	INITIAL RESISTANCE RISE(mΩ/μs)	TIME TO BREAKDOWN μs	SECTION VOLTAGE AT BREAKDOWN KV
P5	97	50	4	41	5	3.7
P6	95	50	4	45	5	3.7
P8	122	100	4	60	7	6.9
P10	185	175	4	117	4	12.5
P13	263	175	3	29	4	13.7
P14	248	175	3	26	4	10.0

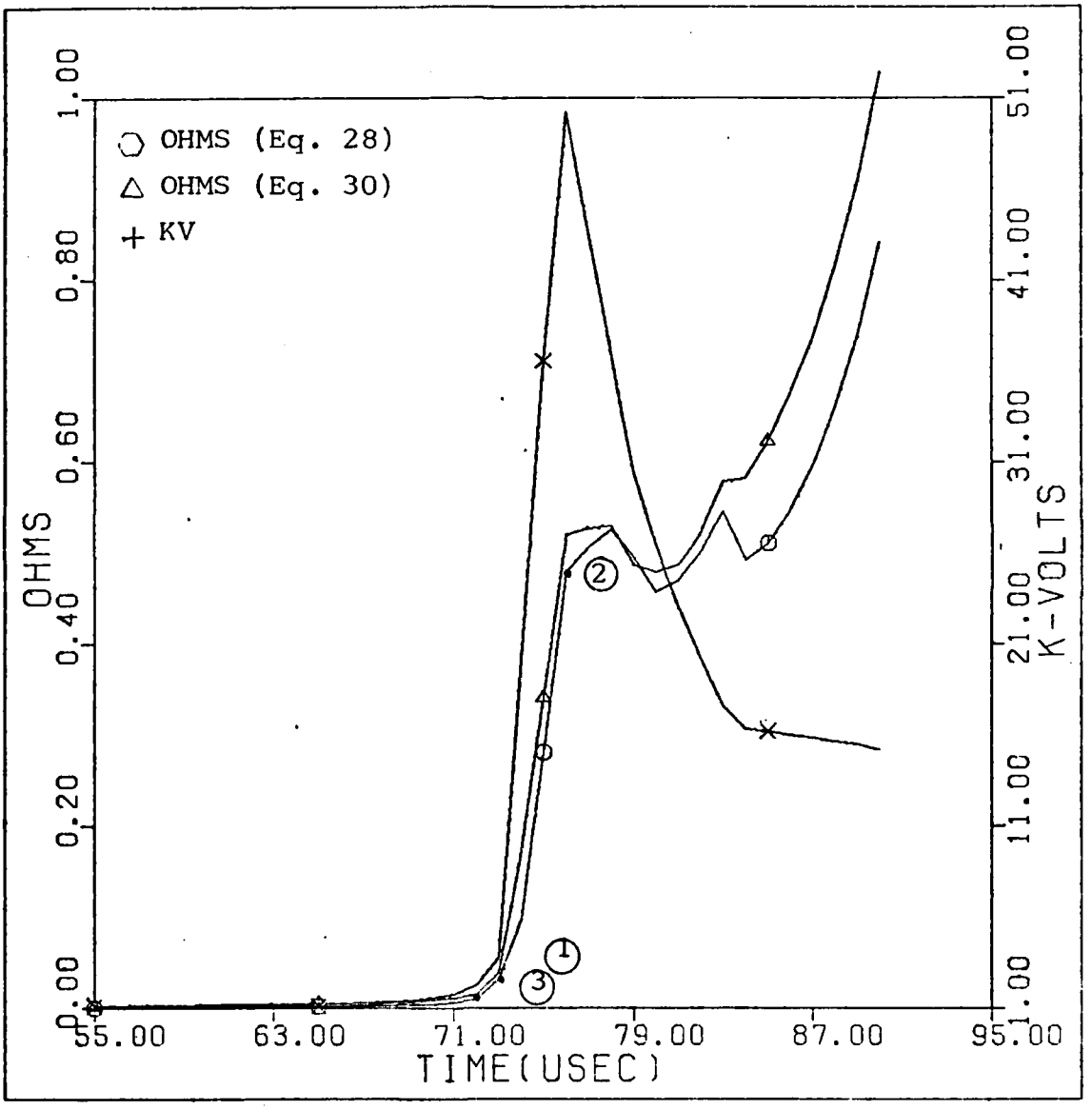

Fig. 17 Plot of Switch P10 Resistance and Voltage

TABLE VI

Planar Switch Current Characteristics

SWITCH NUMBER	DELAY TIME μs	SWITCHING TIME (Δt) μs	MEASURED SWITCH CURRENT KA		PEAK LOAD CURRENT I_{Lp} (KA)	
			t_1	t_2	Measured	Calculated
P5	16	33	94.5	95.6	25.1	56.5
P6	15	36	97.3	1.9	90.8	57.1
P8	12	17	122.0	15.1	79.6	70.1
P10	10	15	185.2	30.5	120.4	109.5
P13	8	15	263.4	69.8	106.5	151.2
P14	8	20	248.1	63.5	119.1	132.4

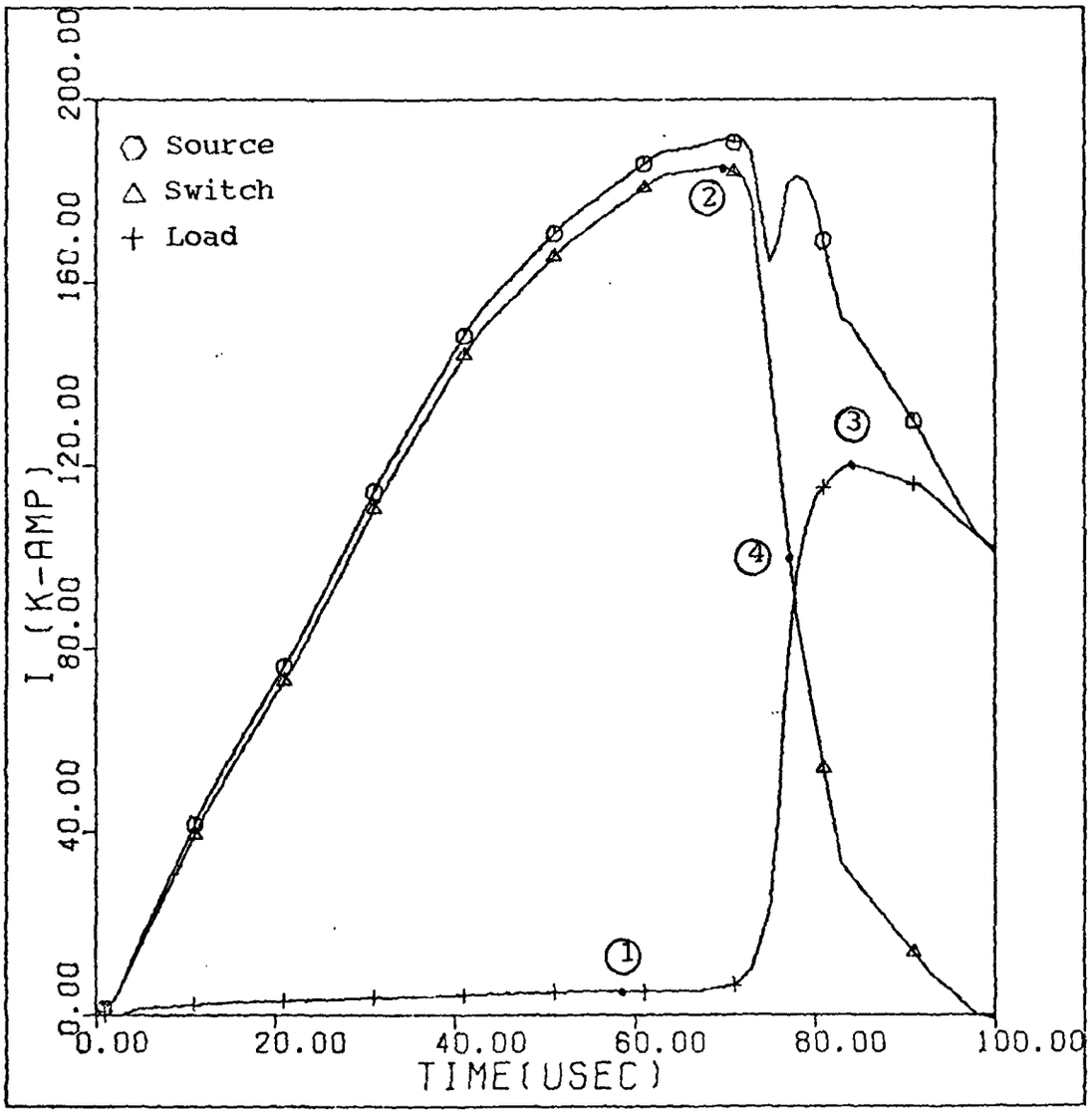

Fig. 18 Plot of Switch P10 Currents

TABLE VII

Planar Switch Energy Distributor

SWITCH NUMBER	STORAGE INDUCTOR ENERGY			PEAK LOAD INDUCTOR ENERGY $W_{L3}(t_2)$ KJ		SWITCH ENERGY $W_{DISS}(t_2)$ KJ		PEAK LOAD POWER MW
	$W_{L1}(t_1)$	$W_{L1}(t_2)$ KJ						
		Measured	Calculated	Measured	Calculated	Measured	Calculated	
5	36.9	49.4	10.8	0.7	3.3	19.9	11.1	176
6	46.9	29.1	11.1	8.6	3.4	11.0	14.1	545
8	55.1	15.1	16.7	5.4	4.2	13.0	15.1	1117
10	124.5	77.4	40.8	12.3	10.2	33.1	34.1	3572
13	131.0	52.8	38.9	4.2	8.6	27.4	42.9	2349
14	126.9	63.5	29.8	5.3	6.6	27.8	41.6	1688

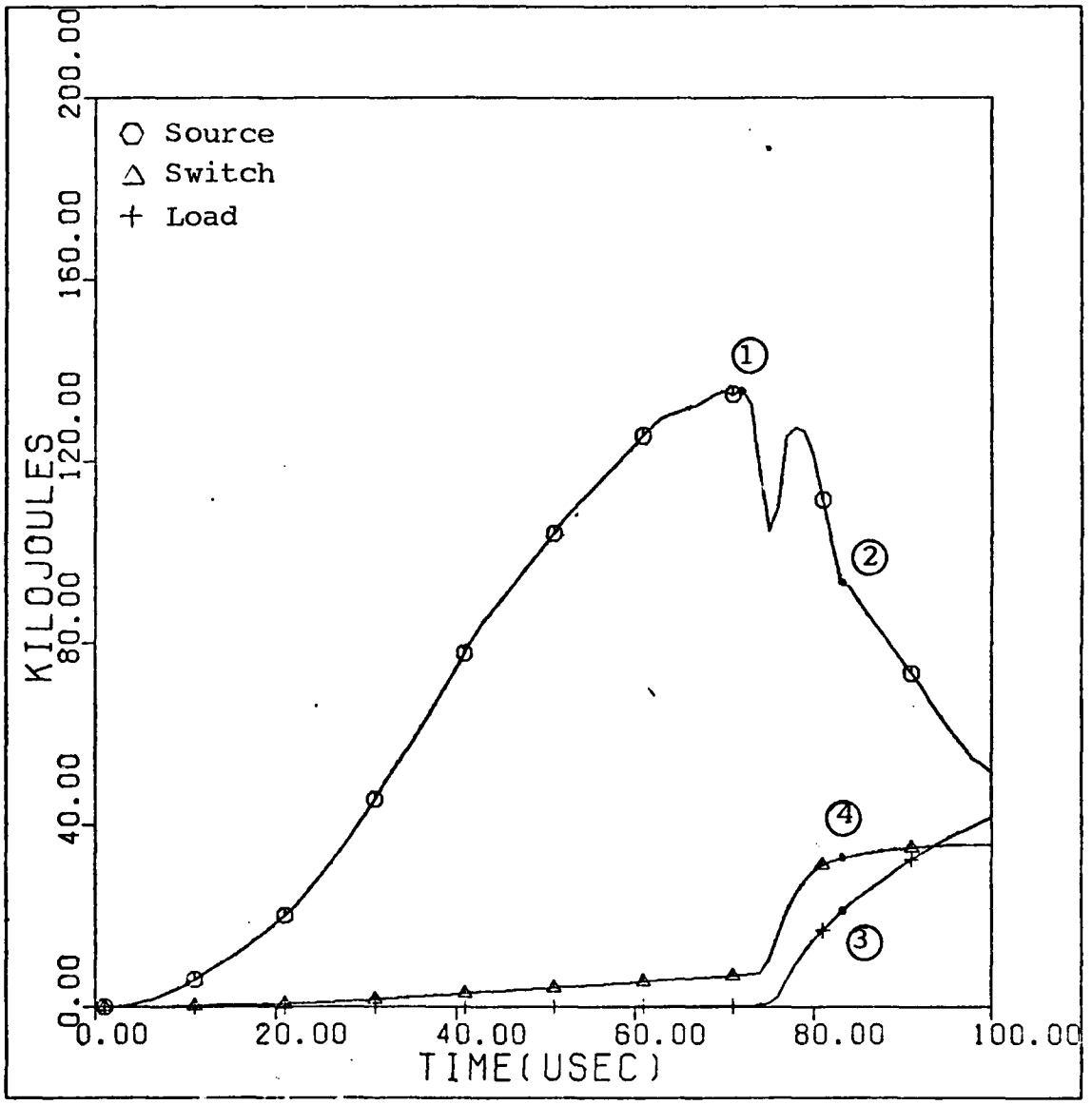

Fig. 19 Plot of Switch P10 Energy Distribution

Table 7 shows the energy distribution at t_2. The peak load power is included as an indication of the effectiveness of the energy transfer. This value is calculated from load current and switch voltage. The storage inductor energy at t_1 is read from point 1 in Figure 19. The energies in the source inductor, load inductor and switch at time t_2 are read from Figure 19 at points 2, 3 and 4. These energies were calculated using equations (25), (26) and (17) and listed for comparison.

Plots of I, $\dot{I}$, V, R, W and P were produced for each switch analysis. These plots are in the appendix.

Conclusions

Both switches demonstrated good switching characteristics. The cylindrical switch was not able to switch more than a few hundred megawatts to the load. The resistance rose faster and interrupted higher currents than have any switches of similar configuration which have been reported (Ref 2). The planar switch tests indicate that this configuration can be competitive with fuse opening switches. When scaled properly, the planar switch should be able to conduct higher currents and open on command very quickly.

Cylindrical Switch. Table 2 shows values of delay time and opening time for each switch tested. CYL3 shows the shortest delay time. This can be attributed to the fact that the 100 gr/ft. detonator cord formed the conductor properly around the bending ring, while the 175 gr/ft. detonator cord tore the conductor at each bending decreasing the

effective arc length between rings. Opening times for each switch were fairly constant indicating that both pusher media cool the arc at the same rate.

Planar Switch. The first two experiments showed that there was little difference between the performance of the tabs and the end blocks. P5 was a Mod 1 switch with tabs at the ends of the channels. P6 was the Mod 2 switch which was the first to use the removable end plugs. The current and voltage characteristics were nearly identical.

The next two tests, P8 and P10 show that the switch performance improves dramatically with increased explosive weight. The best experiment showed a 117 mΩ/μsec resistance rise and a holdoff voltage of 12.5 KV/section.

The delay time for the two 50 gr/ft. tests were longer than the 10.9 μsec predicted in Chapter III. This indicates that the force from the 50 gr/ft. cord needs some time to tear through the 10 mil aluminum conductor. The 100 and 175 gr/ft. tests showed proportionate decreases in the delay time. The 175 gr/ft. cords opened the conductor before the burning was completed. These shots were at increasingly higher currents. This indicates that the increased current at the ends of the switch sections was sufficient to vaporize part of the conductor before it could be torn by the explosive. These switches showed considerable evidence of arcing at the corners of the opened conductors. The center sections were blackened from the detonator cord residue. The corners showed whitened aluminum, indicating a large arc in that region.

The energy predictions appear to give reasonable results if the switching is complete. A condition for the equations in Chapter III was that the load current at t_1 and the switch current at t_2 both be zero. This never occurred since the switches arced over before switching was complete.

Recommendations

Tests of the planar switch are continuing at AFWL. Several specific aspects of these switches should be investigated further.

Zubkov (Ref 6) has experimented with explosive mixtures containing particles of various insulating materials. Some improvement in arc quenching was observed with the insulating particles in the explosive mixtures. A test with standard detonator cord wrapped in teflon tape could accomplish this effect and should be tested.

Scaling experiments should be attempted to investigate the possibility of combining the ruptured conductor characteristics with those of fuses. Quenching media such as glass beads could be placed in the explosive channel. This method is often used for fuses and may improve the switching time. The tests with a 6 in. wide conductor indicate that the conductor may have been partially vaporized by the increased current density. For example, switch P13, interrupting 263 KA, opened in 8 μsec. This is 2.9 μsec before the 10.9 μsec required for the detonator cord to burn, indicating that about one-fourth of the conductor vaporized. This is about 1.5 in. for the 6 in. conductors used. Experiments could be

conducted with reduced conductor widths to better define this effect.

Tests should be performed with additional sections to provide the necessary 10 KV/section voltage protection. This should improve the switching time.

Bibliography

1. Rose, M. F. and A. K. Hyder, Jr. "Opening Switches - Scenarios for Their Use," Workshop on Diffuse Discharge Opening Switches. Workshop notes, January 13-15, 1982. Lubbock, Texas: Texas Tech University, April 23, 1982. (AD A115883).

2. Ford, R. D. and Ihor M. Vitkovitsky. Explosively Actuated 100 kA Opening Switch for High Voltage Applications. NRL Memorandum Report 3561. Washington, D.C.: Naval Research Laboratory, July 1977.

3. Plansey, Robert and Robert E. Collin. Principles and Applications of Electromagnetic Fields. New York: McGraw-Hill Book Company, 1961.

4. Bebie, Jules. Manual of Explosives, Military Pyrotechnics and Chemical Warfare Agents. Boulder, Colorado: Paladin Press. (Tp 270 B37).

5. Ford, R. D. and Ihor M. Vitkovitsky. High Recovery Voltage Switch for Interruption of Large Currents. Unpublished report, Naval Research Laboratory, Washington, D.C., January 11, 1982.

6. Zubkov, P. I. et.al. "Quenching of a Developed Arc Through Shock Compression By Explosive Products," Journal of Applied Mechanics and Technical Physics, 22(5): 701-705 (March, 1982).

7. Schwab, Adolf J. High Voltage Measurement Techniques. Cambridge, Massachusetts: The M.I.T. Press, 1972.

8. Maisonnier, Ch. et. al. "Rapid Transfer of Magnetic Energy by Means of Exploding Foils," The Review of Scientific Instruments, 37(10): 1380-1394 (October 1966).

9. Reinovsky, Robert E, Research Physicist. Personal Correspondence. Air Force Weapons Laboratory, Kirtland AFB, N.M., December 1, 1982.

Appendix

The curves of the measured and calculated data used for the analysis in Chapter VI are presented herein. There are five figures for each of the three cylindrical switches and six planar switches which were analyzed. The currents, current derivatives and voltage were measured during each test. The resistance, energy and power were calculated from the measured values. The constant circuit parameters shown in Figure 2 of the text are listed in Table VIII below for each test.

TABLE VIII

Measured Constant Circuit Parameters

SWITCH	INDUCTANCES (μH)			RESISTANCES (μΩ)	
	L1	L2	L3	R1	R3
C3	6.9	0.6	1.61	9.6	100
C4	6.9	0.6	1.61	9.6	100
C5	9.98	0.6	1.61	9.6	50
P5	6.78	0.45	2.08	9.17	17.3
P6	6.78	0.45	2.08	9.17	17.3
P8	6.8	0.5	1.7	9.1	110.7
P10	6.8	0.5	1.7	9.1	110.7
P13	3.4	0.5	0.75	8.31	48.3
P14	3.4	0.5	0.75	8.31	48.3

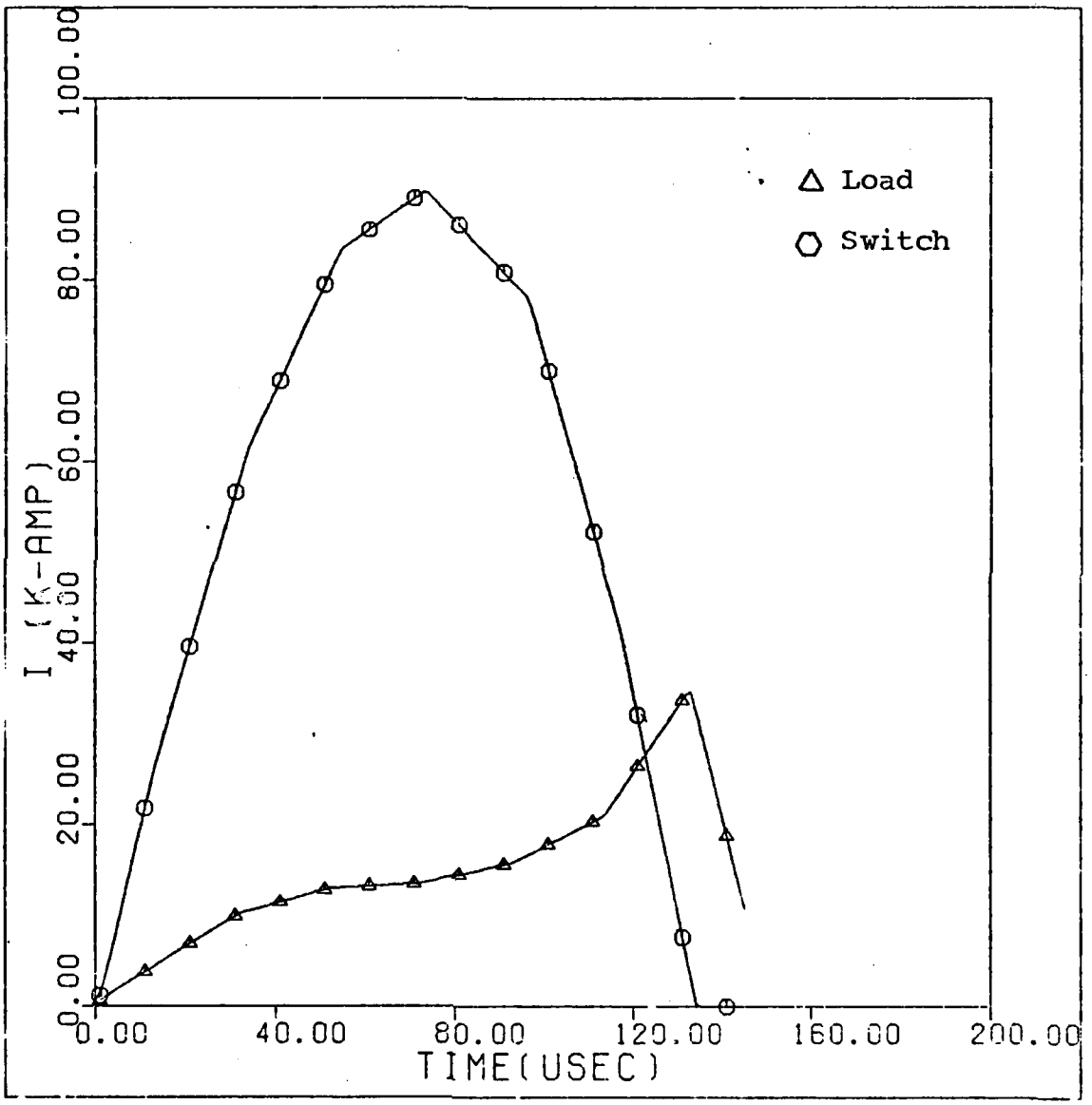

Fig. 20 Switch C3 Currents

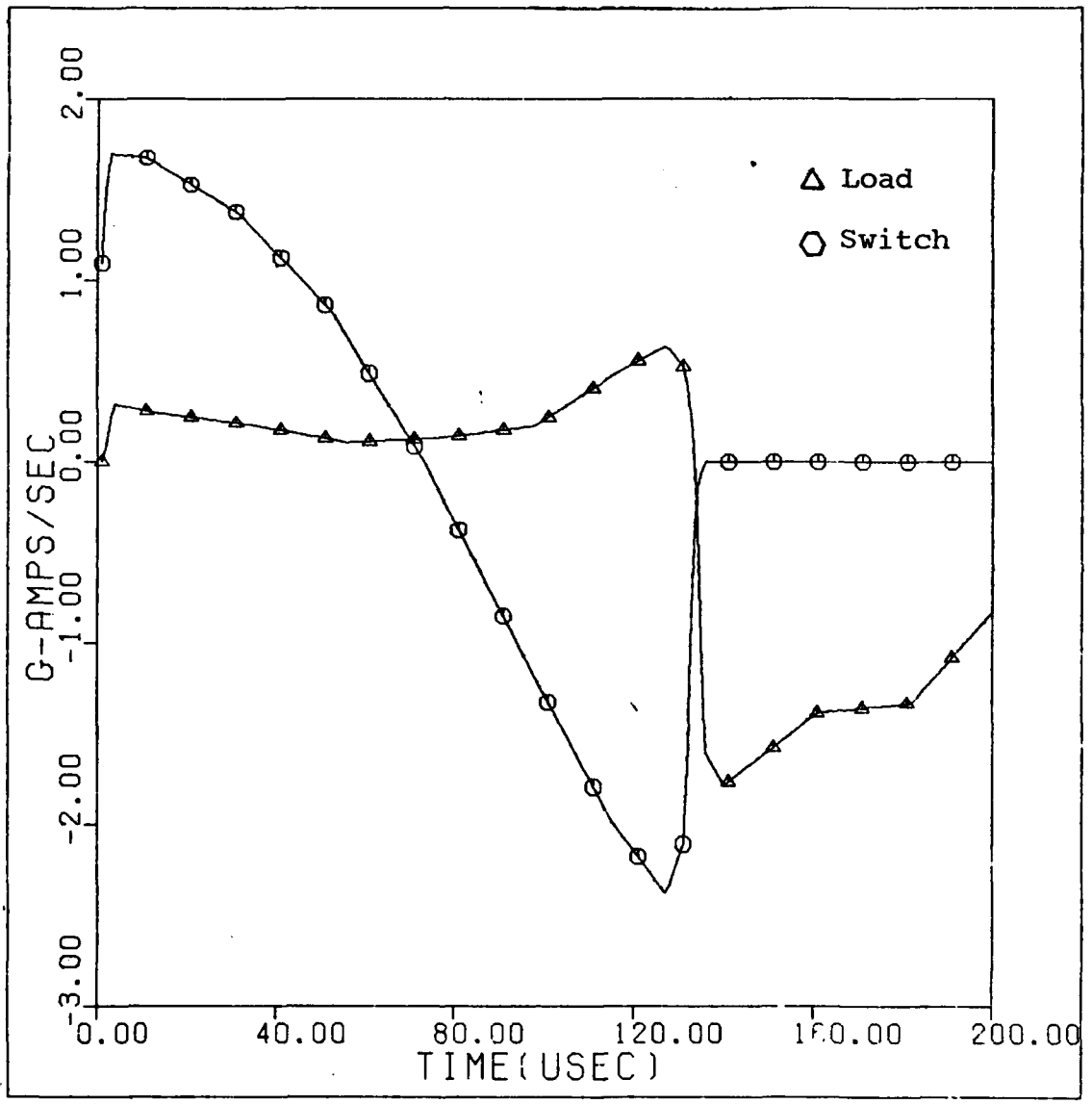

Fig. 21 Switch C3 Current Derivatives

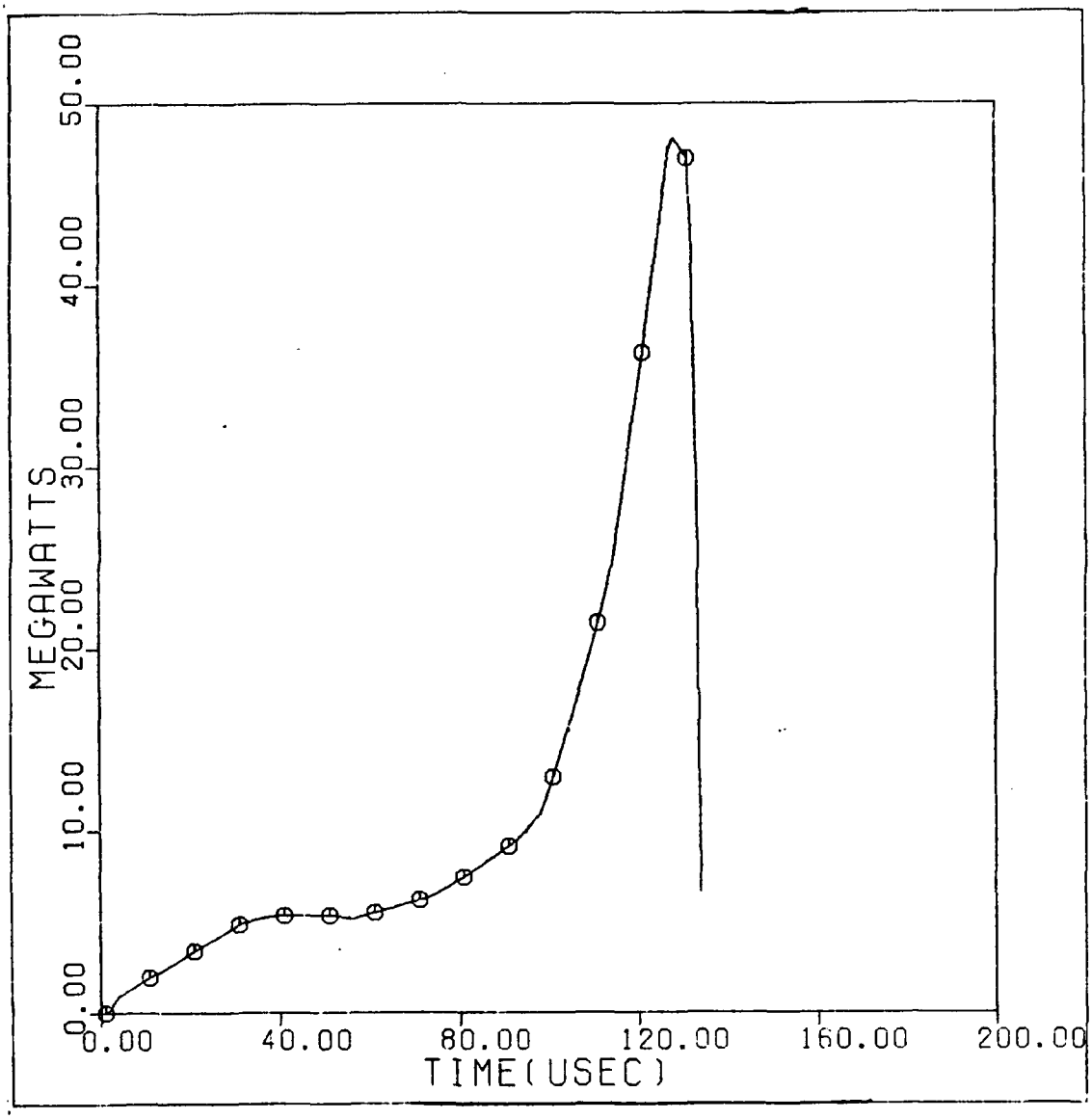

Fig. 22 Switch C3 Load Power

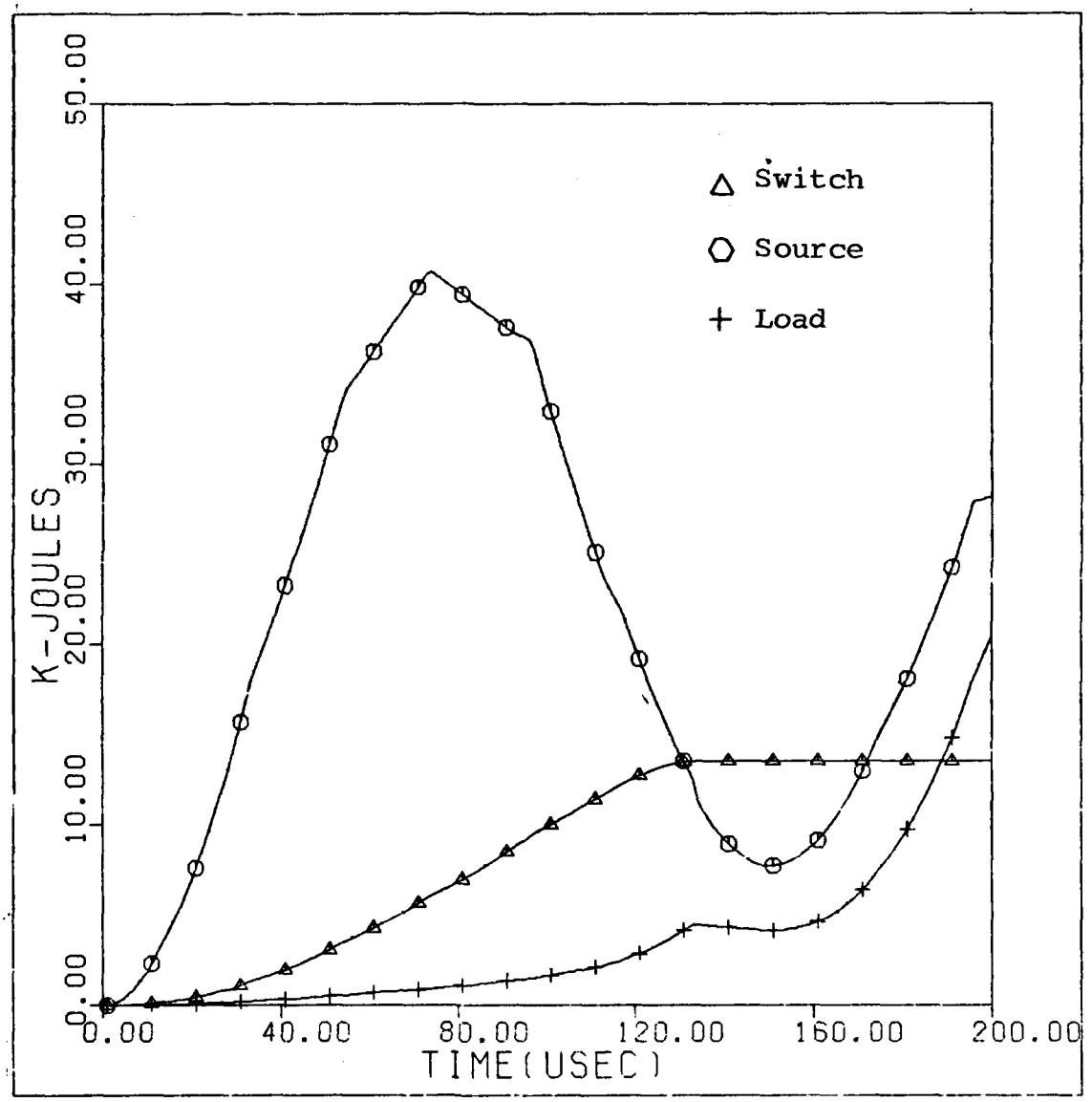

Fig. 23 Switch C3 Energies

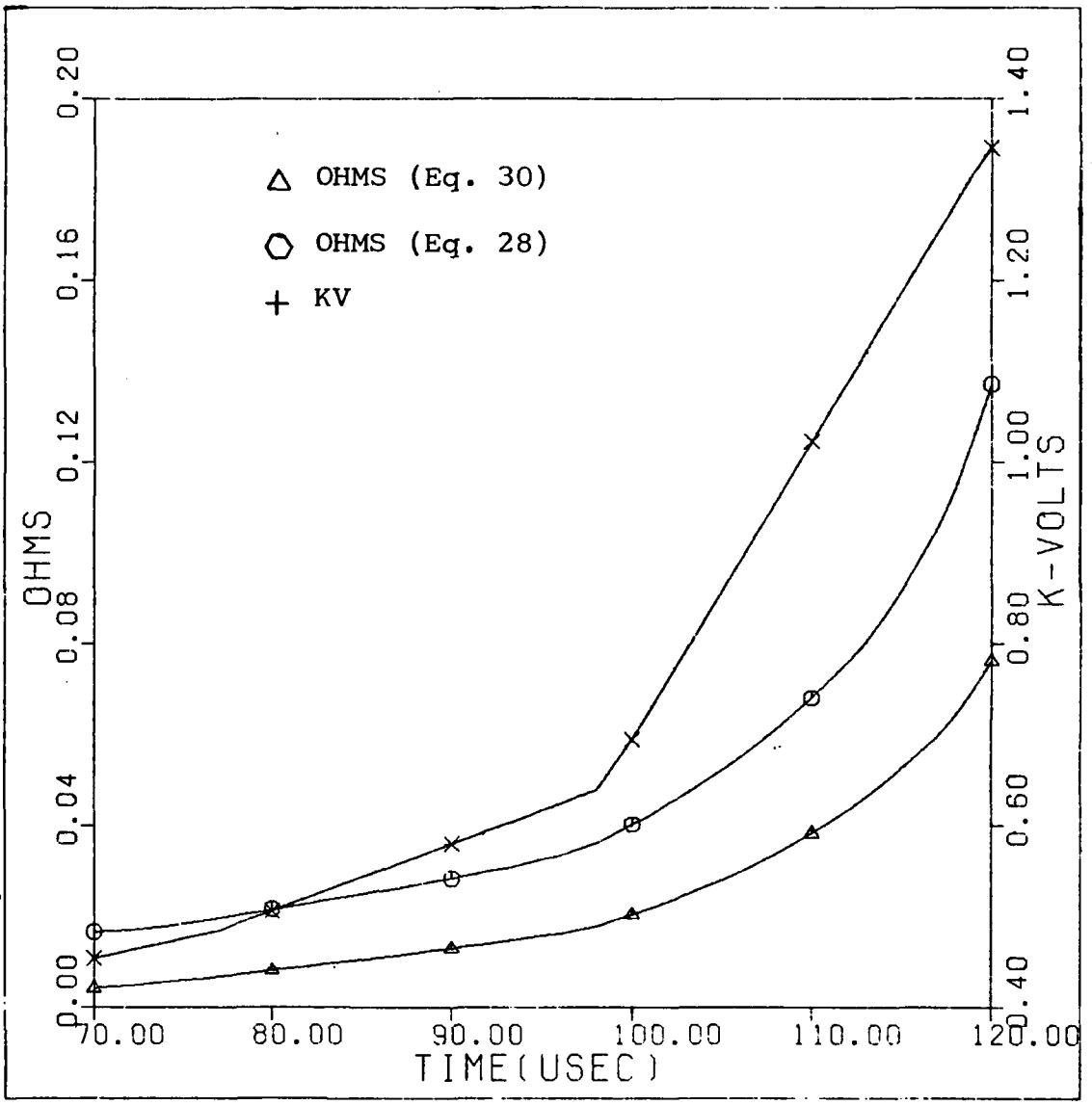

Fig. 24 Switch C3 Resistance and Voltage

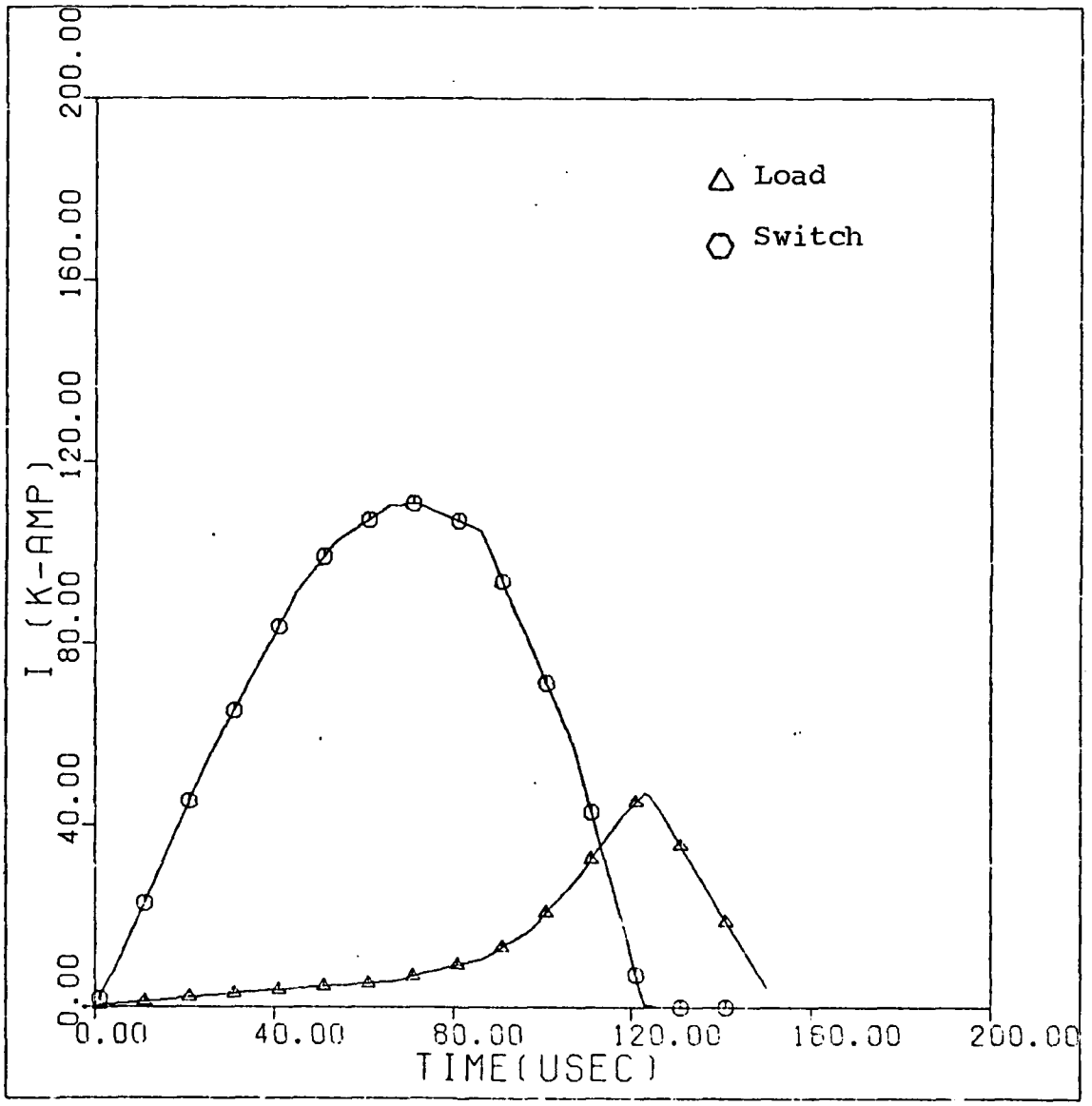

Fig. 25 Switch C4 Currents

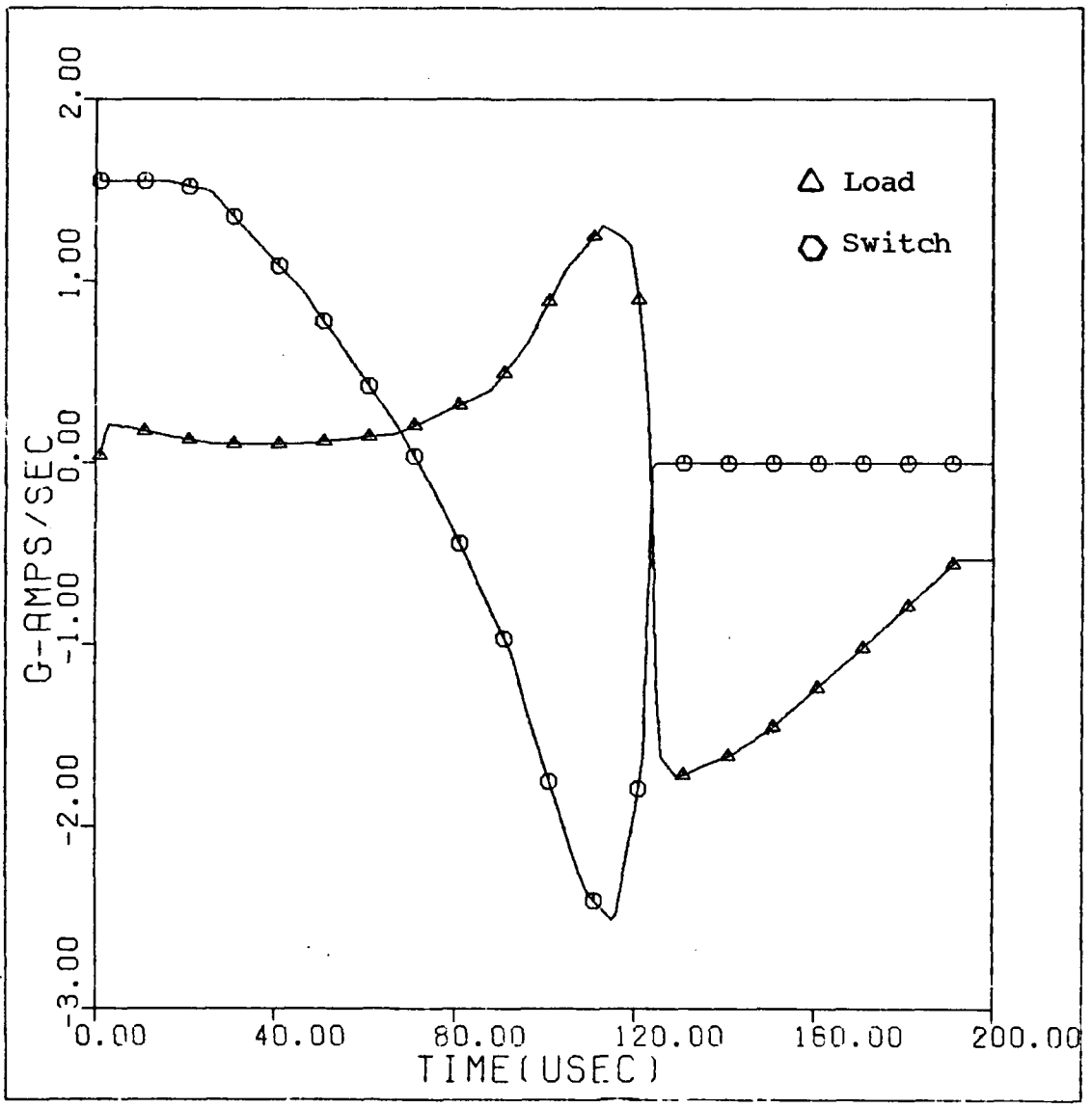

Fig. 26 Switch C4 Current Derivatives

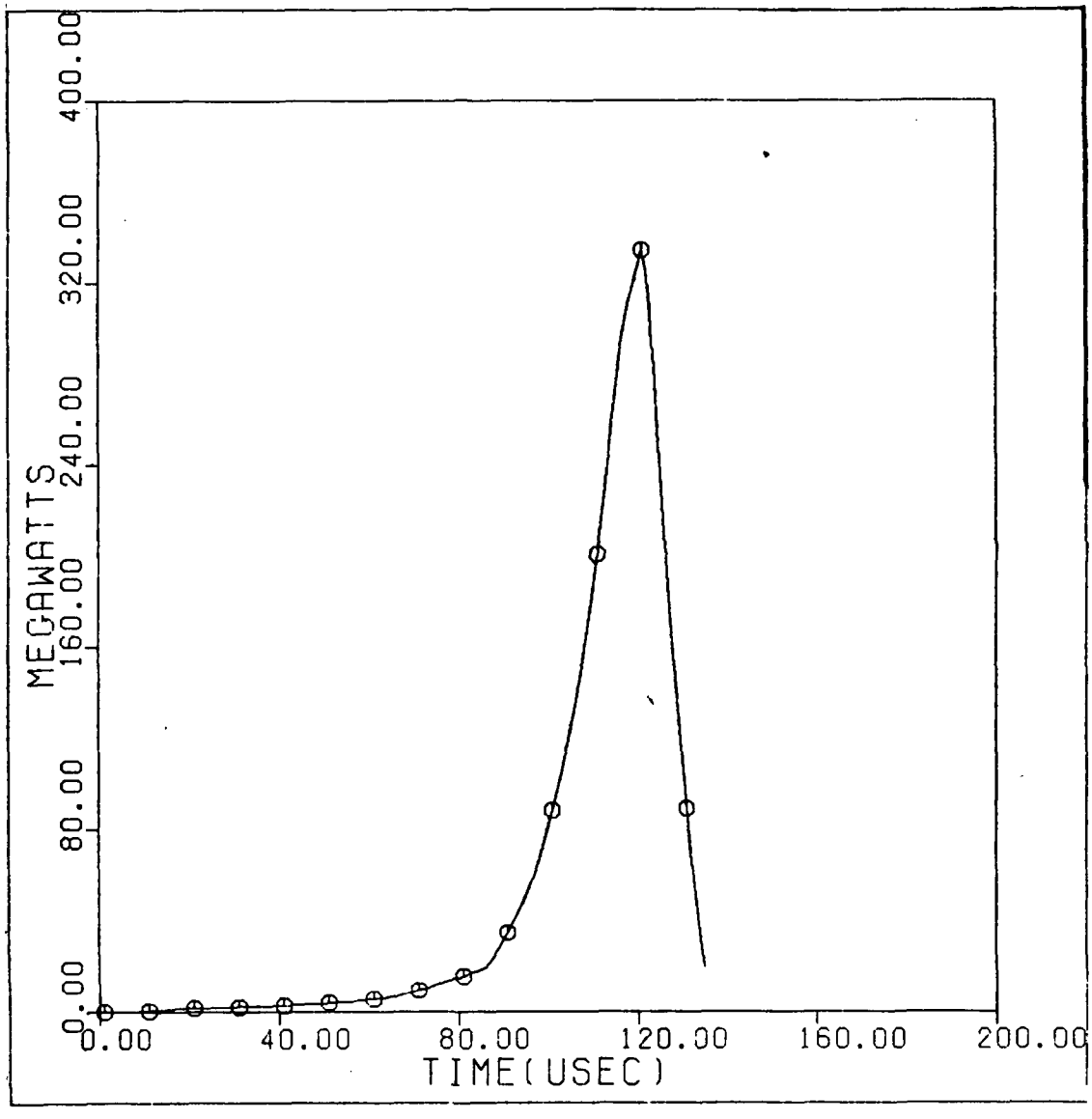

Fig. 27 Switch C4 Load Power

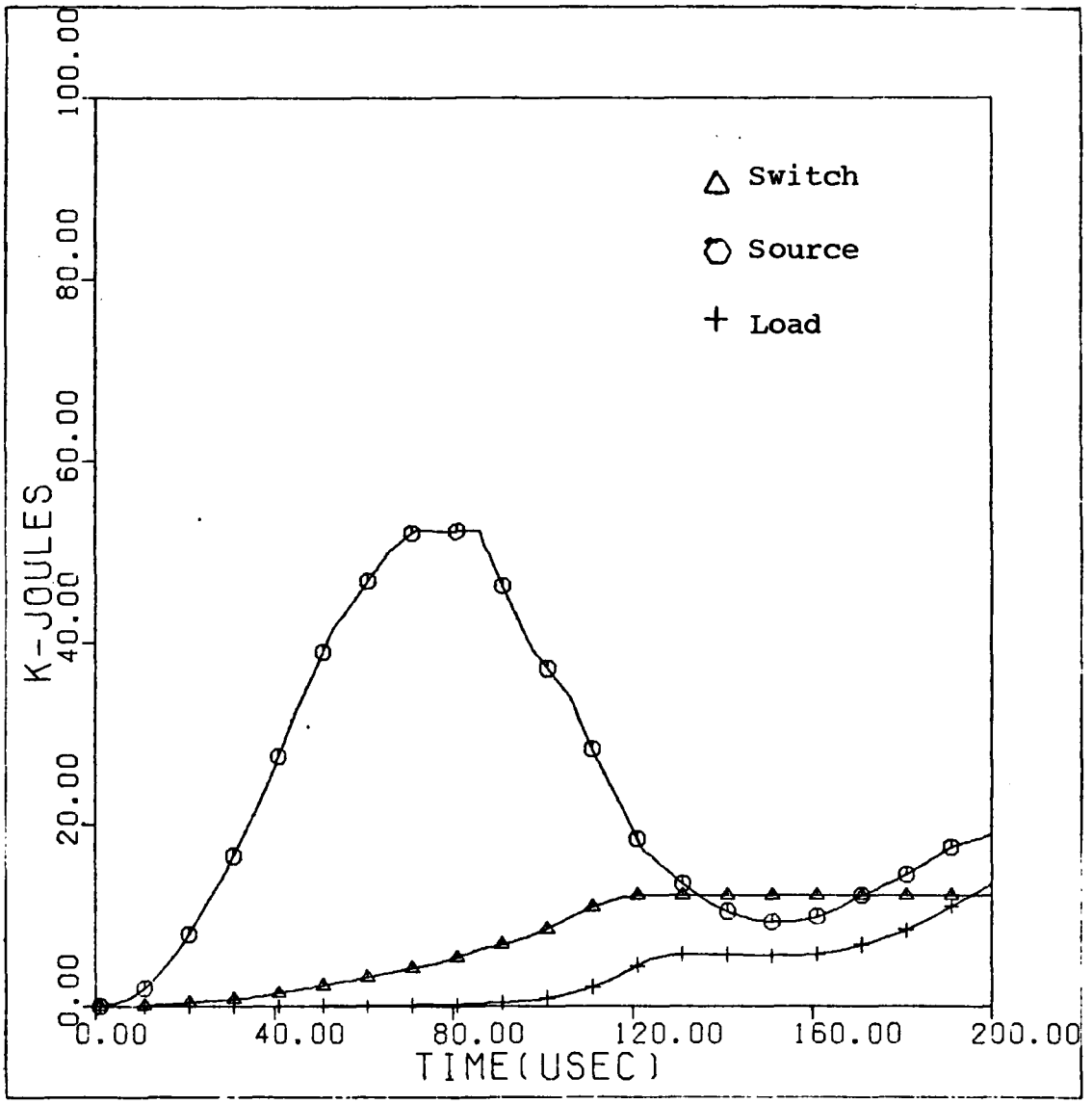

Fig. 28 Switch C4 Energies

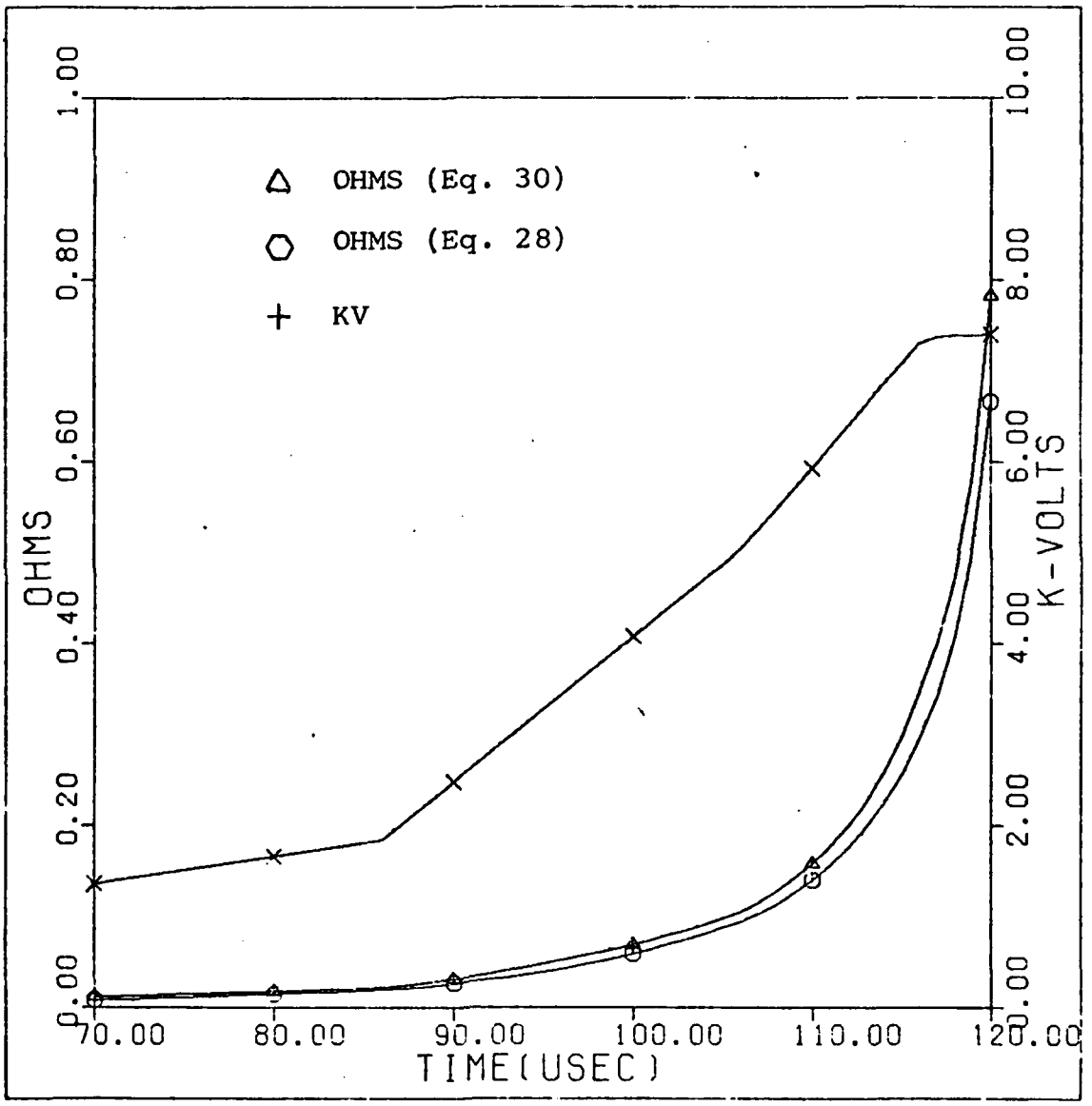

Fig. 29 Switch C4 Resistance and Voltage

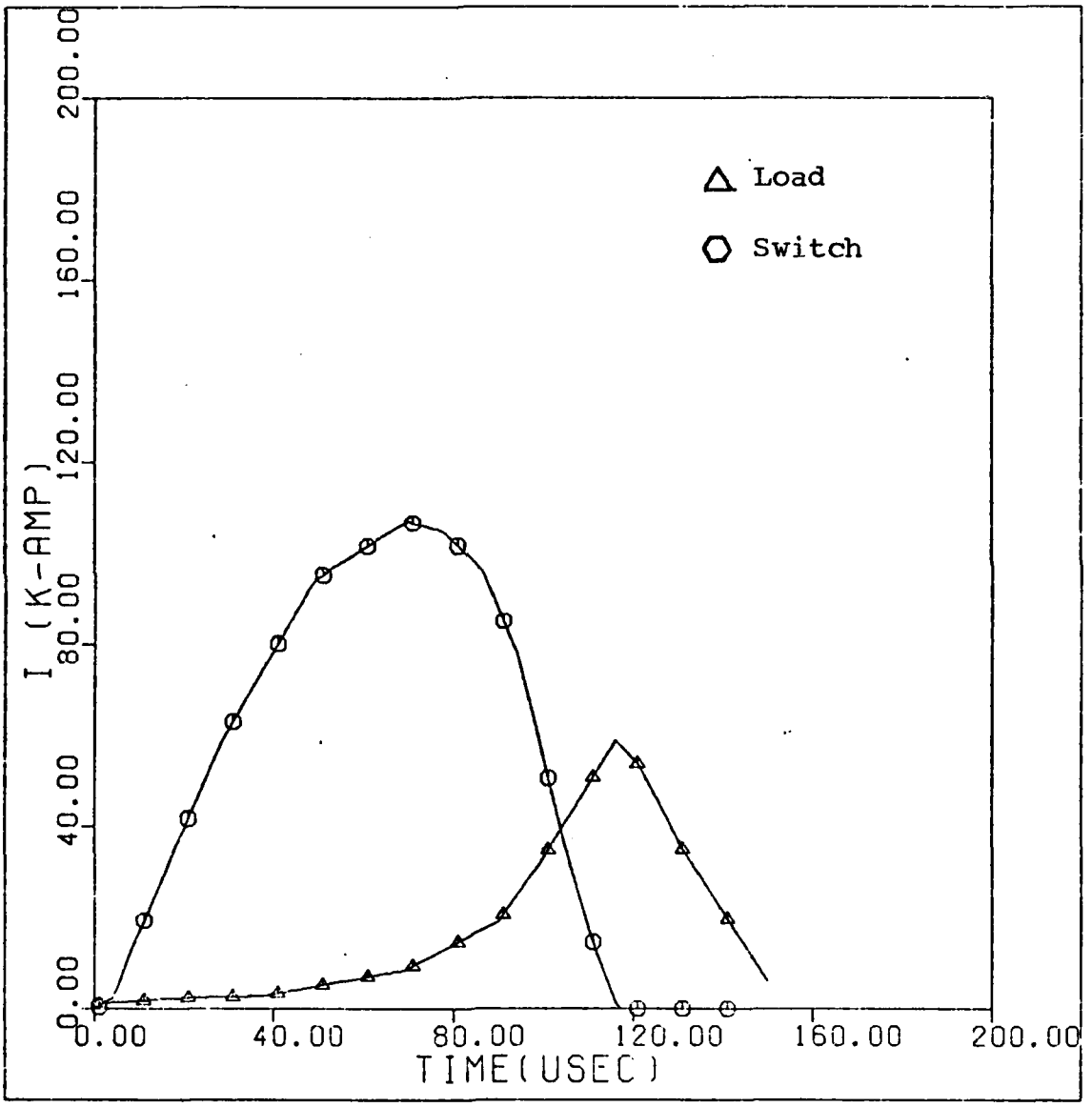

Fig. 30 Switch C5 Currents

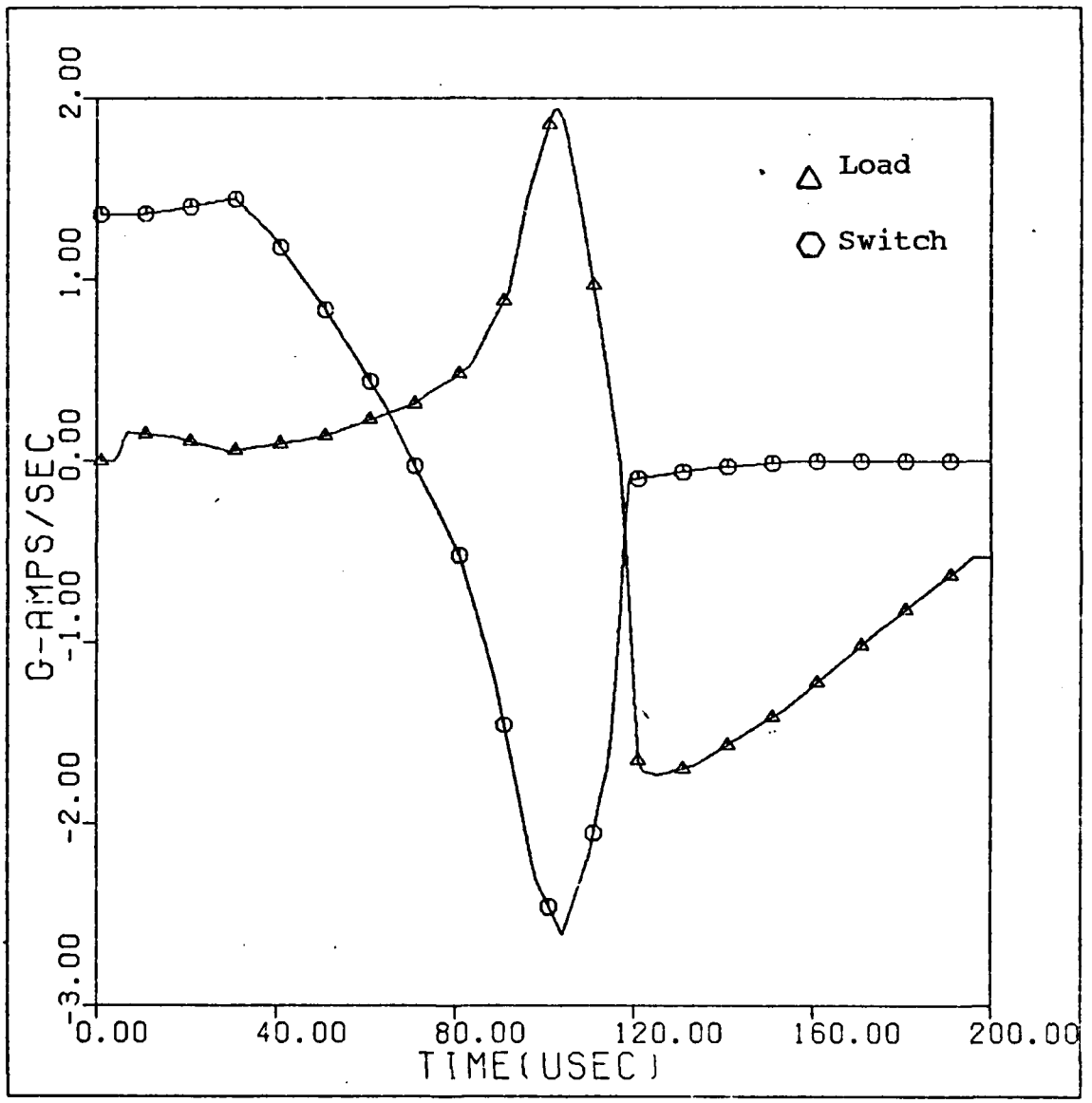

Fig. 31 Switch C5 Current Derivatives

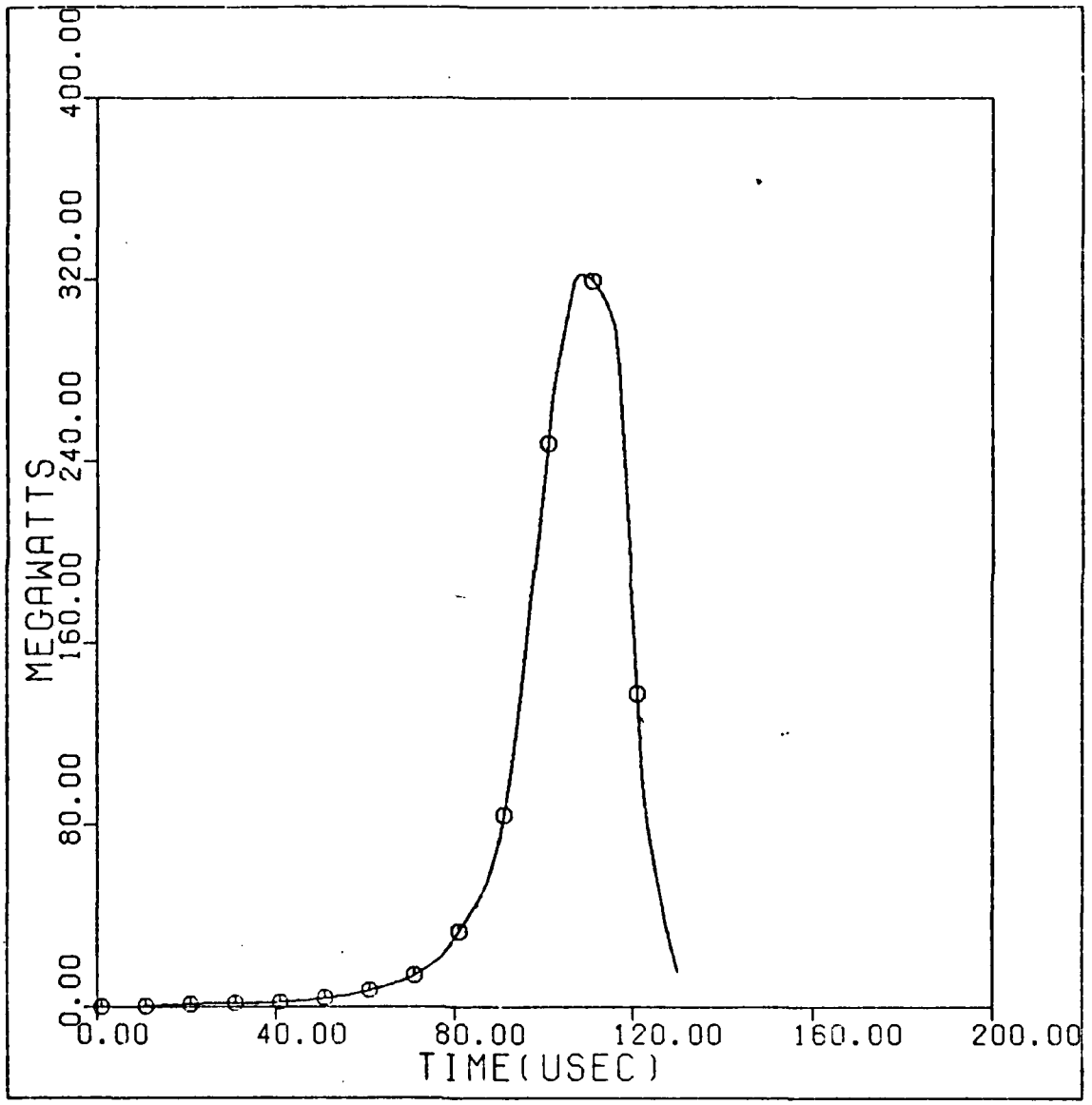

Fig. 32 Switch C5 Load Power

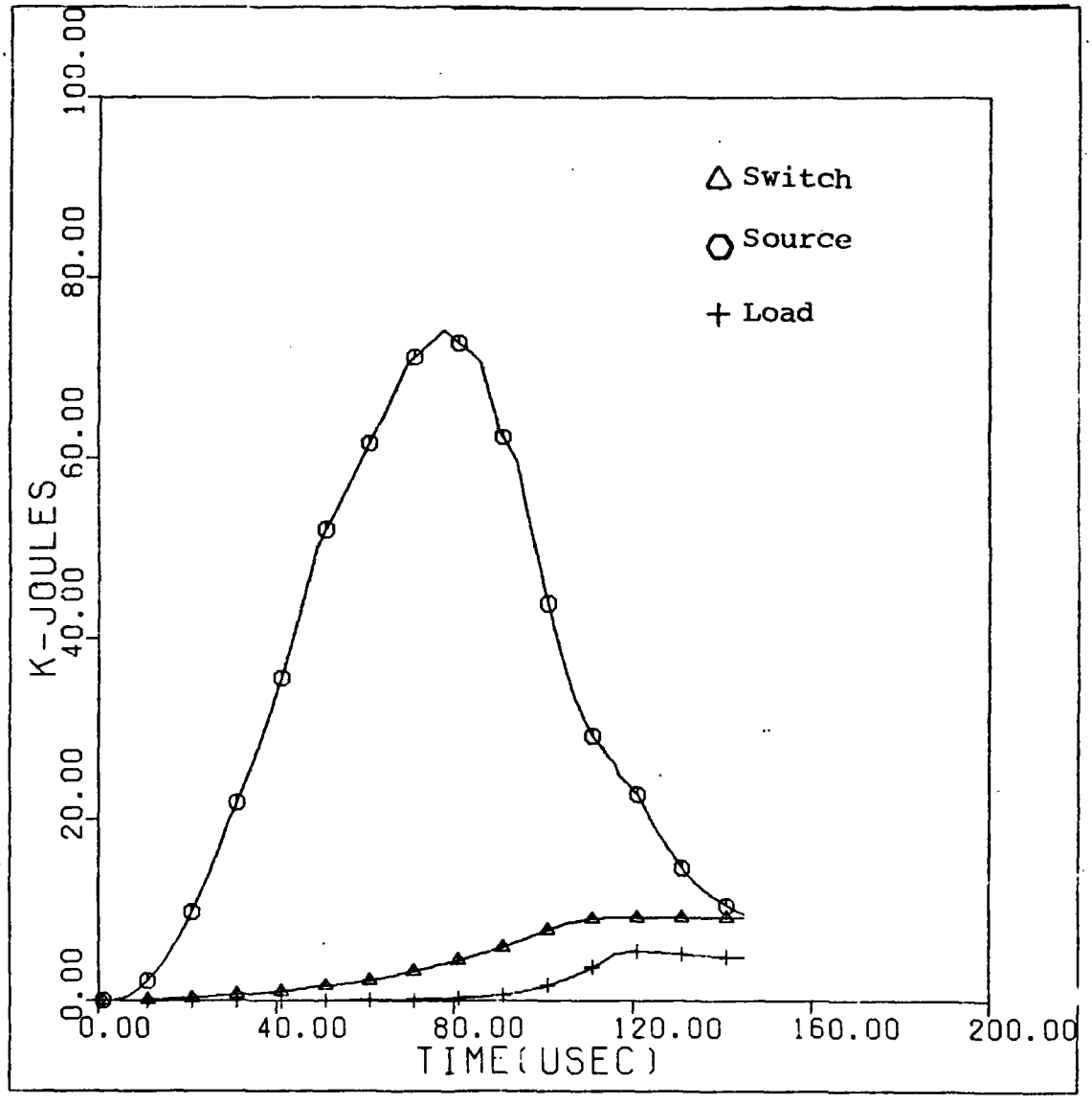

Fig. 33 Switch C5 Energies

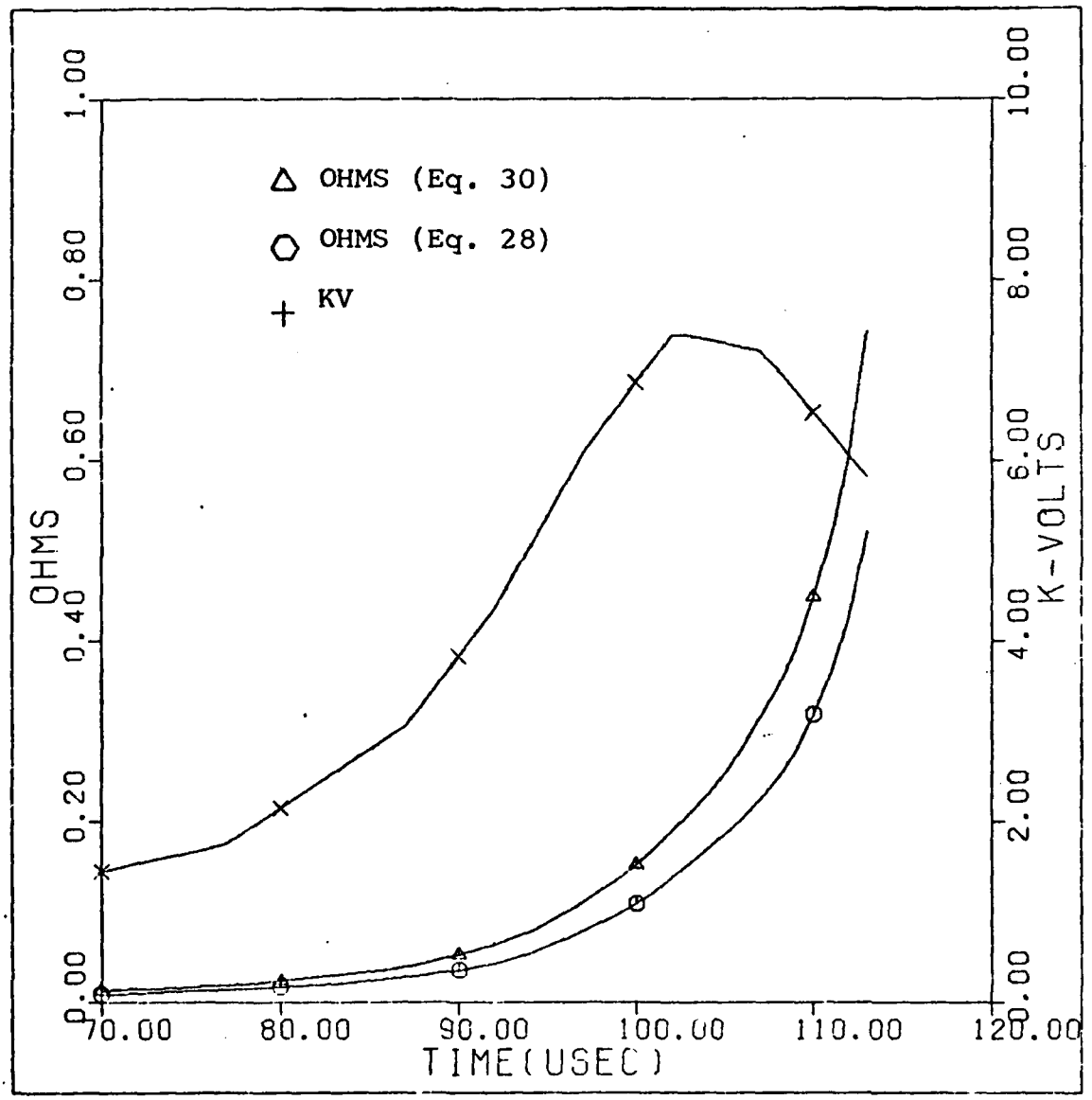

Fig. 34 Switch C5 Resistance and Voltage

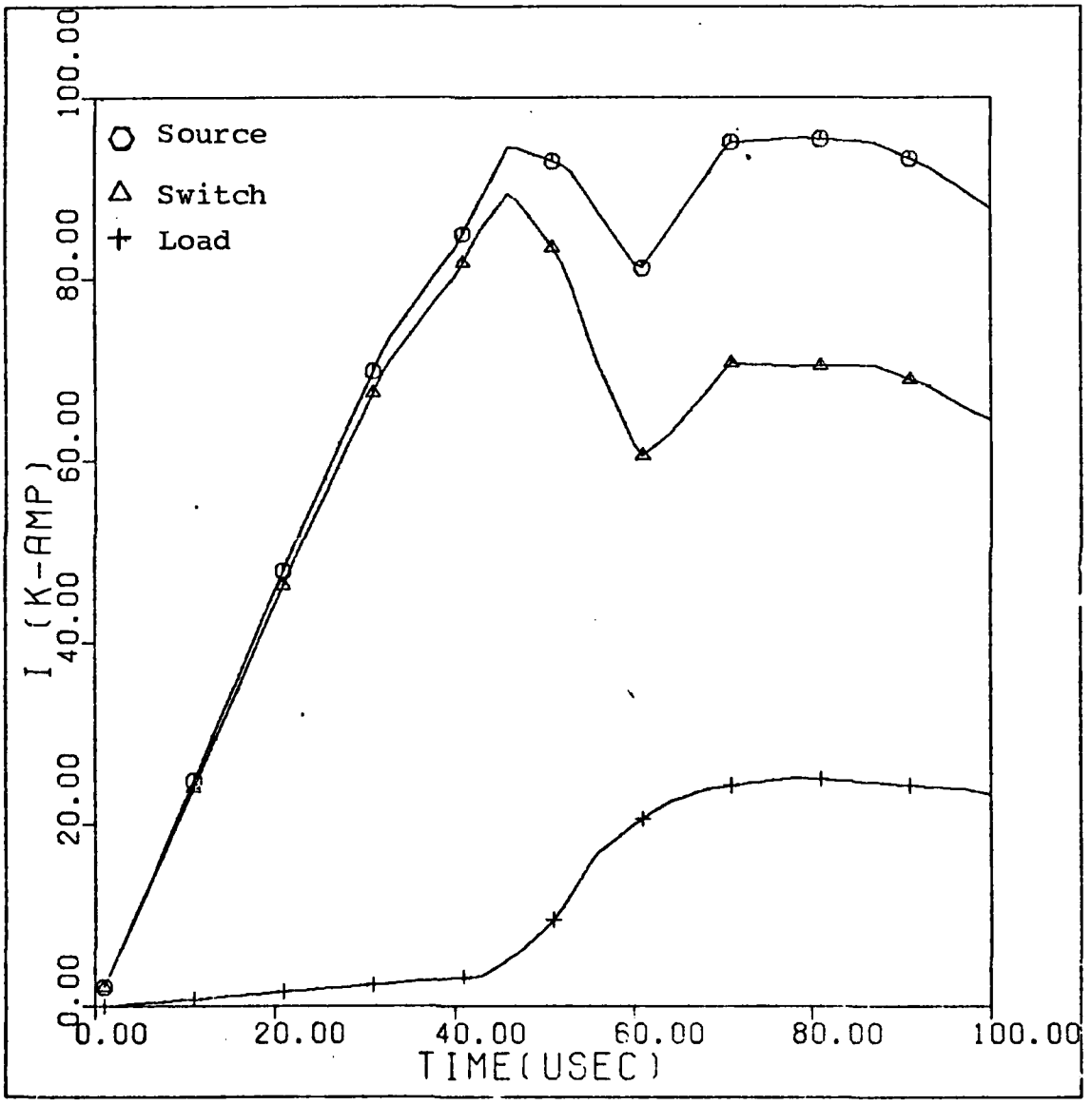

Fig. 35 Switch P5 Currents

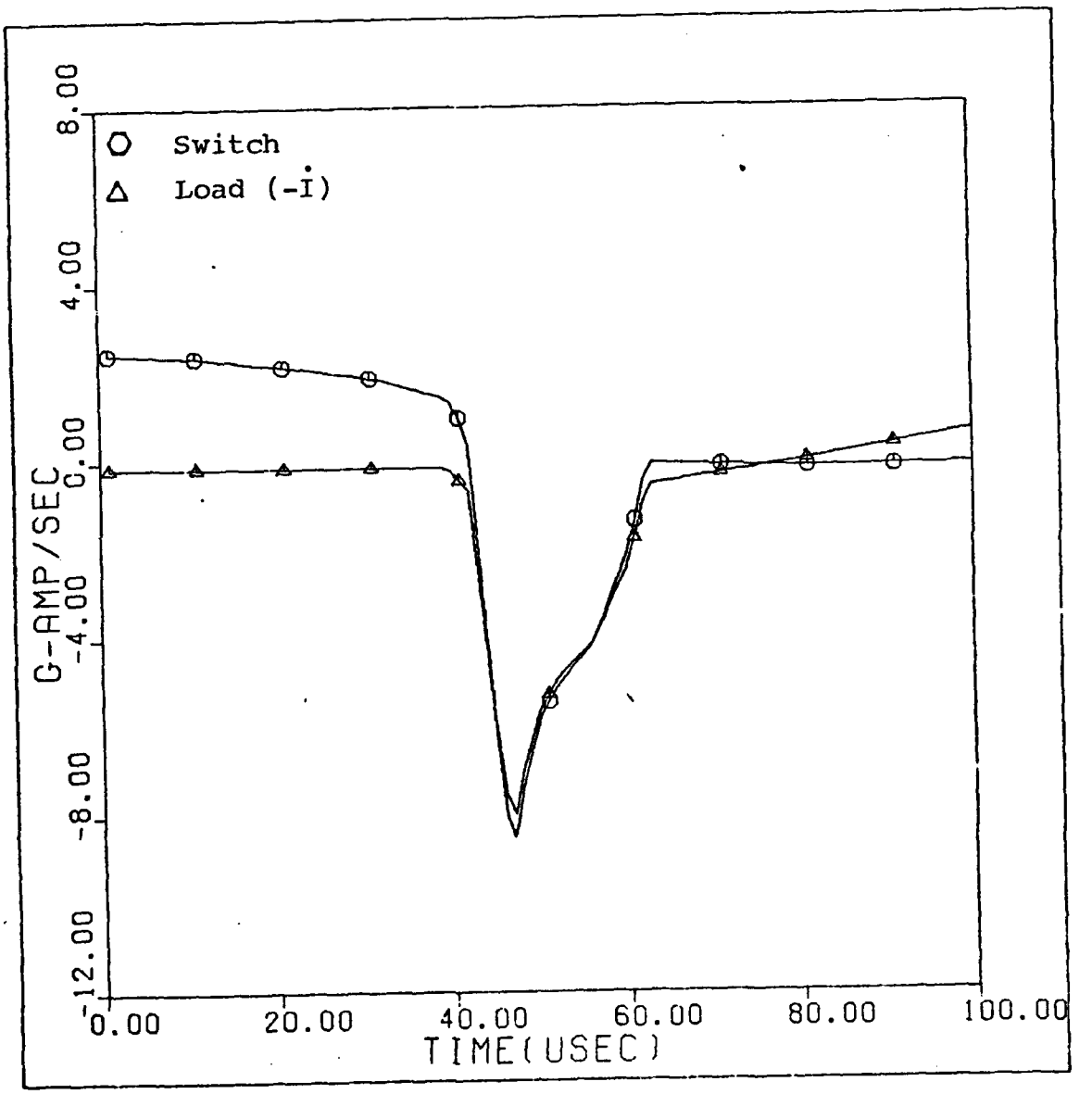

Fig. 36 Switch P5 Current Derivatives

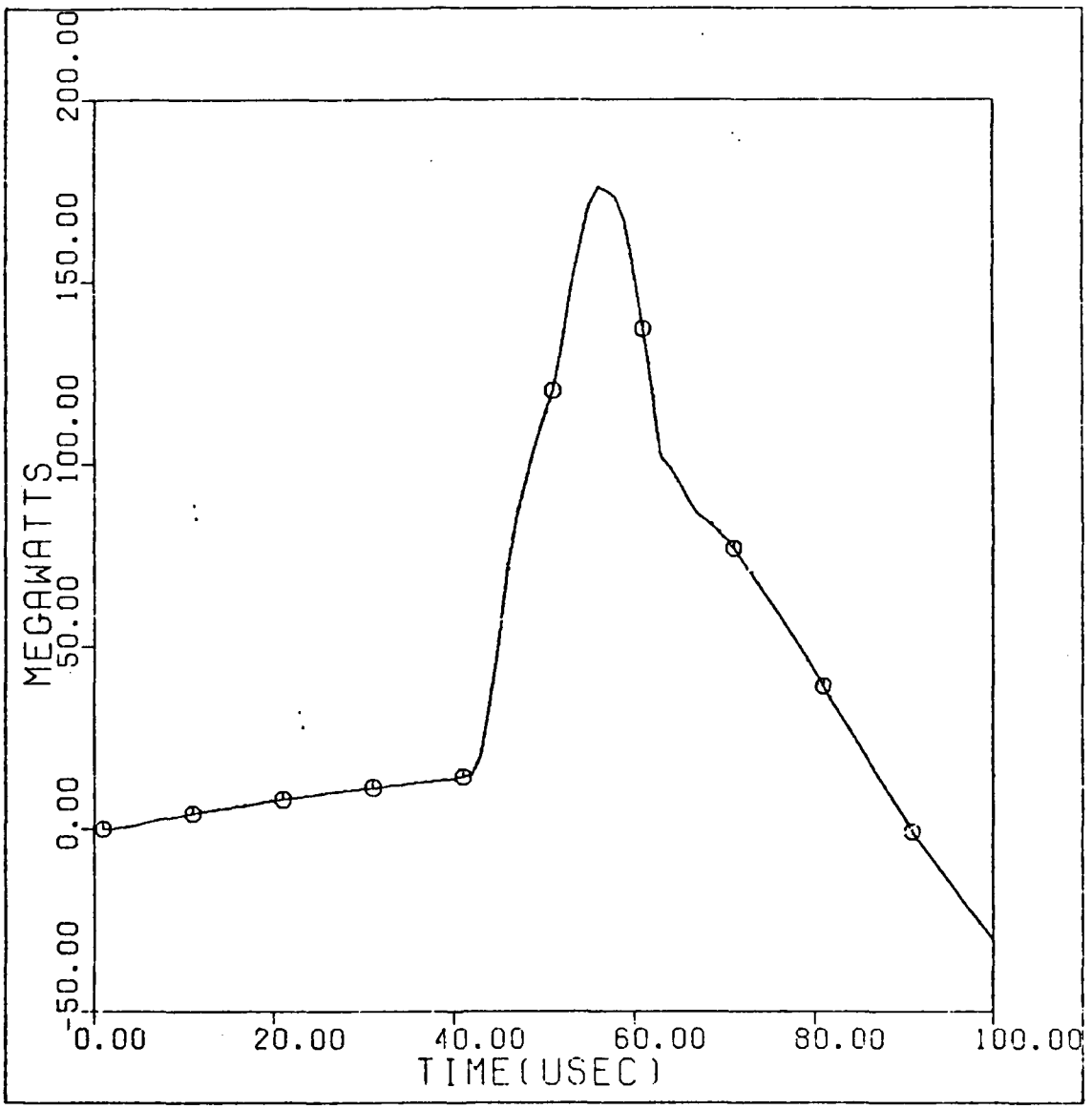

Fig. 37 Switch P5 Load Power

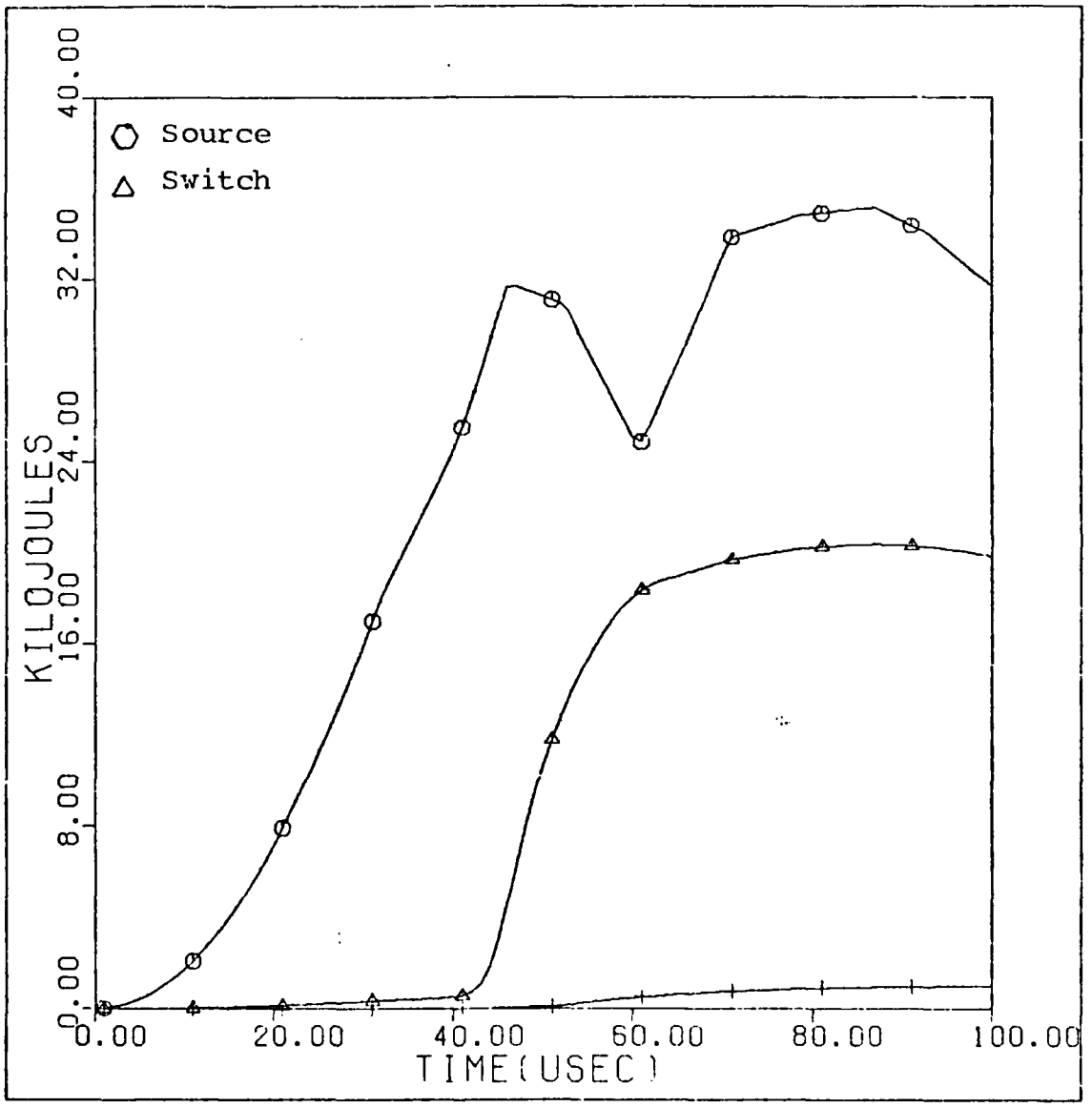

Fig. 38 Switch P5 Energies

AD-A124 671 DEVELOPMENT OF AN IMPROVED EXPLOSIVELY DRIVEN RUPTURED CONDUCTOR OPENING SWITCH(U) AIR FORCE INST OF TECH WRIGHT-PATTERSON AFB OH SCHOOL OF ENGI... 2/2

UNCLASSIFIED J D WATSON ET AL. DEC 82 AFIT/GE/EE/82D-39 F/G 9/1 NL

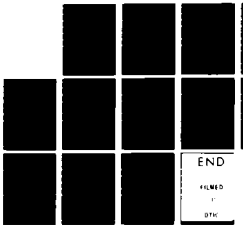

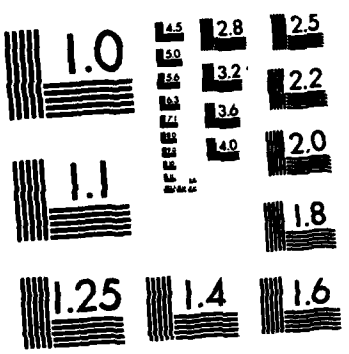

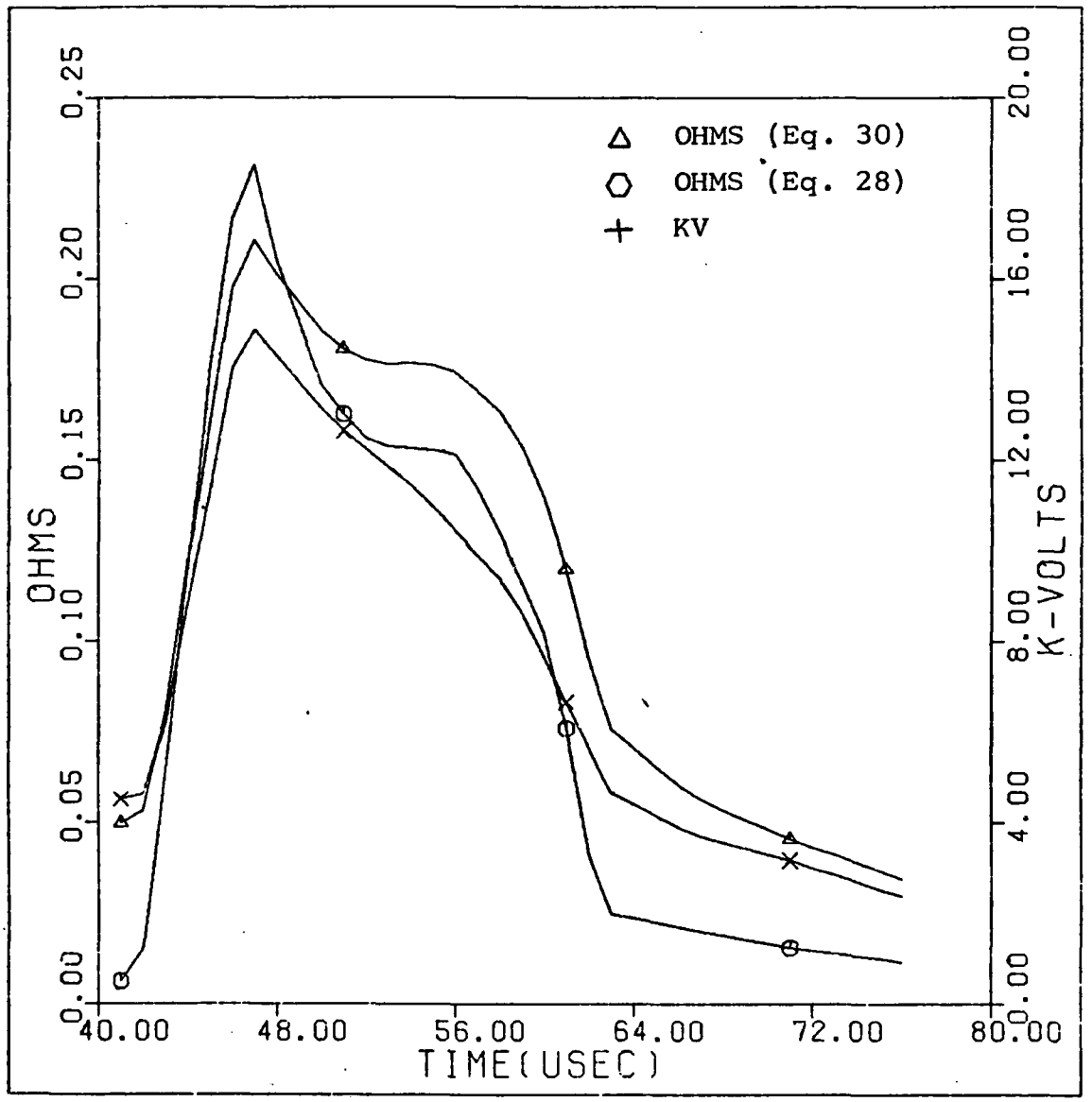

Fig. 39 Switch P5 Resistance and Voltage

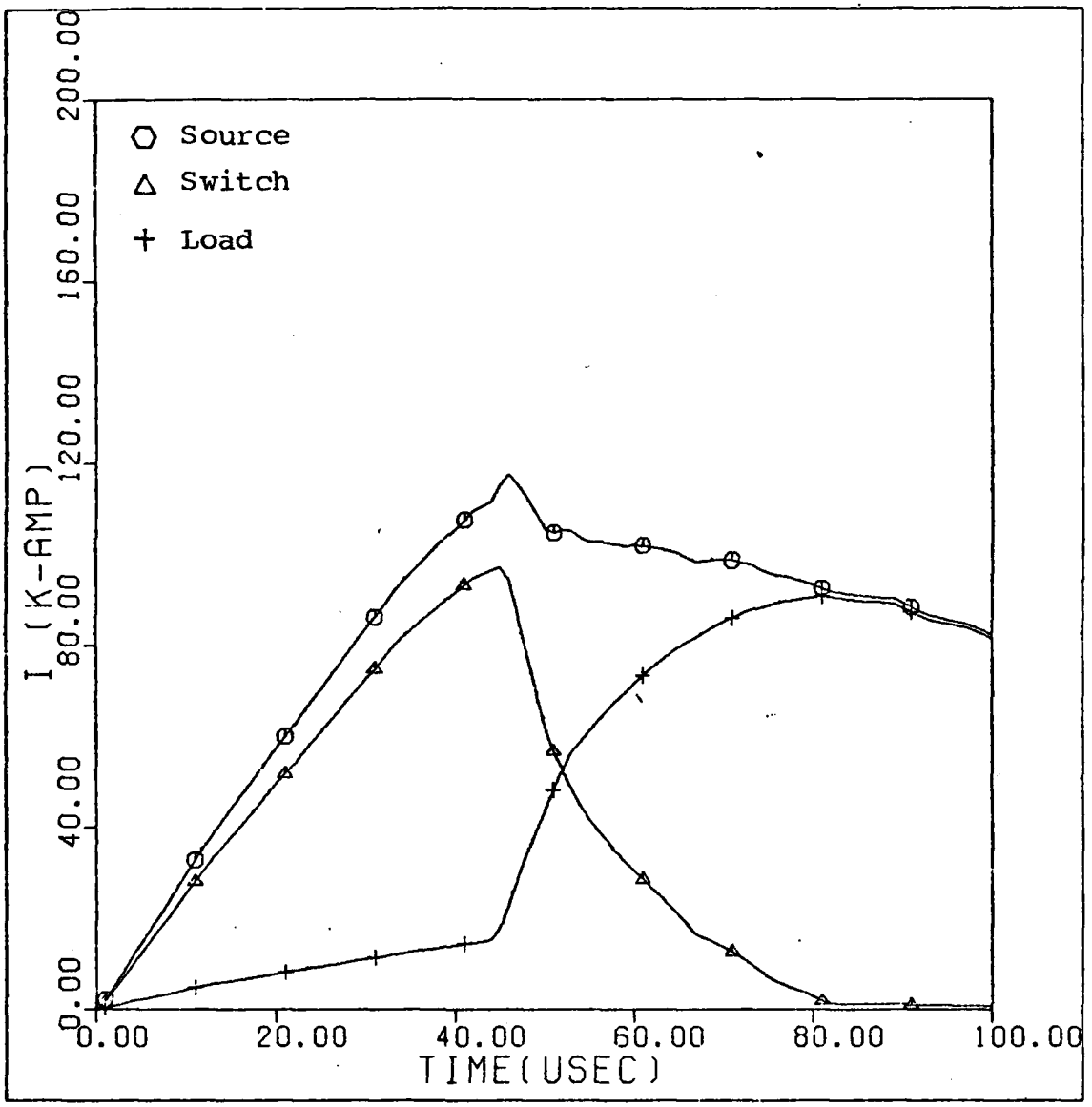

Fig. 40 Switch P6 Currents

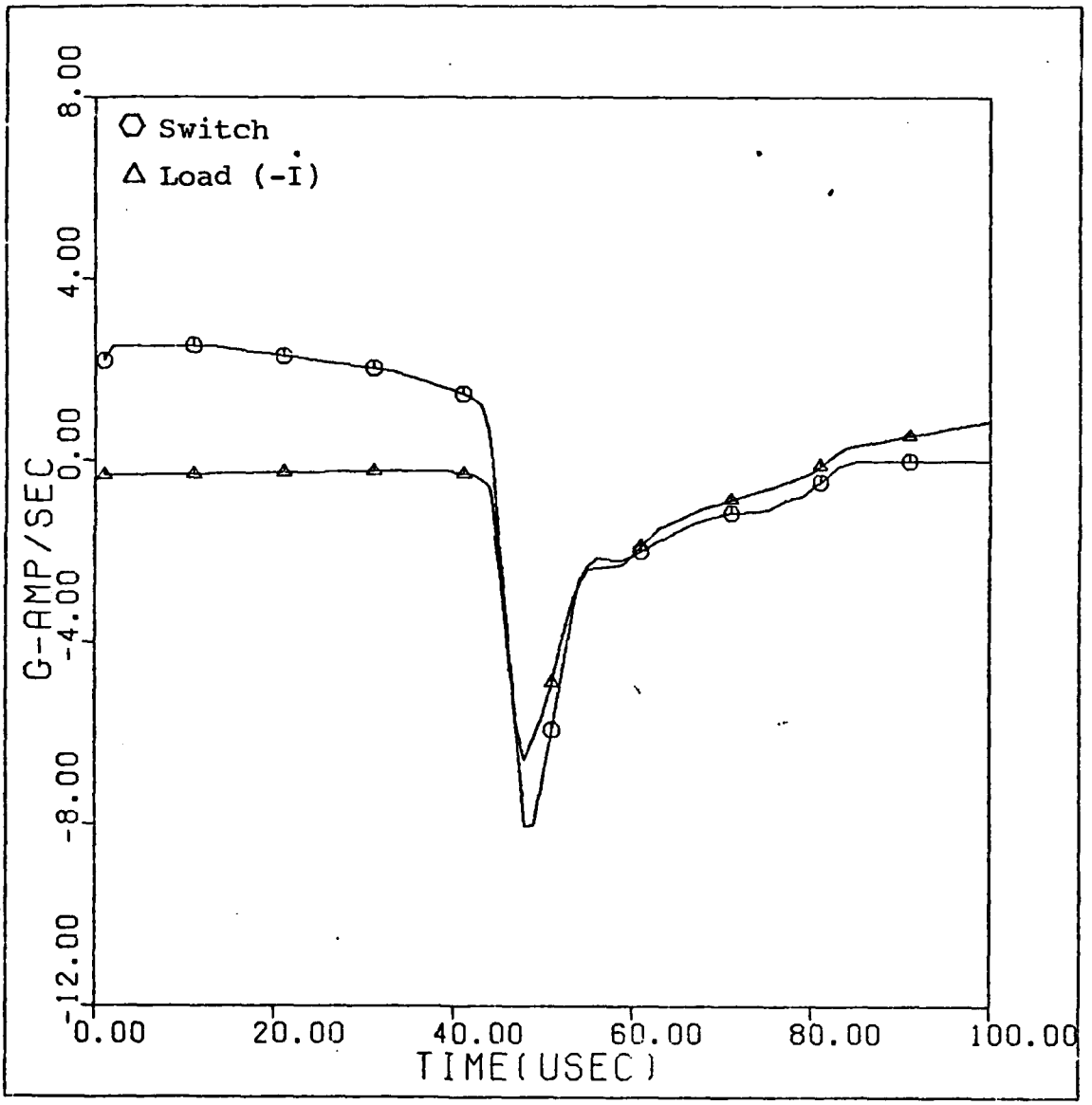

Fig. 41 Switch P6 Current Derivatives

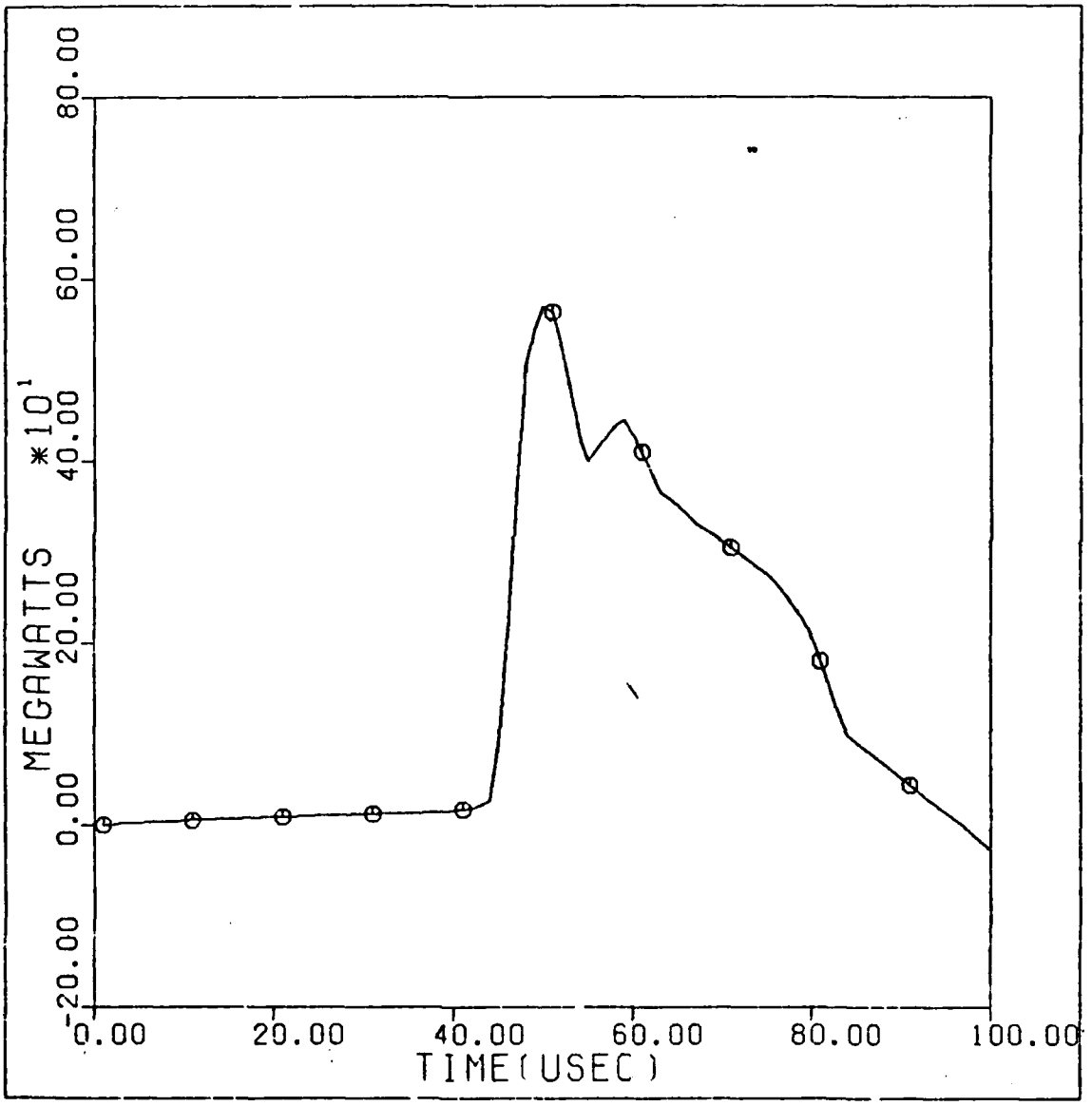

Fig. 42 Switch P6 Load Power

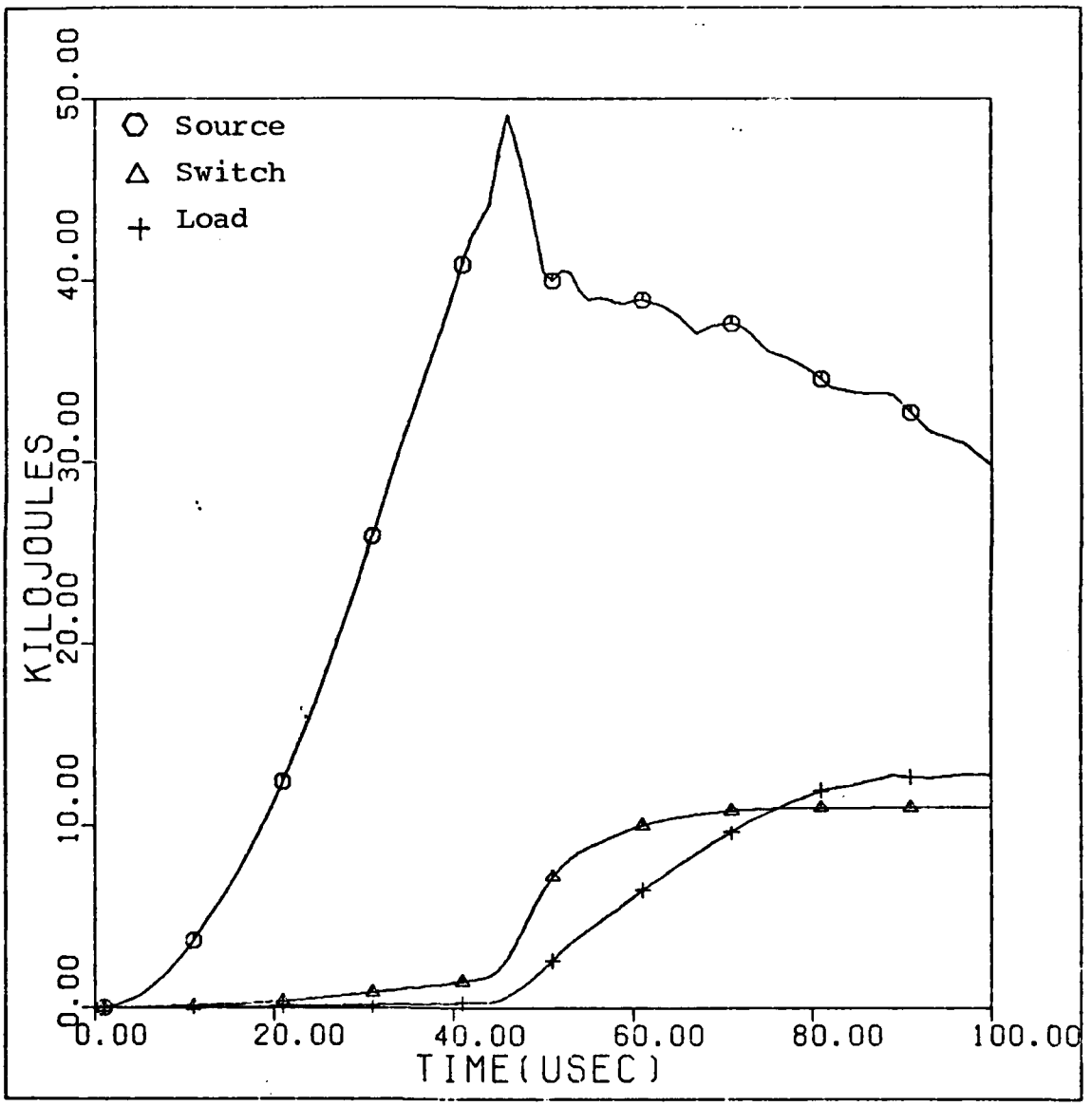

Fig. 43 Switch P6 Energies

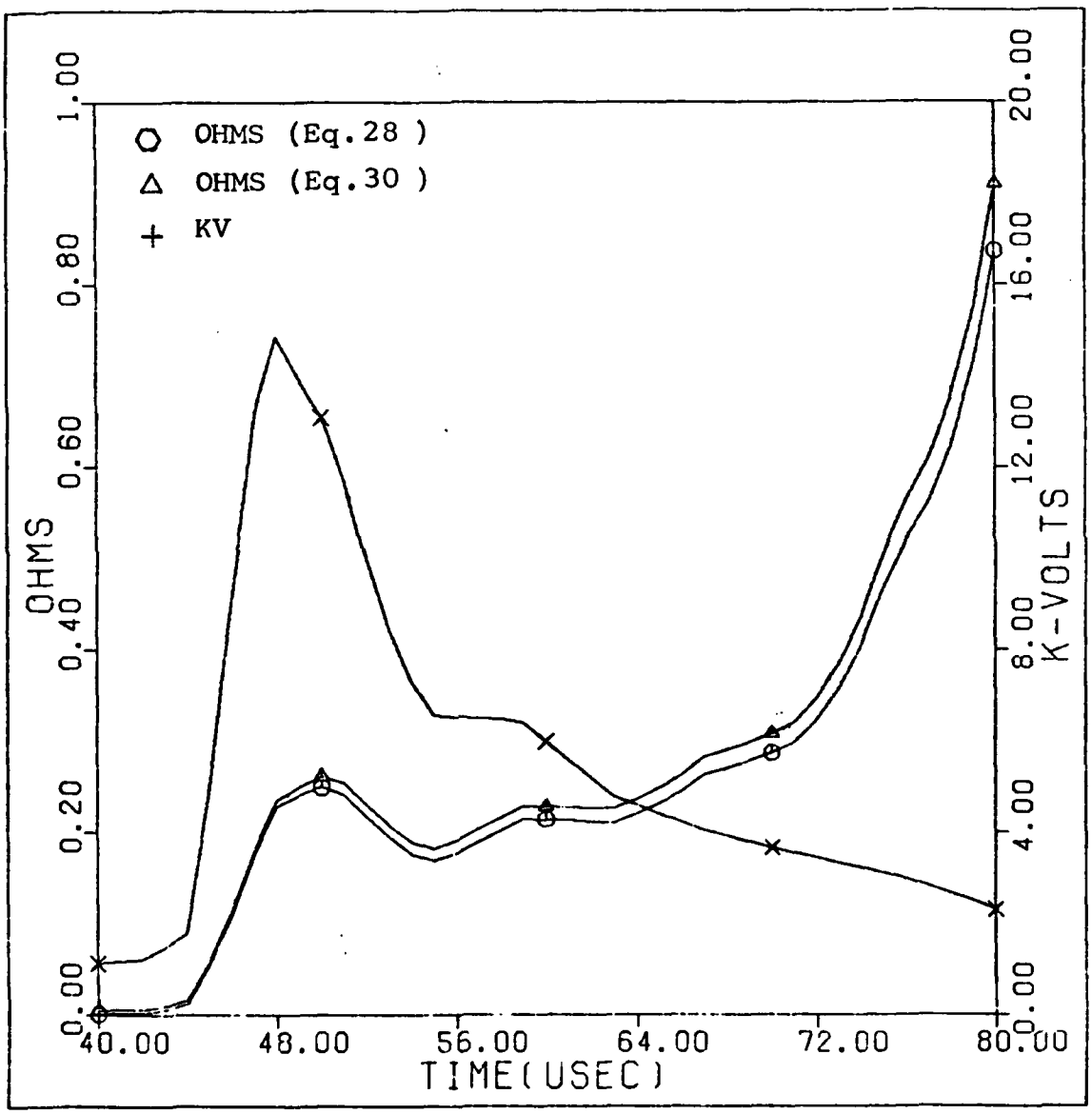

Fig. 44 Switch P6 Resistance and Voltage

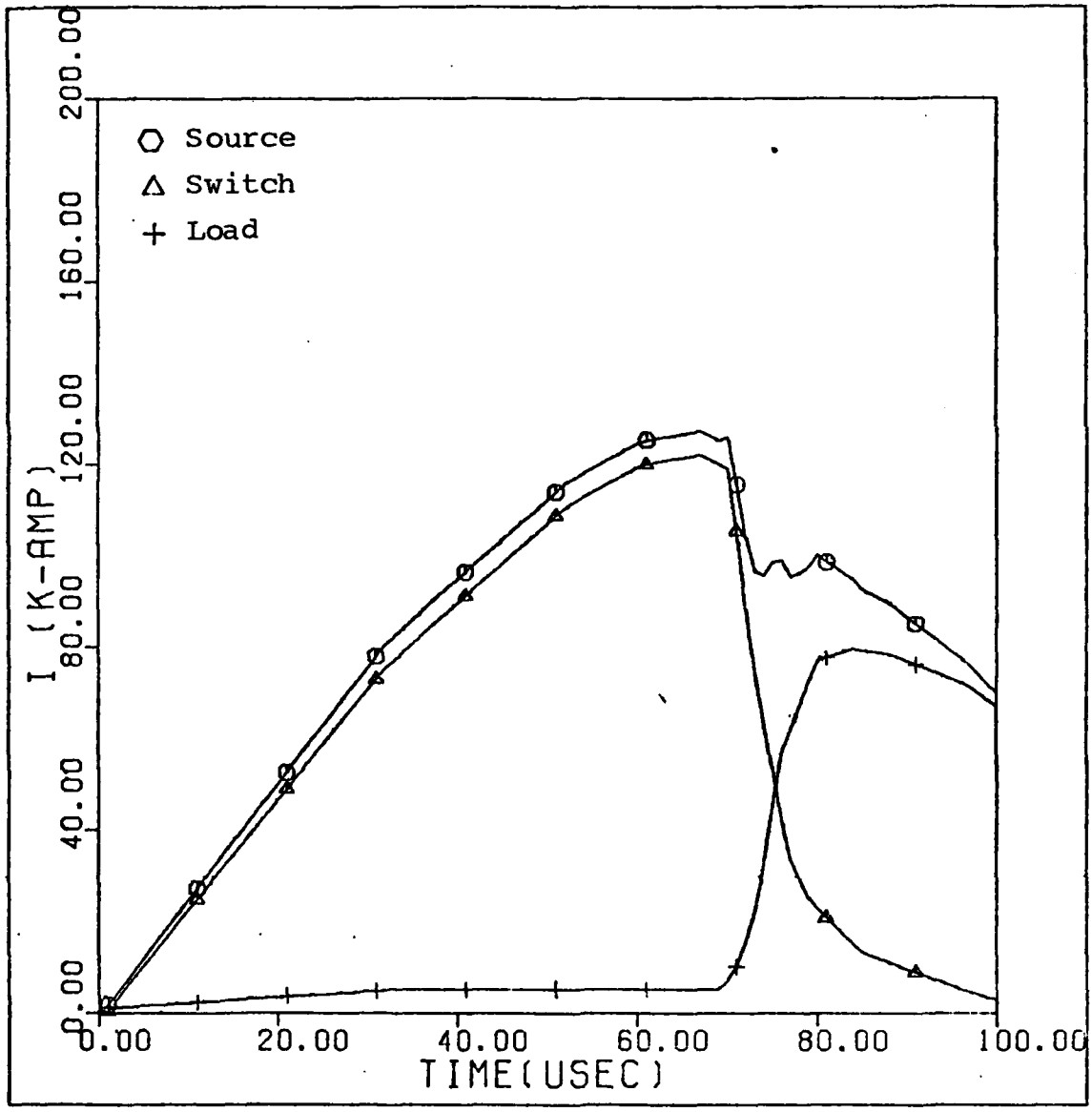

Fig. 45 Switch P8 Currents

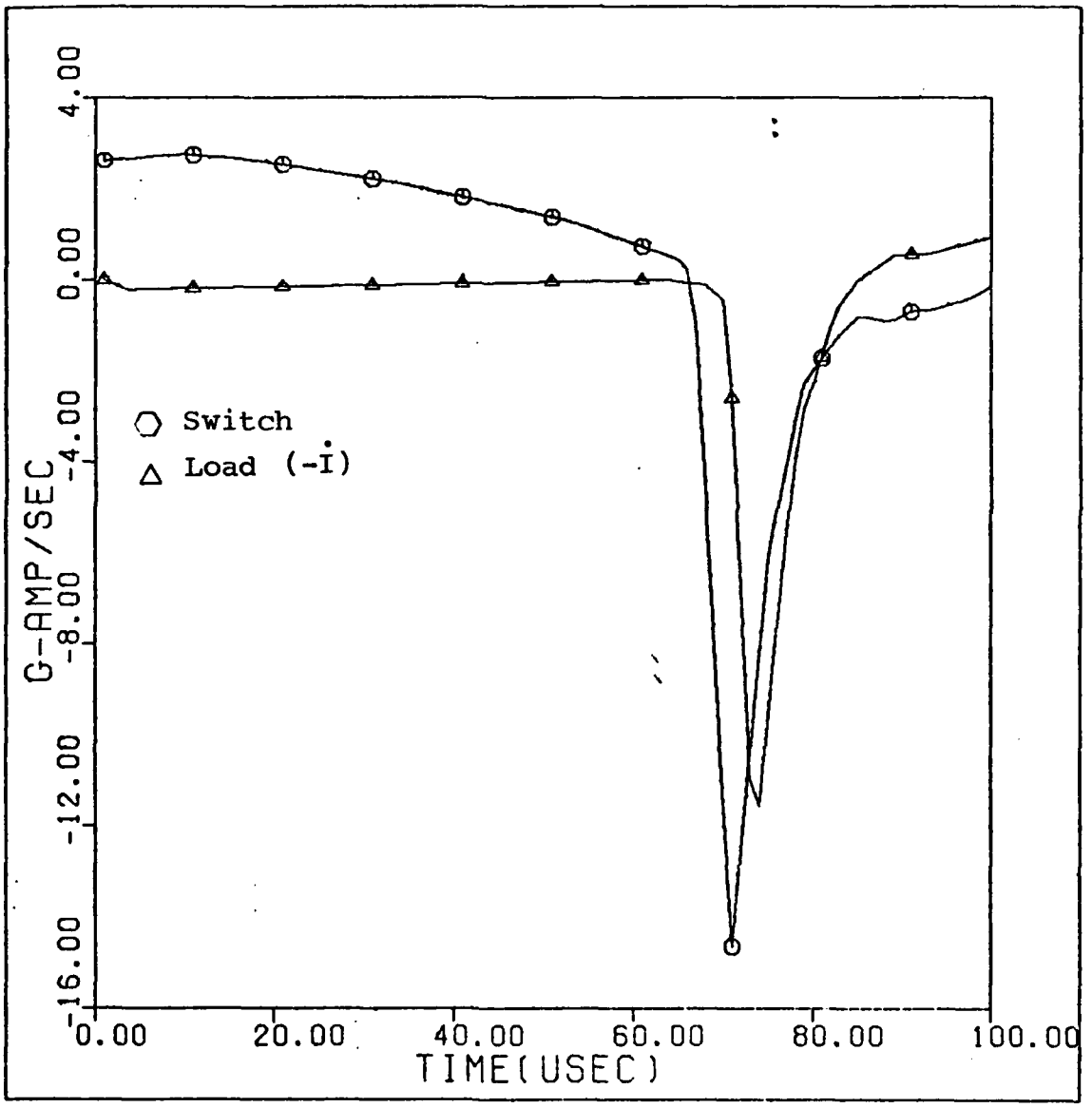

Fig. 46 Switch P8 Current Derivatives

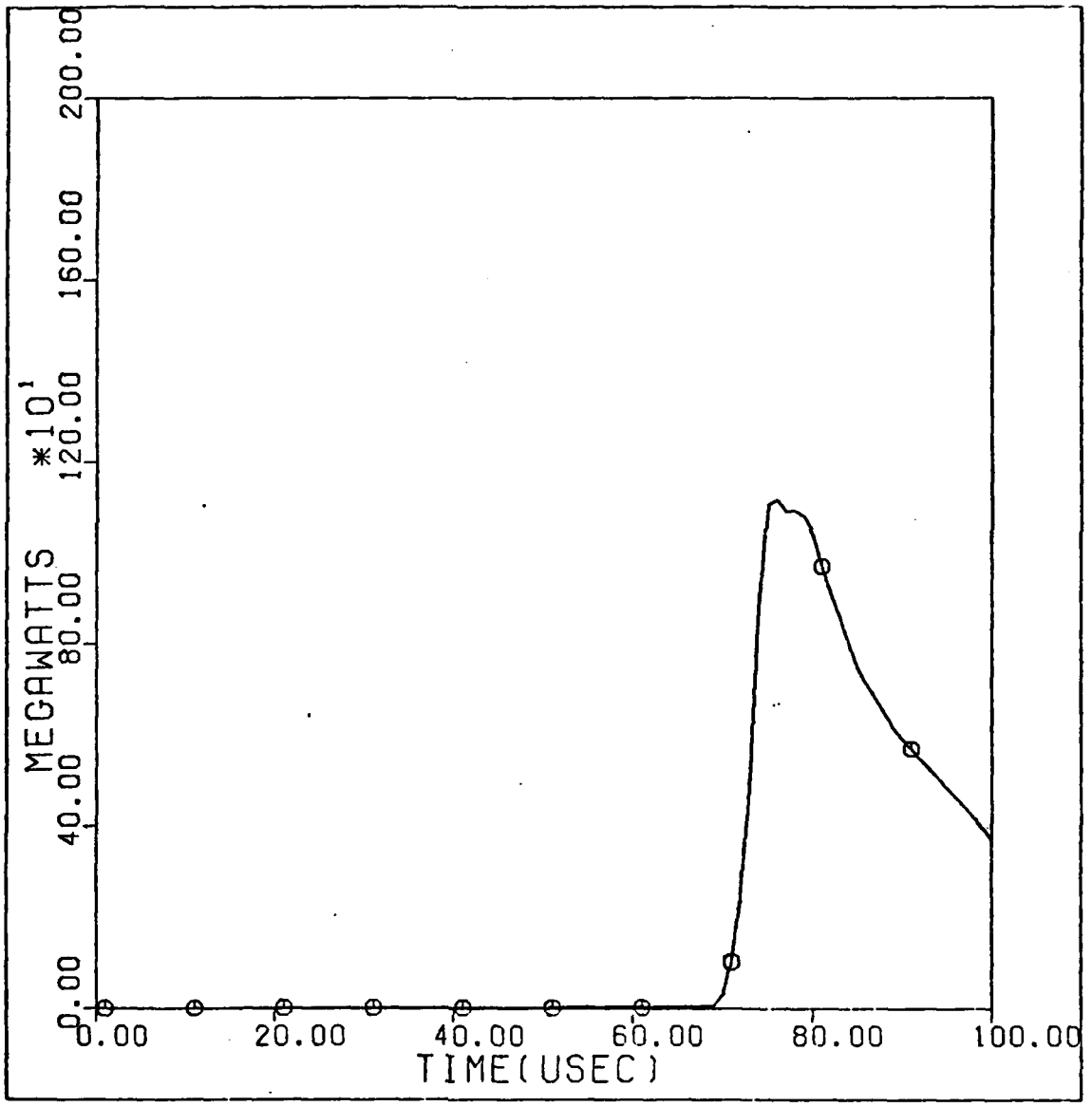

Fig. 47 Switch P8 Load Power

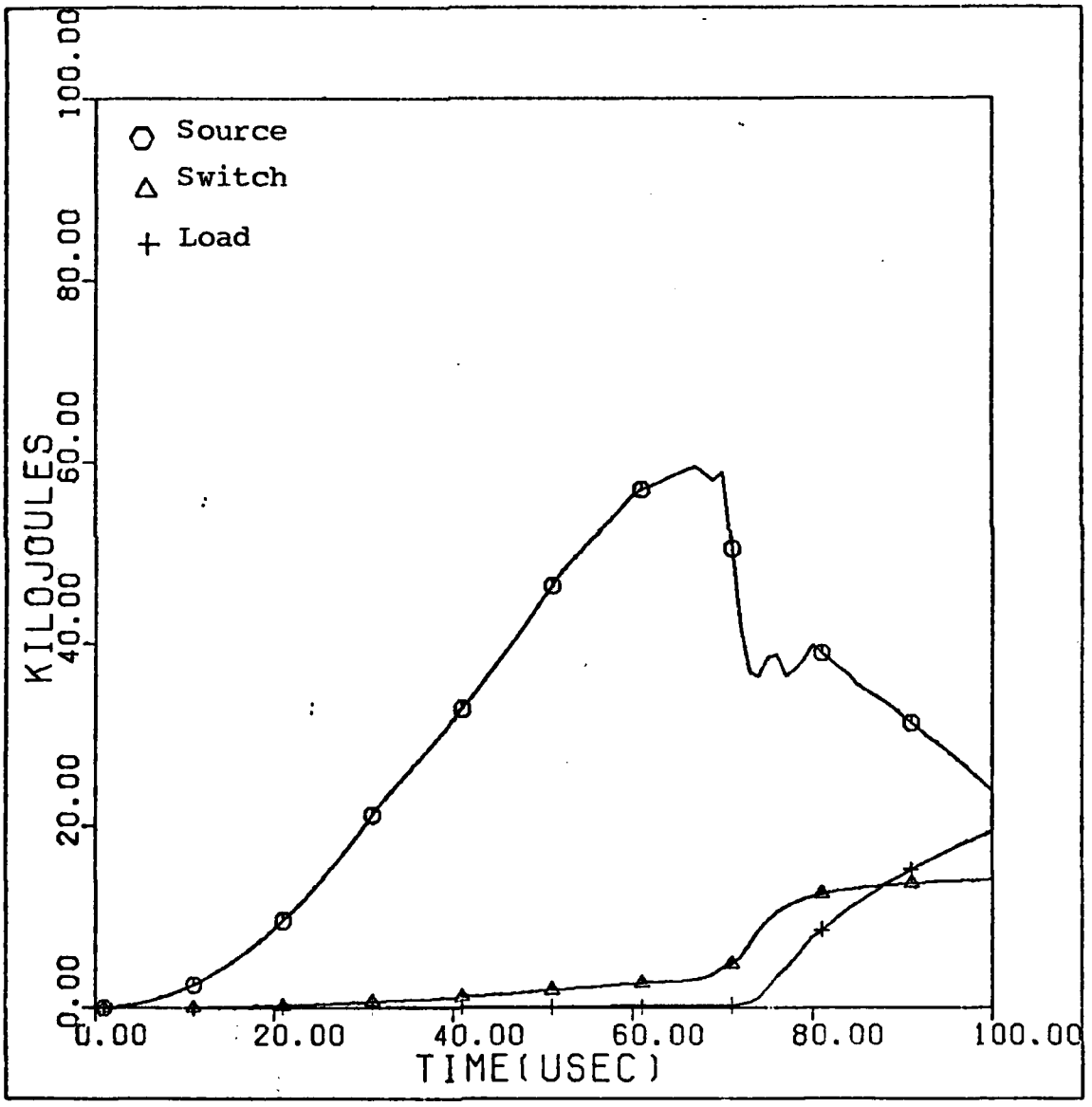

Fig. 48 Switch P8 Energies

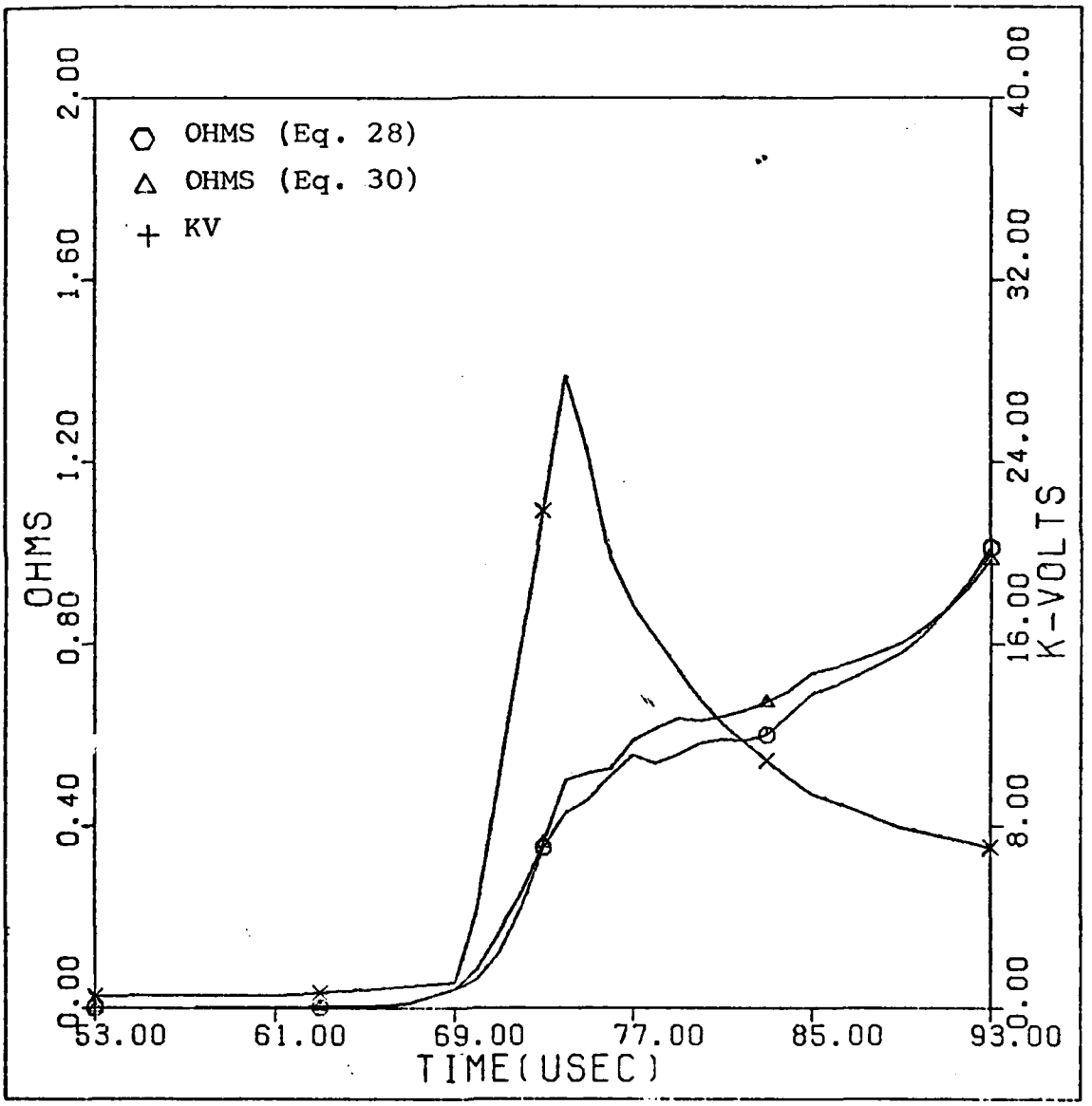

Fig. 49 Switch P8 Resistance and Voltage

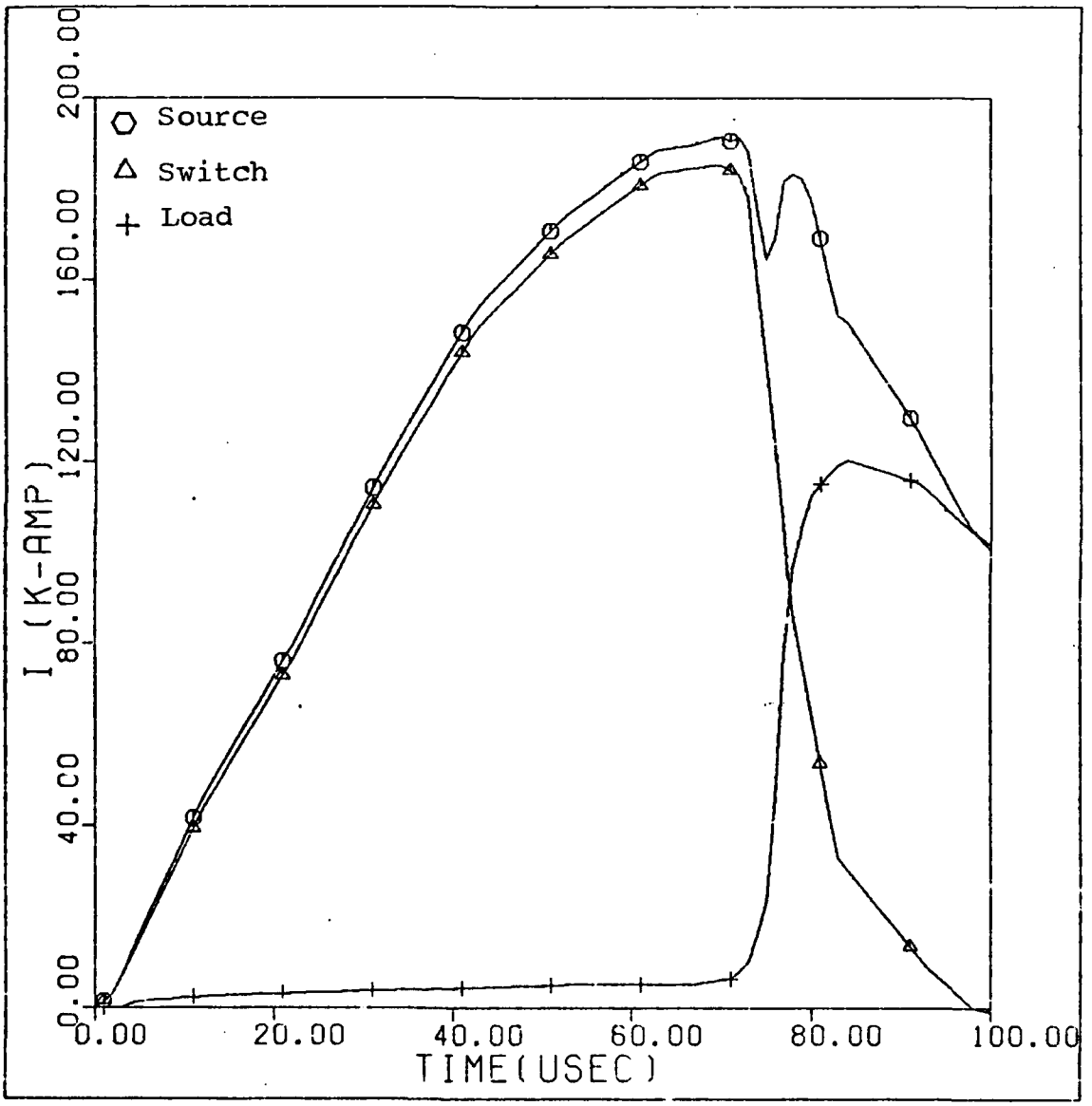

Fig. 50 Switch P10 Currents

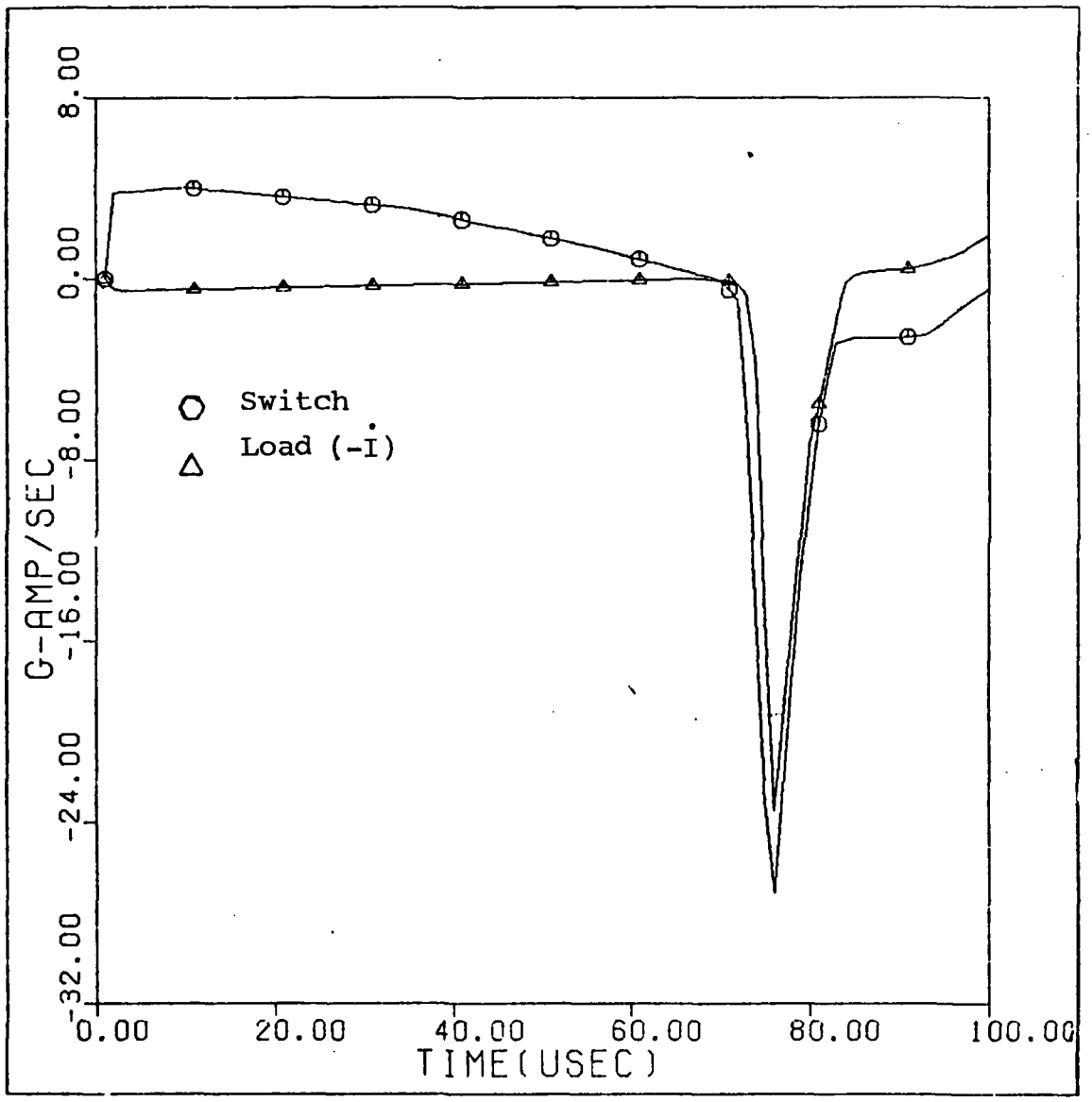

Fig. 51 Switch P10 Current Derivatives

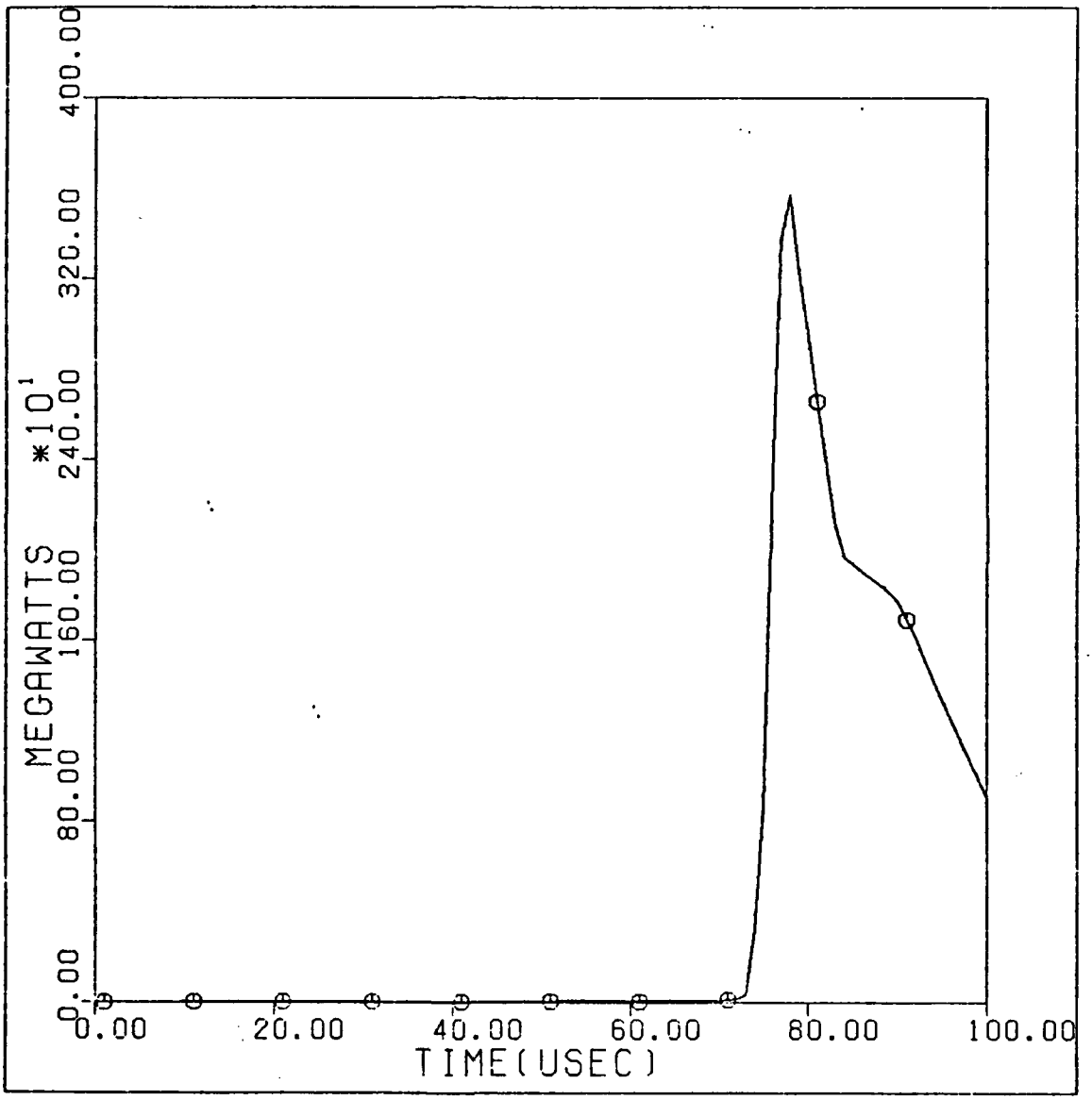

Fig. 52 Switch P10 Load Power

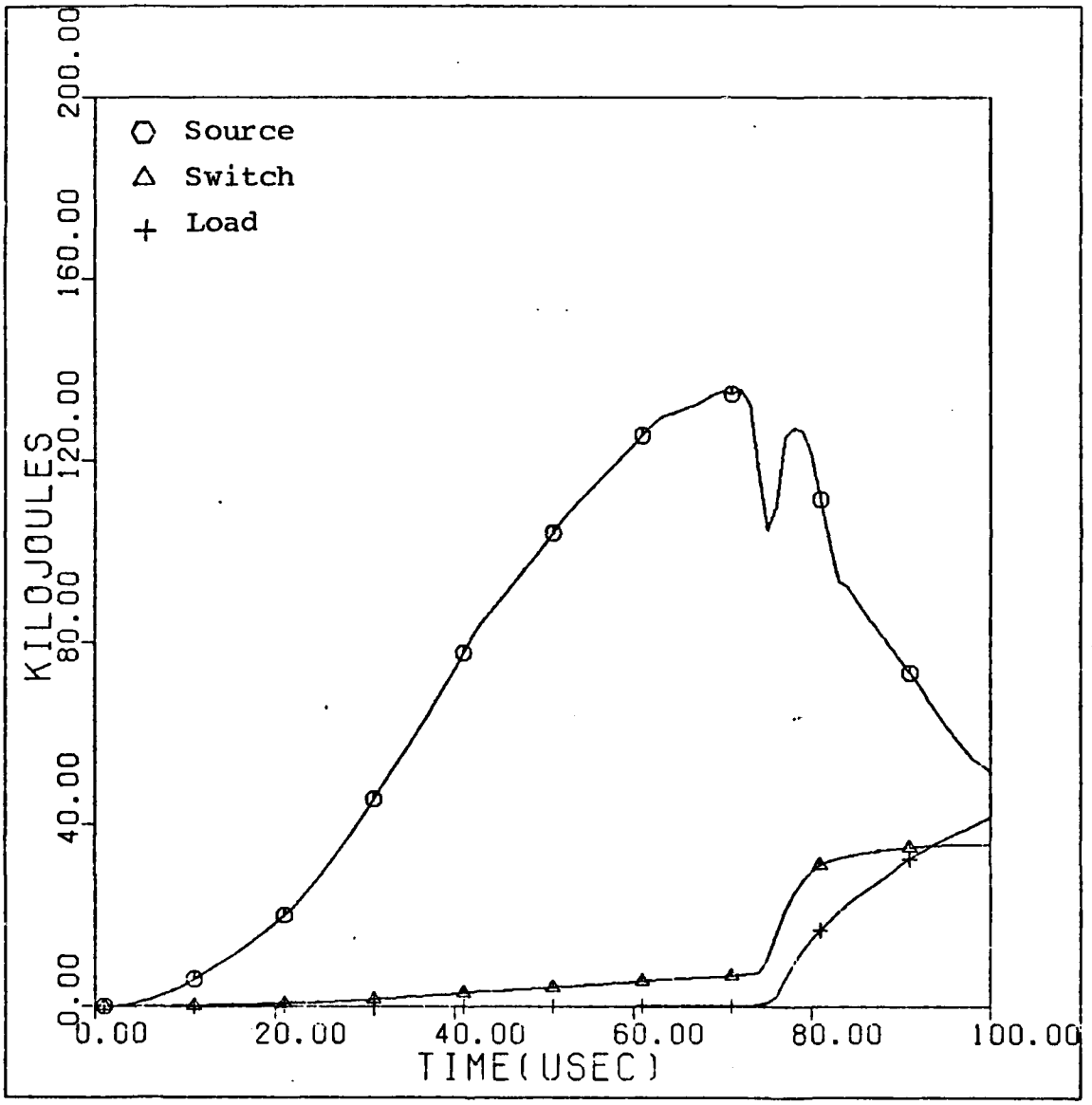

Fig. 53 Switch P10 Energies

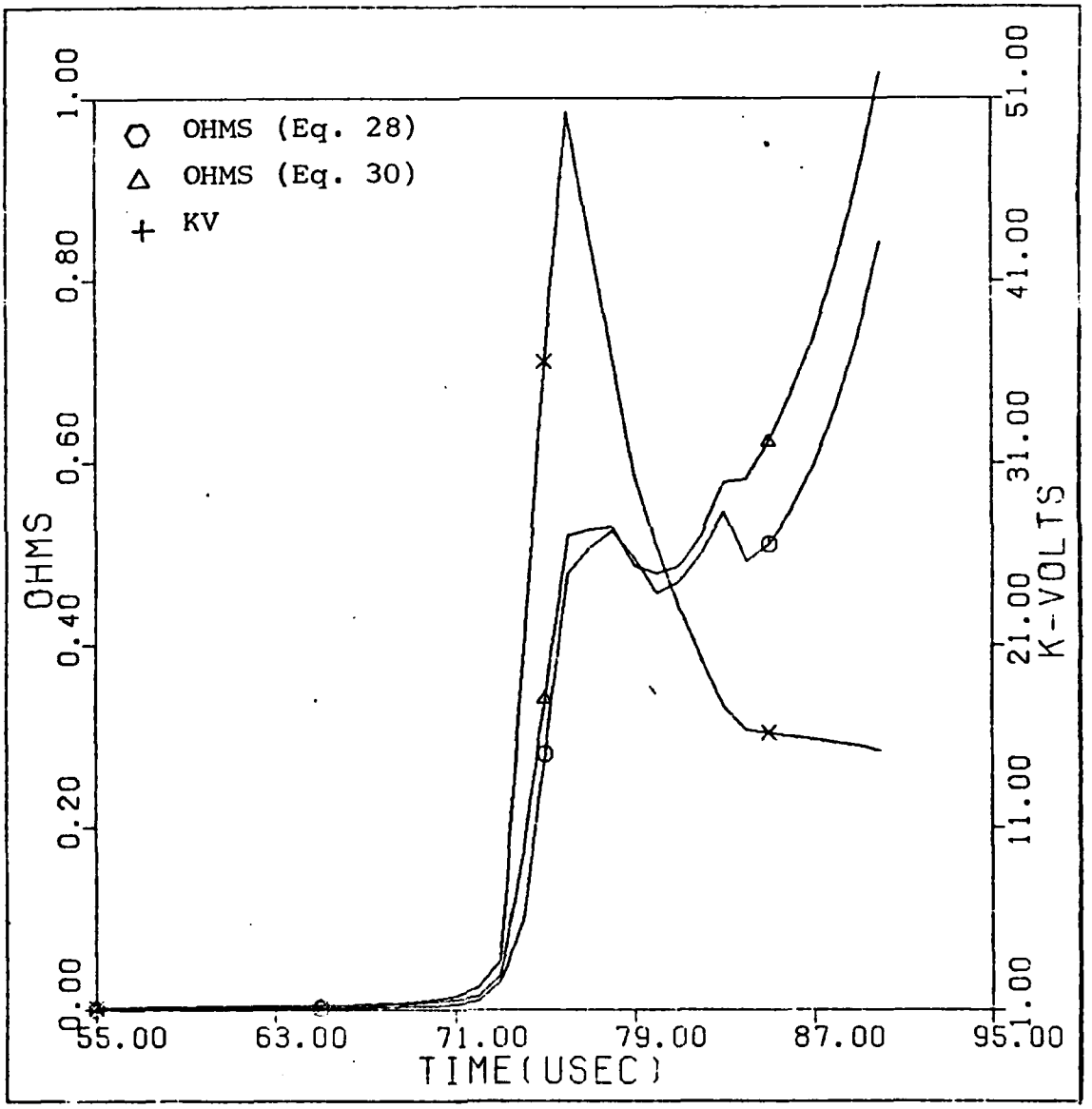

Fig. 54 Switch P10 Resistance and Voltage

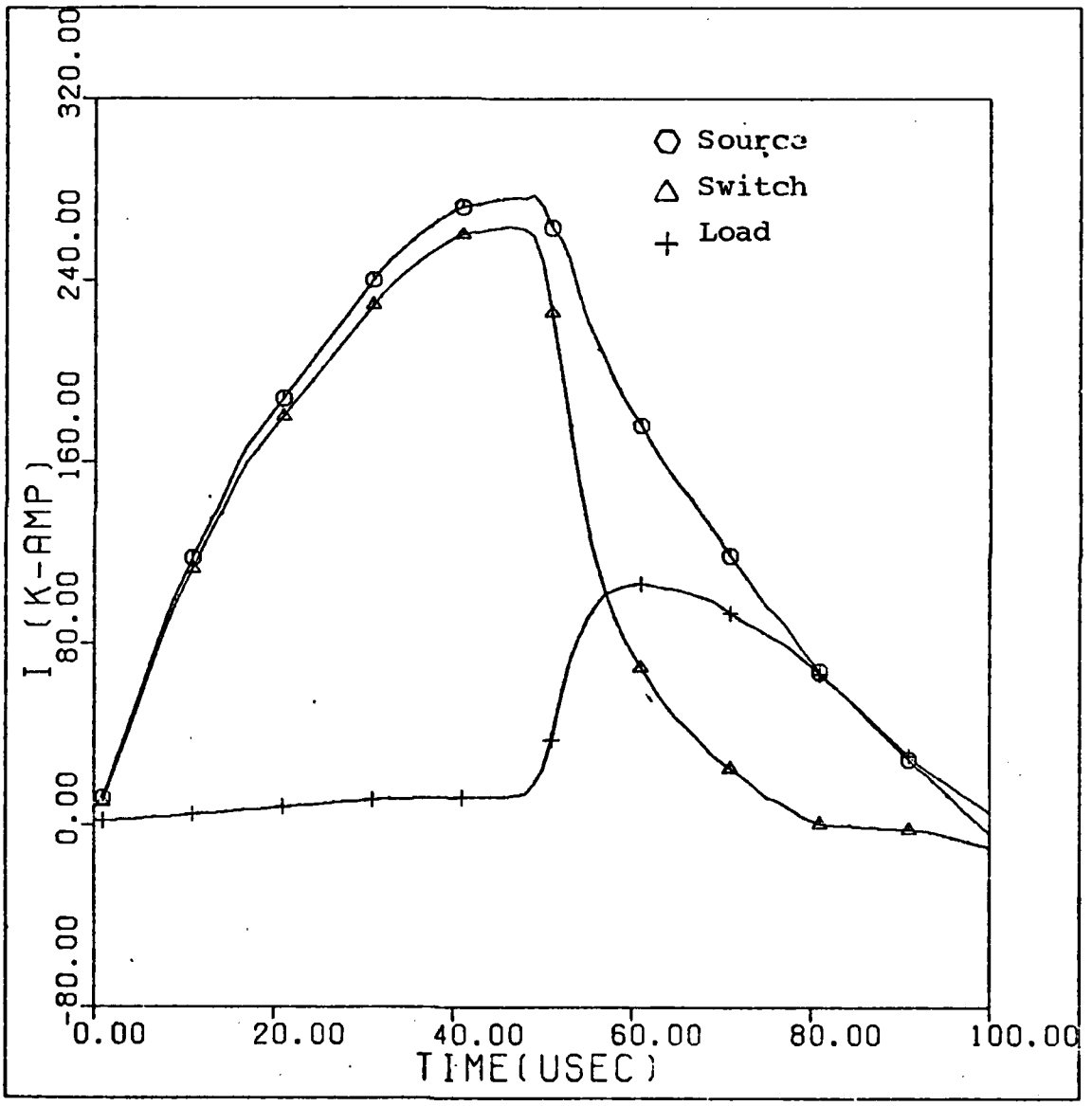

Fig. 55 Switch P13 Currents

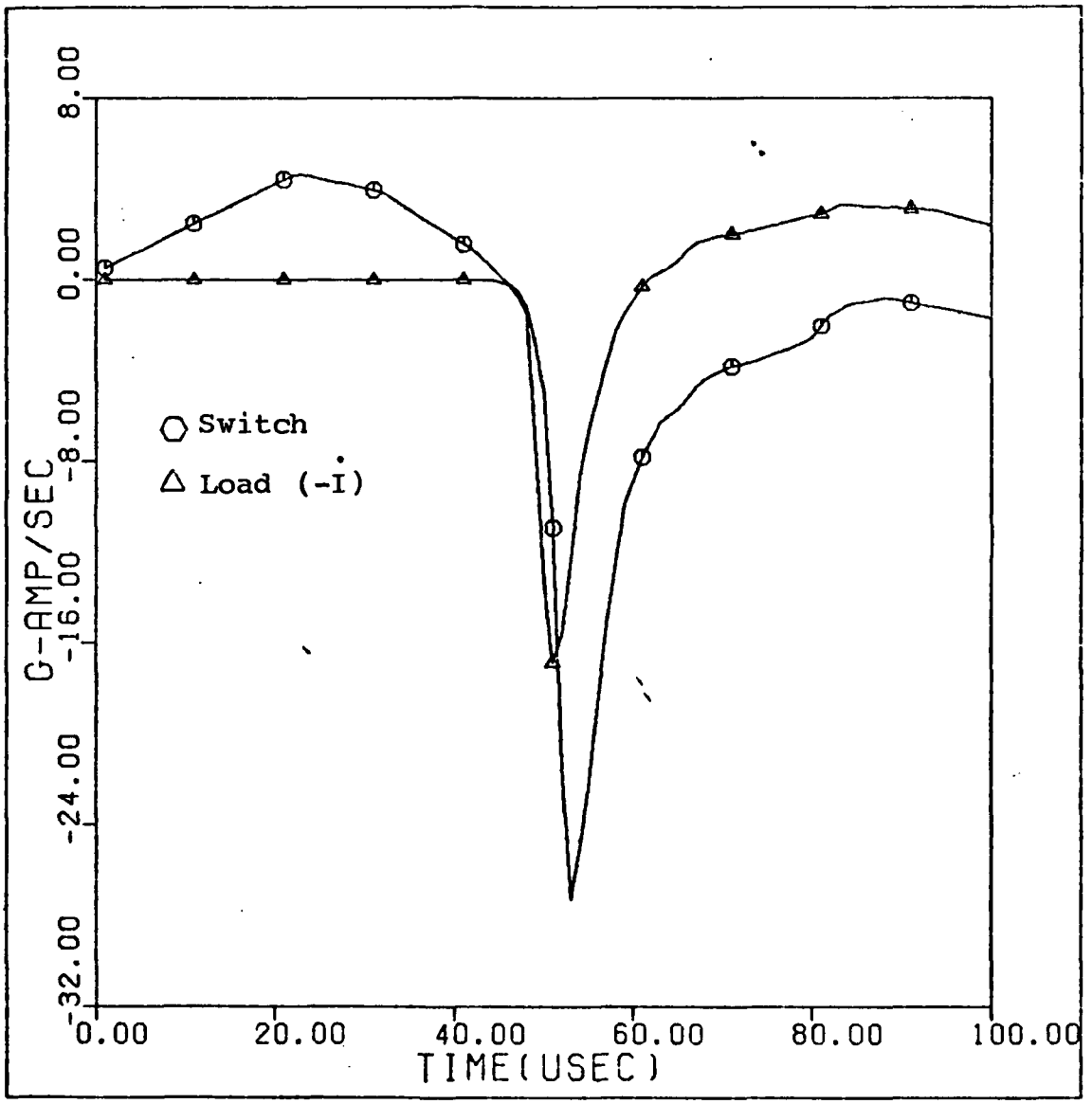

Fig. 56 Switch P13 Current Derivatives

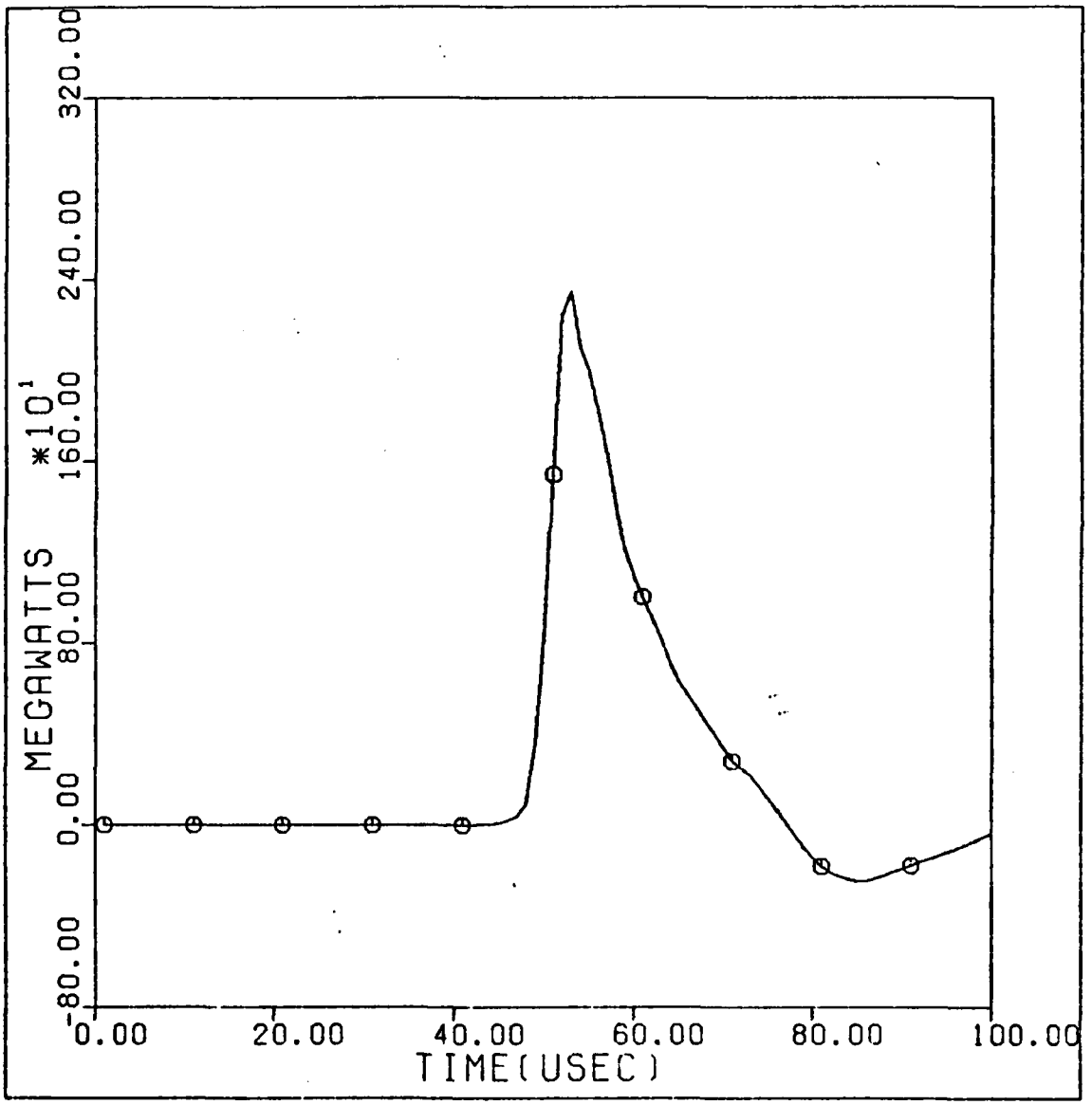

Fig. 57 Switch P13 Load Power

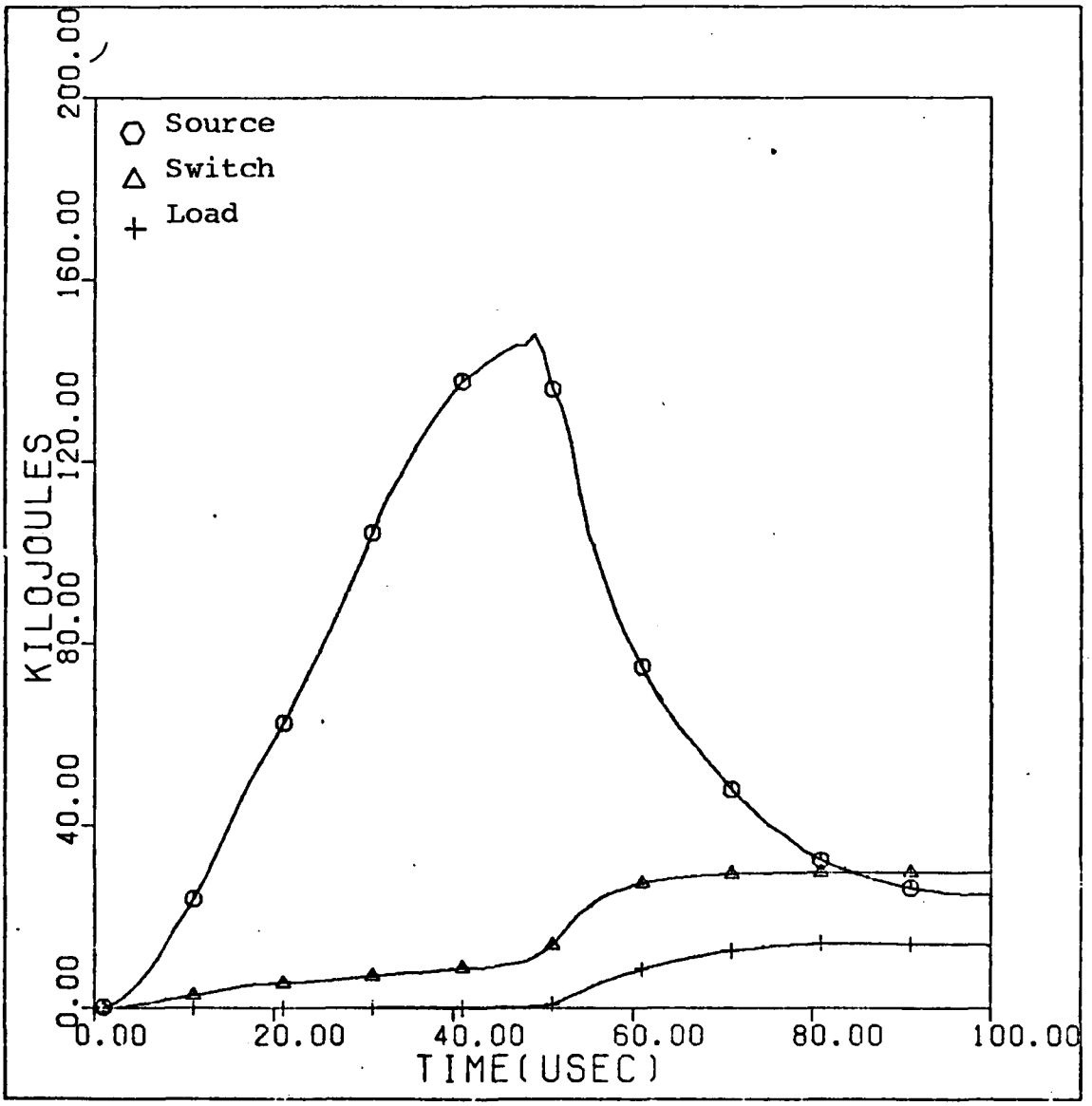

Fig. 58 Switch P13 Energies

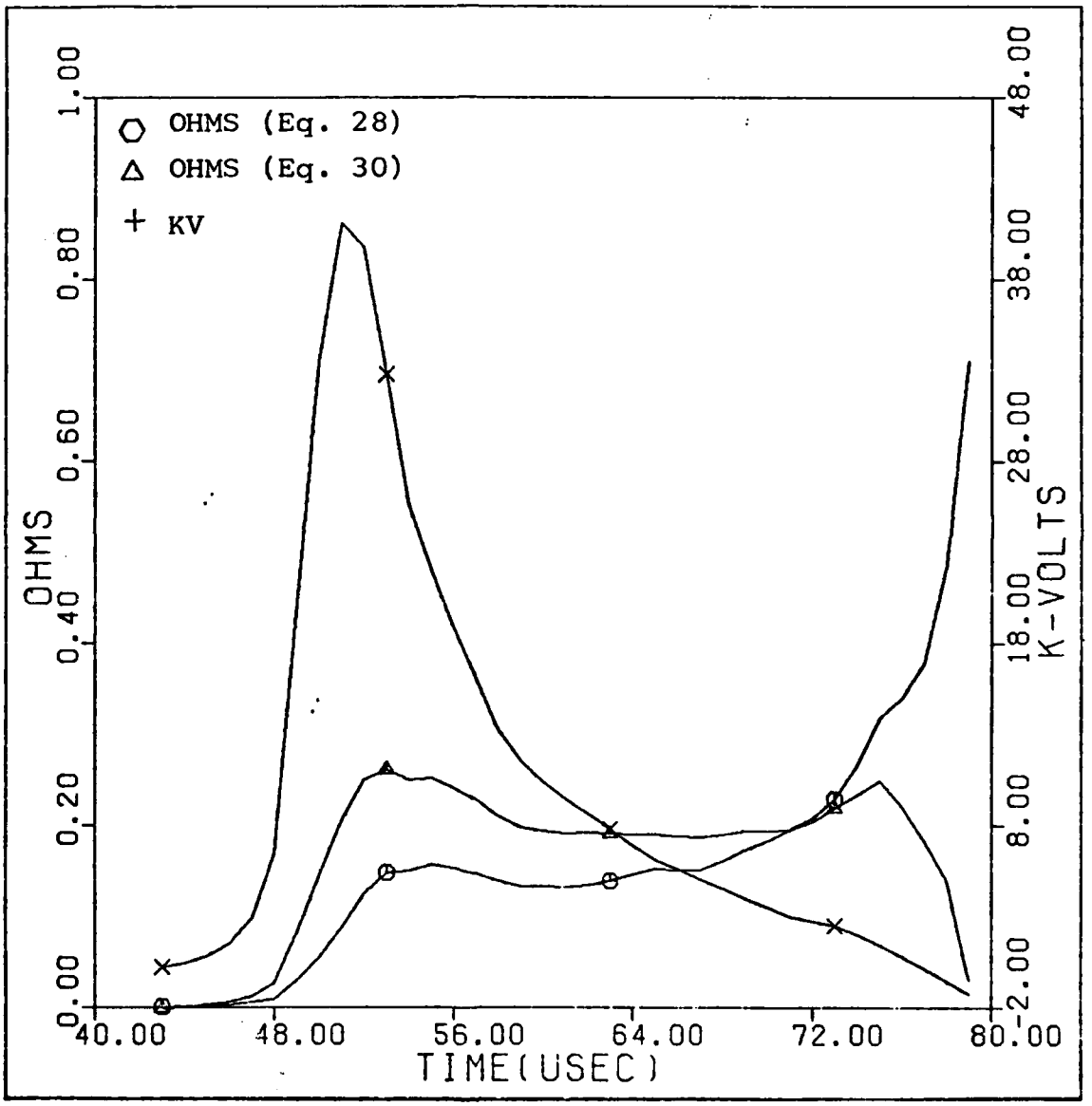

Fig. 59 Switch P13 Resistance and Voltage

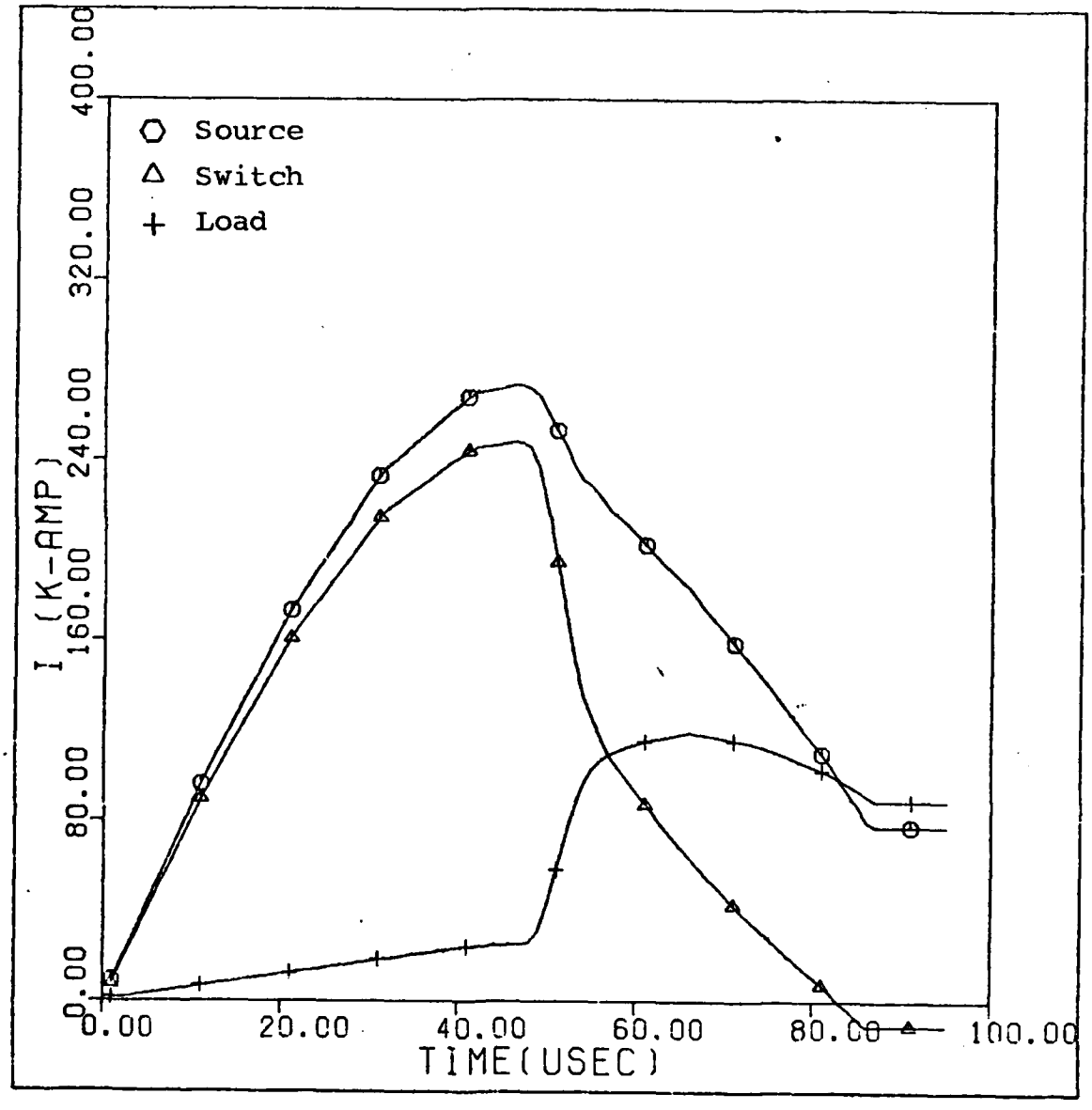

Fig. 60 Switch P14 Currents

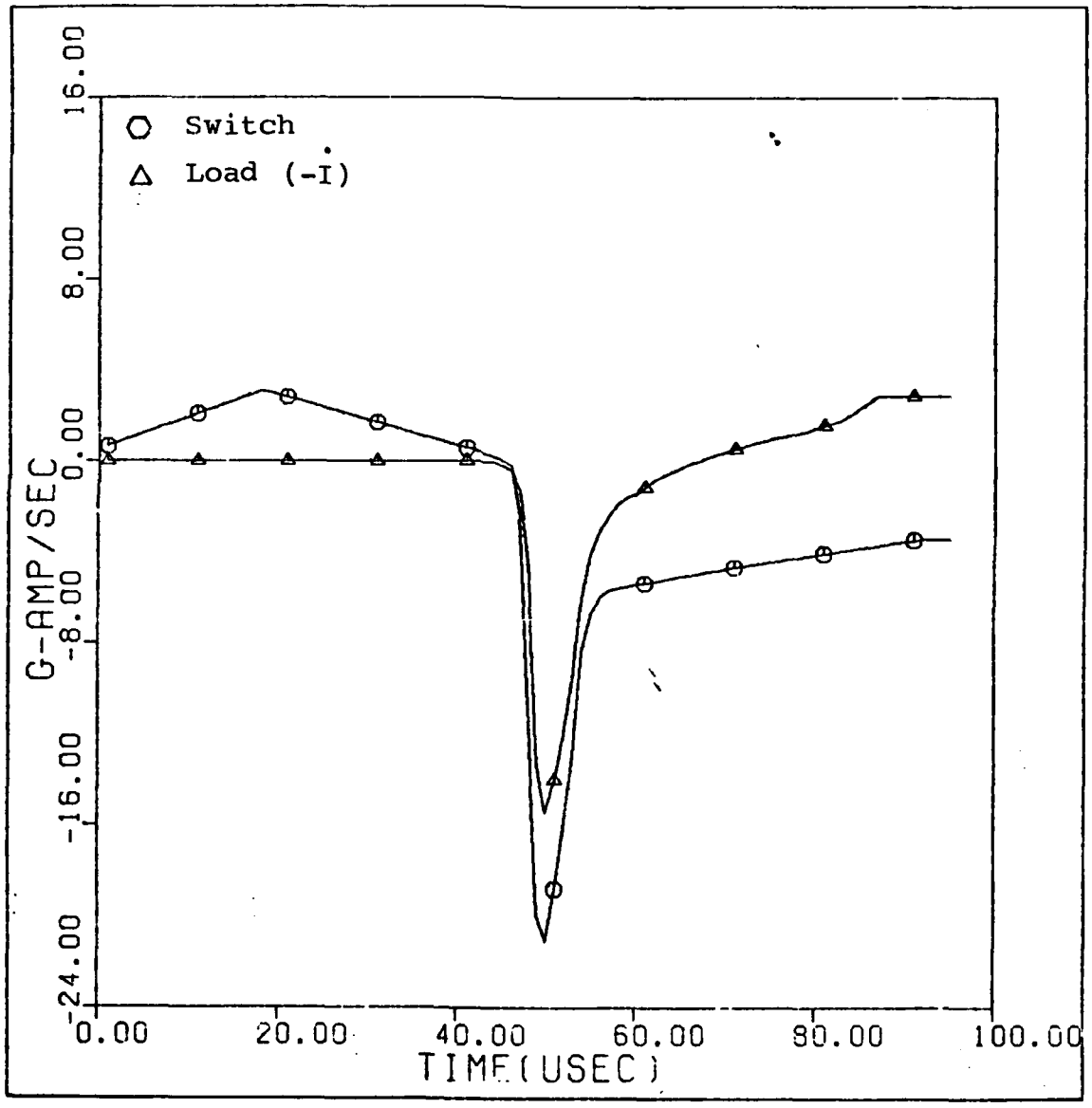

Fig. 61 Switch P14 Current Derivatives

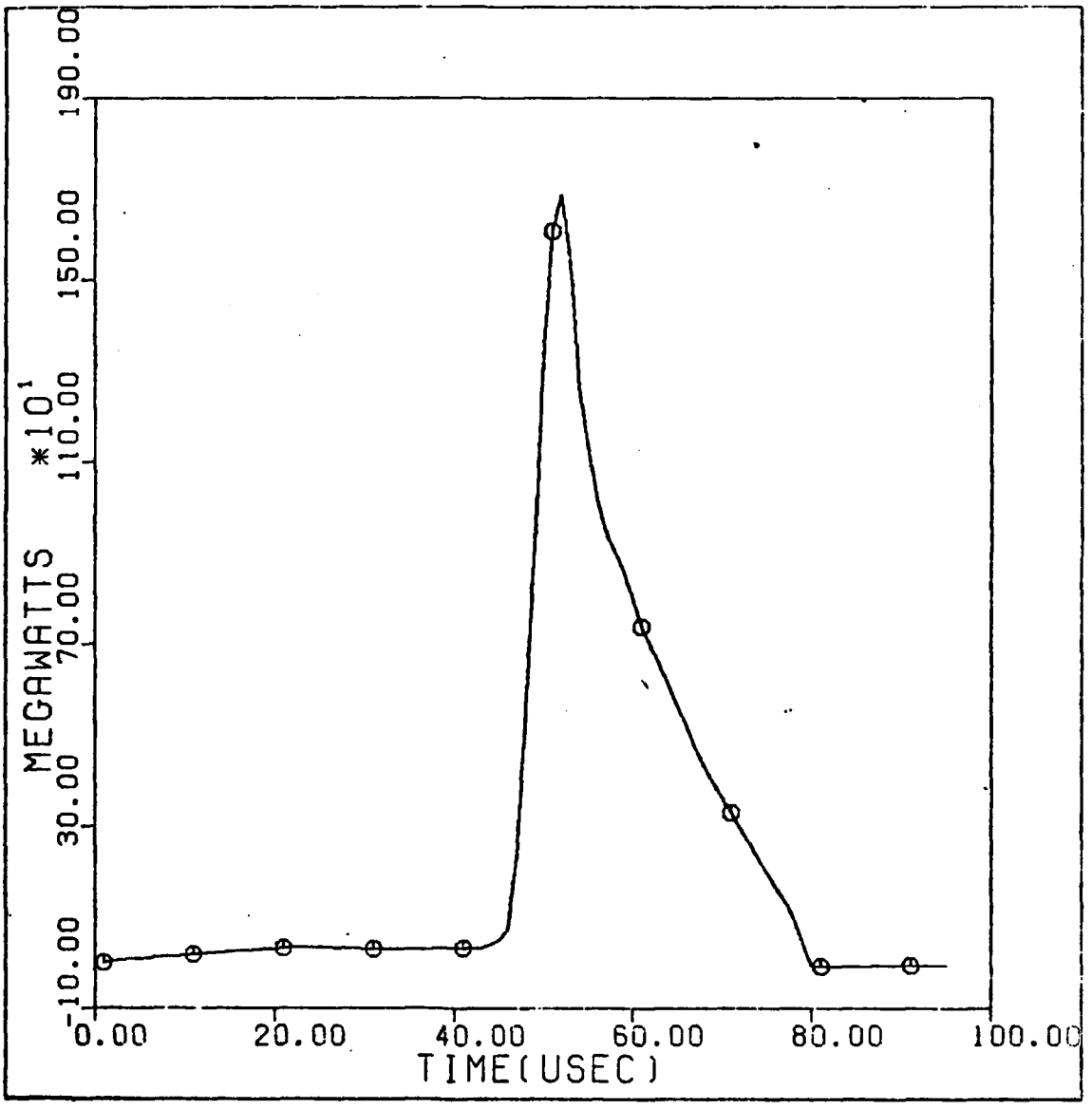

Fig. 62 Switch P14 Load Power

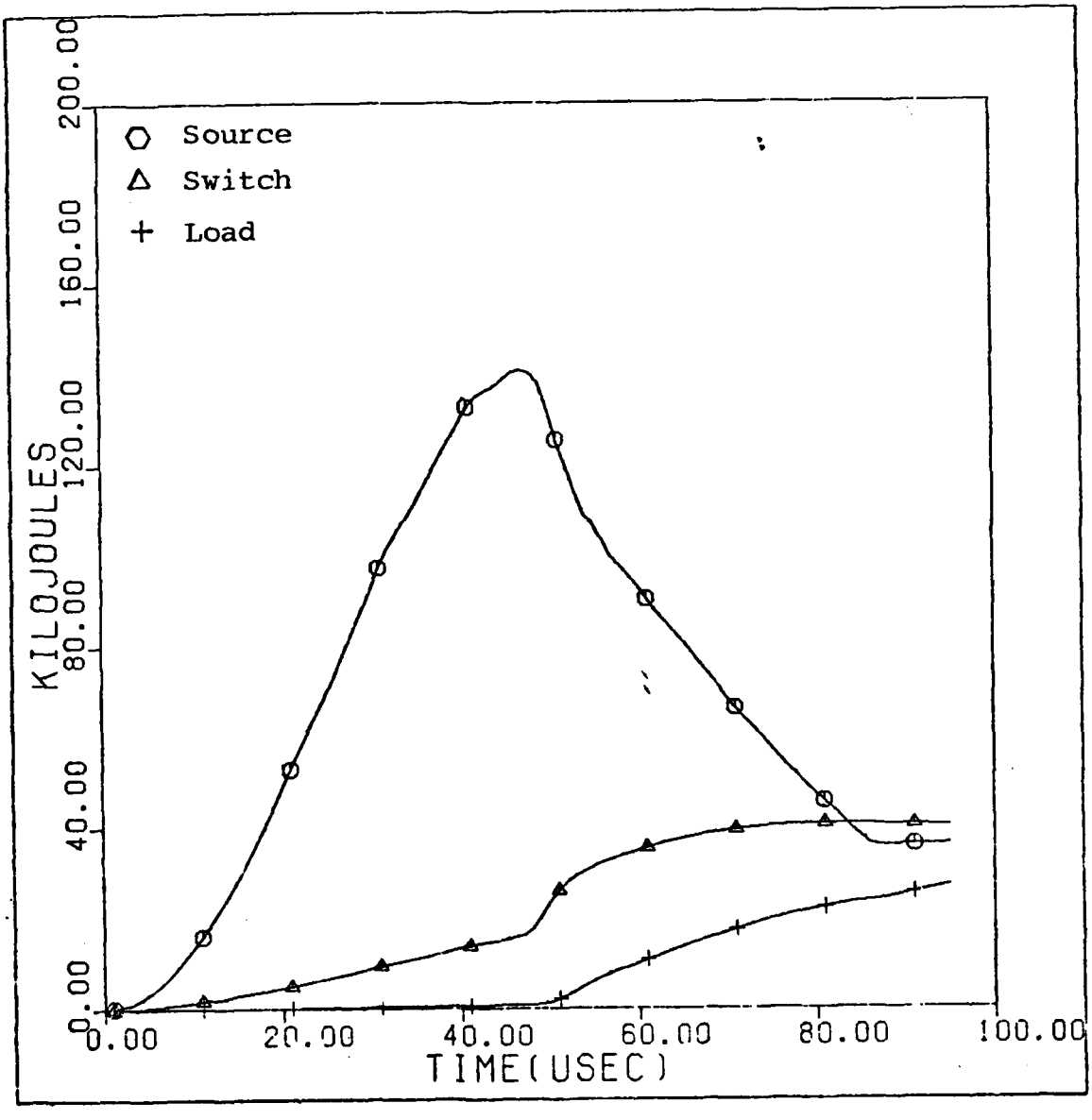

Fig. 63 Switch P14 Energies

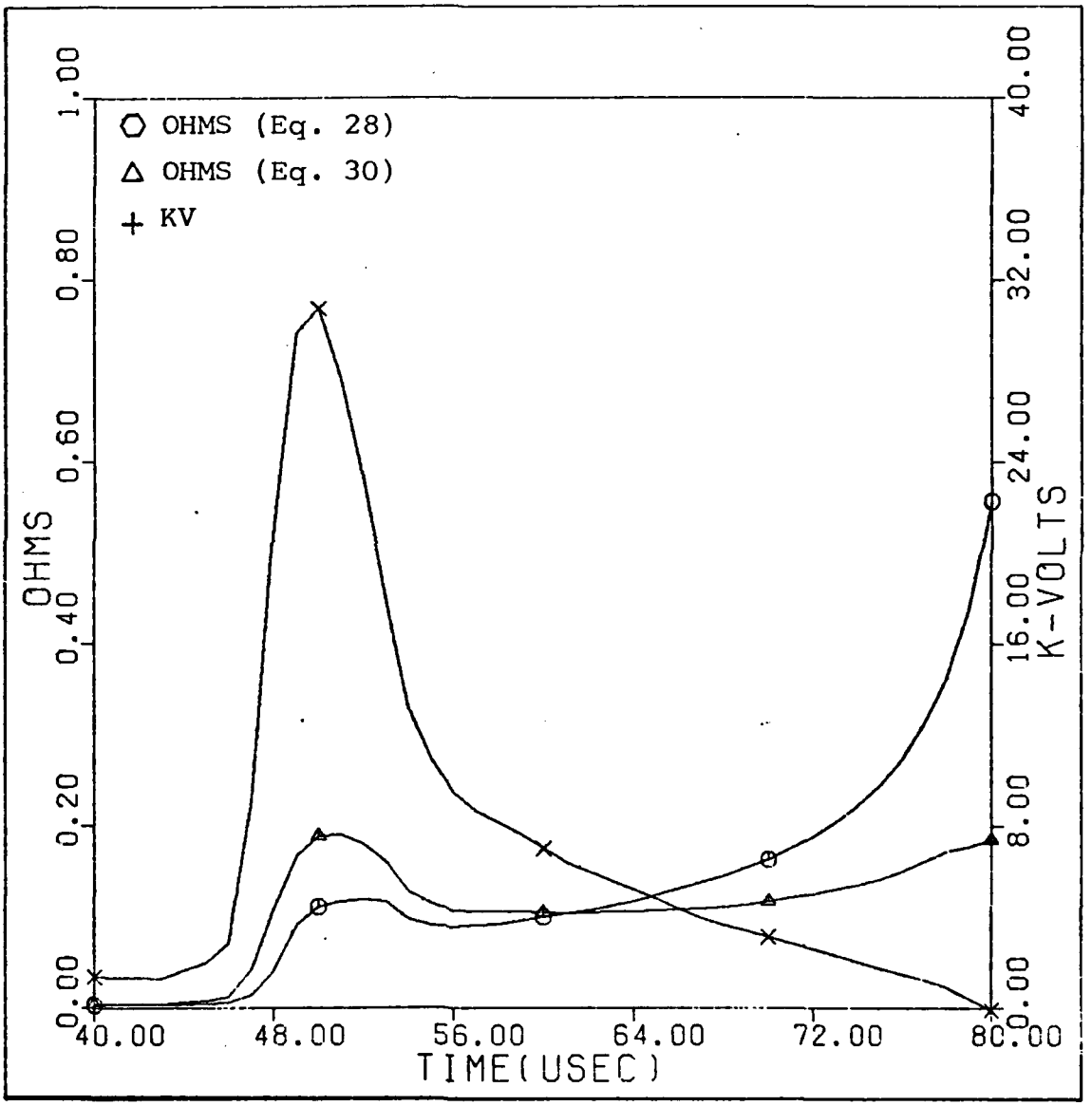

Fig. 64 Switch P14 Resistance and Voltage

VITA

David Watson

John David Watson was born 5 July 1948 in Fayetteville, North Carolina. He graduated from high school in Fayetteville in 1966 and attended North Carolina State University for one year. He enlisted in the USAF in 1967 and served as an aircraft weapons technician until 1975. He returned to North Carolina State University and received the degree of Bachelor of Science in Electrical Engineering in December 1977. Upon graduation, he entered the USAF OTS and received a commission in April 1978. He served as a Satellite Systems Engineer at the 2d Communications Squadron, Buckley ANGB, Colorado until entering the School of Engineering, Air Force Institute of Technology, in June, 1981.

Permanent address: P.O. Drawer 70
Lumber Bridge, North Carolina 28357

Michael Hines

Michael Lee Hines was born on 26 September 1950 in Marietta, Ohio. He graduated from high school in Stewart, Ohio in 1968. He entered the Air Force in 1969 and served as a communications specialist. He attended Ohio University, Athena, Ohio from which he received the degree of Bachelor of Science in Electrical Engineering in 1981. He received his Air Force Commission through ROTC in 1981. He entered the School of Engineering, Air Force Institute of Technology, in June 1981.

Permanent address: Box 123
Amesville, Ohio 45711

UNCLASSIFIED
SECURITY CLASSIFICATION OF THIS PAGE (When Data Entered)

REPORT DOCUMENTATION PAGE		READ INSTRUCTIONS BEFORE COMPLETING FORM
1. REPORT NUMBER AFIT/GE/EE/82D-39	2. GOVT ACCESSION NO. AD-A124 67	3. RECIPIENT'S CATALOG NUMBER
4. TITLE (and Subtitle) DEVELOPMENT OF AN IMPROVED EXPLOSIVELY DRIVEN RUPTURED CONDUCTOR OPENING SWITCH		5. TYPE OF REPORT & PERIOD COVERED MS Thesis 6. PERFORMING ORG. REPORT NUMBER
7. AUTHOR(s) John D. Watson, Capt, USAF Michael L. Hines, 2Lt, USAF		8. CONTRACT OR GRANT NUMBER(s)
9. PERFORMING ORGANIZATION NAME AND ADDRESS Air Force Institute of Technology (AFIT-EN) Wright-Patterson AFB, Ohio 45433		10. PROGRAM ELEMENT, PROJECT, TASK AREA & WORK UNIT NUMBERS
11. CONTROLLING OFFICE NAME AND ADDRESS Advanced Concepts Branch (AFWL-NTYP) Air Force Weapons Laboratory Kirtland AFB, NM 87117		12. REPORT DATE December 1982 13. NUMBER OF PAGES 121
14. MONITORING AGENCY NAME & ADDRESS(if different from Controlling Office)		15. SECURITY CLASS. (of this report) Unclassified 15a. DECLASSIFICATION/DOWNGRADING SCHEDULE

16. DISTRIBUTION STATEMENT (of this Report)

Approved for public release; distribution unlimited

17. DISTRIBUTION STATEMENT (of the abstract entered in Block 20, if different from Report)

18. SUPPLEMENTARY NOTES

Approved for public release: IAW AFR 190-17.
LYNN E. WOLAVER
Dean for Research and Professional Development
Air Force Institute of Technology (ATC)
Wright-Patterson AFB OH 45433

4 JAN 198

19. KEY WORDS (Continue on reverse side if necessary and identify by block number)

Current Interruptor
High Speed Opening Switch
Fuse
Pulse Compression
Explosive Switch
Energy Storage - Inductive

20. ABSTRACT (Continue on reverse side if necessary and identify by block number)

Two types of explosively driven ruptured conductor opening switches were tested. Each used a length of detonator cord to rupture an aluminum conductor. The first type used a cylindrical conductor with pusher media of either paraffin or water to break the conductor and absorb the arc energy. The second type used detonator cord in direct contact with a flat conductor. This design used the high pressure from the explosive to break the conductor and extinguish the arc.

DD FORM 1 JAN 73 1473 EDITION OF 1 NOV 65 IS OBSOLETE

UNCLASSIFIED
SECURITY CLASSIFICATION OF THIS PAGE (When Data Entered)

The cylindrical switches interrupted 115 KA in approximately 35 μsec with switching delays of 68 μsec to 87 μsec. Peak load powers of up to 334 MW were achieved using a 61 KJ supply circuit. Increasing the explosive weight was found to have a detrimental effect on the switch opening time.

The flat conductor switches interrupted 185 KA with initial resistance rise rates of up to 117 mΩ/μsec. Peak load powers of up to 3.5 GW were achieved using a 137 KJ supply circuit.

The planar switch showed characteristics of both a ruptured conductor opening switch and a fuse opening switch. As the switch current was increased, the opening time decreased, eventually to a time smaller than the detonator cord burn time. This indicated that after the detonator cord was ignited, the unsevered portion of the conductor was burned open like a fuse due to the increased current density.

END

FILMED

3-83

DTIC